UNIVERSIDADE FEDERAL DO PARANÁ

GIOVANA LAIS RUVIARO TULESKI

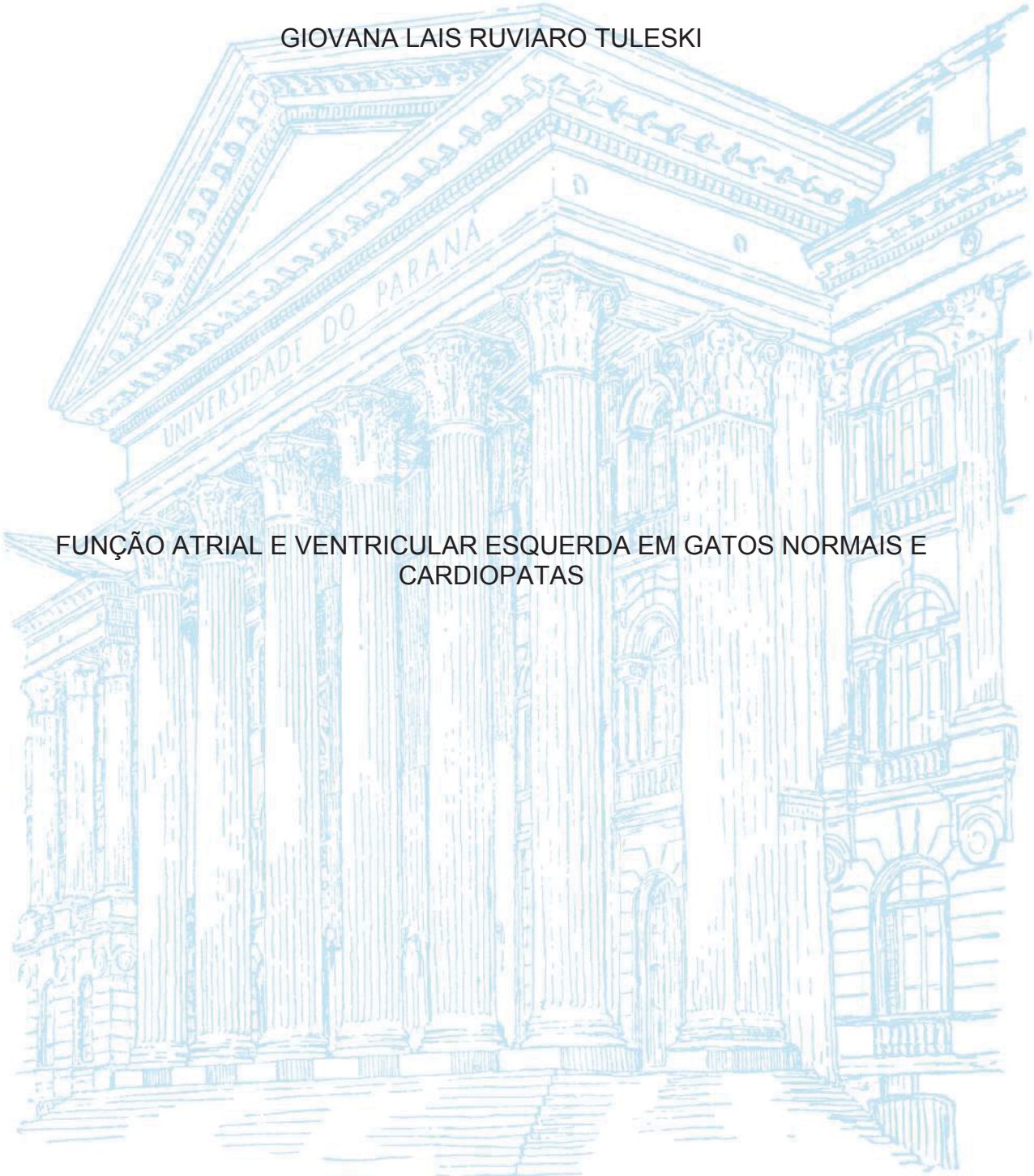

FUNÇÃO ATRIAL E VENTRICULAR ESQUERDA EM GATOS NORMAIS E CARDIOPATAS

CURITIBA
2022

UNIVERSIDADE FEDERAL DO PARANÁ

GIOVANA LAIS RUVIARO TULESKI

FUNÇÃO ATRIAL E VENTRICULAR ESQUERDA EM GATOS NORMAIS E CARDIOPATAS

Tese apresentada ao curso de Pós-Graduação em Ciências Veterinárias, Setor de Ciências Agrárias, Universidade Federal do Paraná, como requisito parcial à obtenção do título de Doutor.

Orientador: Prof. Dr. Marlos Gonçalves Sousa

CURITIBA
2022

DADOS INTERNACIONAIS DE CATALOGAÇÃO NA PUBLICAÇÃO (CIP)
UNIVERSIDADE FEDERAL DO PARANÁ
SISTEMA DE BIBLIOTECAS – BIBLIOTECA

Tuleski, Giovana Lais Ruviaro
Função atrial e ventricular esquerda em gatos normais e cardiopatas. / Giovana Lais Ruviaro Tuleski. – Curitiba, 2022.
1 recurso online: PDF.

Tese (Doutorado) – Universidade Federal do Paraná, Setor de Ciências Agrárias, Programa de Pós-Graduação Ciências Veterinárias.

Orientador: Prof. Dr. Marlos Gonçalves Sousa.

1. Coração – Ventrículo esquerdo. 2. Cardiologia veterinária. I. Sousa, Marlos Gonçalves. II. Universidade Federal do Paraná. Programa de Pós-Graduação Ciências Veterinárias. III. Título.

Bibliotecário: Douglas Alex Jankoski CRB-9/1167

TERMO DE APROVAÇÃO

Os membros da Banca Examinadora designada pelo Colegiado do Programa de Pós-Graduação CIÊNCIAS VETERINÁRIAS da Universidade Federal do Paraná foram convocados para realizar a arguição da tese de Doutorado de **GIOVANA LAIS RUVIARO TULESKI** intitulada: **FUNÇÃO ATRIAL E VENTRICULAR ESQUERDA EM GATOS NORMAIS E CARDIOPATAS**, sob orientação do Prof. Dr. MARLOS GONÇALVES SOUSA, que após terem inquirido a aluna e realizada a avaliação do trabalho, são de parecer pela sua APROVAÇÃO no rito de defesa.

A outorga do título de doutora está sujeita à homologação pelo colegiado, ao atendimento de todas as indicações e correções solicitadas pela banca e ao pleno atendimento das demandas regimentais do Programa de Pós-Graduação.

CURITIBA, 19 de Abril de 2022.

Assinatura Eletrônica
19/04/2022 17:04:08.0
MARLOS GONÇALVES SOUSA
Presidente da Banca Examinadora

Assinatura Eletrônica
06/05/2022 08:22:52.0
KARINA PREISINGAPTEKMANN
Avaliador Externo (UNIVERSIDADE FEDERAL DO ESPÍRITO SANTO)

Assinatura Eletrônica
19/04/2022 17:25:15.0
JUAN CARLOS DUQUE MORENO
Avaliador Interno (UNIVERSIDADE FEDERAL DO PARANÁ)

Assinatura Eletrônica
20/04/2022 09:03:09.0
MARIA LUCIA GOMES LOURENÇO
Avaliador Externo (UNIVERSIDADE EST.PAULISTA JÚLIO DE MESQUITA FILHO/BOTUCATU)

Assinatura Eletrônica
21/04/2022 09:09:51.0
SIMONE TOSTES DE OLIVEIRA STEDILE
Avaliador Interno (UNIVERSIDADE FEDERAL DO PARANÁ)

Dedico essa tese à minha filha Lara.

AGRADECIMENTOS

Ao Hospital Veterinário da UFPR e todos os que o constituem: residentes, alunos, servidores, professores, terceirizados e comunidade.

Ao professor Marlos Gonçalves Sousa, que sempre acredita no potencial dos seus alunos e tem uma maneira de orientar que possibilita que façamos nossos próprios caminhos.

À minha família, que deu apoio incondicional.

À minha filha Lara, que compreendeu que a mamãe também é uma cientista e necessita tempo, e iluminou meus dias com seu carinho e alegria.

Ao meu pai, que sempre compartilhou comigo o amor aos animais.

À minha mãe Cleme, cujos olhos brilham de entusiasmo a cada passo que dou na vida acadêmica.

À minha irmã Vanessa, incentivadora, parceira e conselheira.

À minha irmã Valéria, entusiasta dos estudos, uma torcedora solidária e carinhosa.

Ao Oscar, que me acompanhou boa parte do Doutorado, e sempre enfatizou a importância da saúde do corpo para abastecer a mente.

Aos amigos que fiz no doutorado, principalmente Tais Casonato, que compartilhou comigo as dúvidas e as alegrias dessa etapa da vida.

Aos gatos.

Sombra

Busco a mim mesmo
Fico feliz quando acho a sombra
estou perto

Autor desconhecido

Um dia vai ser

Pelos caminhos que ando
um dia vai ser
só não sei quando.

Paulo Leminski

RESUMO

A função sistólica longitudinal do ventrículo esquerdo em gatos saudáveis foi avaliada por meio do deslocamento tecidual do anel mitral (TMAD), comparando-o ao strain longitudinal (LSt), ambas técnicas baseadas na ecocardiografia Speckle Tracking. Adicionalmente, foram observadas as alterações provocadas pela administração prévia de drogas para diminuir a frequência cardíaca, como o timolol, ou para tranquilizar os gatos, como a gabapentina e a melatonina. Dessa forma, esse trabalho foi subdividido em introdução e três capítulos. O primeiro capítulo investigou a utilização do TMAD como método diagnóstico da função sistólica longitudinal em gatos saudáveis, realizando ecocardiografia em 193 gatos de diferentes raças, pesos e idades. A técnica apresentou moderada variação inter e intra-observador, mostrando-se uma ferramenta confiável para avaliação da função sistólica longitudinal do ventrículo esquerdo em gatos. O segundo capítulo verificou o efeito de uma gota de solução oftálmica de timolol a 0,5% sobre a função sistólica do ventrículo esquerdo (VE) e átrio esquerdo (AE) em gatos, buscando também confirmar se essa droga realmente auxilia na avaliação da função diastólica. Participaram ao total de 41 gatos saudáveis de tutores, submetidos a duas ecocardiografias com 20 minutos de intervalo. Animais do grupo timolol (33 gatos) receberam uma gota de solução de timolol após o primeiro exame. O timolol reduziu a função sistólica, diminuindo as variáveis ecocardiográficas mais comuns, como fração de encurtamento do VE e AE. Quanto à avaliação diastólica, embora a FC tenha diminuído, a droga não separou as ondas diastólicas mitrais como esperado. Finalmente, o terceiro capítulo descreve o experimento randomizado e duplo-cego com 75 gatos saudáveis comparando dois tratamentos tranquilizantes distintos (gabapentina, melatonina) com placebo, administrados imediatamente após os exames de controle: eletrocardiografia (ECG) , aferição de pressão arterial sistêmica e ecocardiografia (PAS). O intervalo para reavaliação foi de 60 minutos para o segundo ECG e PAS, e 70 minutos para a segunda ecocardiografia. Foram observadas alterações mínimas nas variáveis, nenhuma capaz de comprometer o diagnóstico. Quanto ao comportamento, tanto a gabapentina como a melatonina conseguiram tranquilizar os gatos, embora a primeira droga tenha provocado sedação em um maior número de animais.

Palavras-chave: Speckle-tracking; ventrículo esquerdo; função sistólica longitudinal;, beta-bloqueador, medicação pré-consulta, tranquilizante

ABSTRACT

Left ventricular longitudinal systolic function in healthy cats was evaluated through tissue motion annular displacement (TMAD) of the mitral annulus, compared to longitudinal strain (LSt), both techniques based on speckle tracking echocardiography (STE). Additionally, changes caused by a previous administration of drugs to decrease heart rate, such as timolol, or to calm cats, such as gabapentin and melatonin. Thus, this work was subdivided into an introduction and three chapters. The first chapter investigated the use of TMAD as a diagnostic method of longitudinal systolic function in healthy cats, performing echocardiography in 193 cats of different breeds, weights and ages. The technique showed moderate inter-and intra-observer variation, proving a reliable tool for assessing left ventricular longitudinal systolic function in cats. The second chapter verified the effect of a drop of 0.5% timolol ophthalmic solution on the systolic function of the left ventricle (LV) and left atrium (LA) in cats, also seeking to confirm whether this drug helps in the evaluation of the diastolic function. A total of 41 client-owned healthy cats were submitted to two echocardiograms 20 minutes apart. Animals in the timolol group (33 cats) received a drop of timolol solution after the first examination. Timolol reduced systolic function, decreasing the most common echocardiographic variables, such as LV and LA shortening fraction. As for the diastolic assessment, although the HR decreased, the drug did not separate the mitral diastolic waves as expected. Finally, the third chapter describes the randomized, double-blind trial with 75 healthy cats comparing two different tranquillizing treatments (gabapentin, melatonin) with placebo, administered immediately after the control exams: electrocardiography (ECG), measurement of systemic blood pressure (SBP) and echocardiography. The reassessment interval was 60 minutes for the second ECG and SBP and 70 minutes for the second echocardiography. Minimal changes were observed in the variables observed, none capable of compromising the diagnosis. As for behaviour, both gabapentin and melatonin managed to calm the cats, although the first drug caused sedation in a more significant number of animals.

Keywords: Speckle-tracking; Left ventricle; longitudinal systolic function; beta-blocker; pre-appointment medication; tranquillizer.

LISTA DE ILUSTRAÇÕES

LISTA DE TABELAS

SUMARIO

INTRODUÇÃO

A avaliação da função sistólica do ventrículo esquerdo (VE) auxilia na escolha terapêutica e no prognóstico. Para tanto, a fração de encurtamento obtida pela ecografia bidimensional é o índice sistólico mais utilizado, o qual verifica principalmente a contração transversal das fibras musculares cardíacas. A função sistólica longitudinal geralmente é avaliada por meio do *strain* longitudinal (LSt) e da excursão sistólica do plano do ânulo mitral (MAPSE), o qual mede o deslocamento do anel mitral durante a sístole usando-se o Modo-M. Ja o deslocamento tecidual de movimento do anel mitral (TMAD - *Tissue motion annular displacement*) do ventrículo esquerdo, é muito semelhante ao MAPSE, exceto por utilizar o a tecnologia speckle-tracking para essa aferição.

Considerando a importância da função sistólica longitudinal, as médias de TMAD e LSt também foram aferidas nos outros capítulos dessa dissertação. O capítulo 2 avalia os efeitos da solução oftálmica de timolol instilada previamente à ecocardiografia. Tal procedimento foi sugerido para que a diminuição da frequência cardíaca provocada por esse fármaco permita a avaliação diastólica durante a ecocardiografia. No entanto, como beta-bloqueador, é esperado que o timolol também diminua a força de contração.

O capítulo 3 compara os efeitos tranquilizantes e cardíacos da gabapentina, melatonina ou placebo administrados via oral setenta minutos antes da ecocardiografia, ou sessenta minutos antes da eletrocardiografia e aferição da pressão arterial sistêmica. Busca-se efetivo relaxamento sem consequências hemodinâmicas substanciais que comprometam a avaliação cardíaca desses animais.

CAPÍTULO 1- Deslocamento tecidual do anel mitral para avaliar a função sistólica do ventrículo esquerdo em gatos saudáveis

Giovana Lais Ruviaro Tuleski[a*], M.Sc; Marcela Wolf[a], M.Sc; Maria Jose Garcia Ribeiro Pscheidt, BSc[b]; Júlio Pereira dos Santos[a], M.Sc; Marlos Gonçalves Sousa[a], PhD.

[a] Laboratory of Comparative Cardiology, Department of Veterinary Medicine, Federal University of Paraná (UFPR), Rua dos Funcionários, 1540, CEP 80035-050, Curitiba, Paraná, Brazil.

[b] Autonomous veterinarian, Curitiba, Paraná, Brazil

*Corresponding author. Email address: gtuleski@yahoo.com.br. Giovana L. R. Tuleski - ORCID 0000-0002-0817-3470

Publicado no revista *Veterinary Research Communications* no dia 8 de Março de 2022, citado a seguir:

Tuleski, Giovana Lais Ruviaro, et al. "Tissue motion annular displacement to assess the left ventricular systolic function in healthy cats." Veterinary Research Communications (2022): 1-14.

Abstract

The tissue motion annular displacement (TMAD) measures the longitudinal displacement of the mitral annulus during systole, using speckle-tracking echocardiography (STE). The main objective was to determine the TMAD means in healthy cats, exploring the correlations with systolic surrogates. The influence of age, body surface area (BSA), heart rate, and systemic blood pressure on the indices was also analyzed. One hundred ninety-three healthy, client-owned cats participated in this prospective, cross-sectional observational study undergoing conventional and STE. Apical four-chamber (AP4) and two-chamber (AP2) images were recorded for offline calculations. Mean TMAD values were similar to mitral annulus plane systolic excursion (MAPSE), varying between 4 to 4.8 millimeters depending on the annulus and image used. No significant differences between age and BSA categories were detected, except for AP4 MP%, reduced in the heavier group. TMAD variables showed moderate correlation with longitudinal strain (LSt) and MAPSE, but not with fraction shortening (FS) and ejection fraction (EF). The median time required for the offline calculation was 12.2 s for AP4 and 11.8 s for AP2. The technique showed moderate inter and intraobserver variation, proving a reliable tool for assessing left ventricular longitudinal systolic function in cats.

Keywords: speckle tracking; strain; longitudinal function; reference range

Abbreviations

AP2	Apical 2-chamber image
AP4	Apical 4-chamber image
BSA	Body surface area
ECG	Electrocardiography
FS	Fractional shortening
FW	Free wall
EF	Ejection fraction
GLS	Global longitudinal strain
HCM	Hypertrophic cardiomyopathy
HR	Heart rate
IVS	Interventricular septum
LA	Left atrium
LSt	Longitudinal strain
LV	Left ventrilce
MAPSE	Mitral Annular Plane Systolic Excursion
ROI	Regions of interest
SBP	Systolic blood pressure
STE	Speckle-tracking echocardiography
TDI	Tissue Doppler imaging
TMAD	Tissue Motion Annular Displacement
TMAD MP	The displacement (in mm) of a virtual midpoint between the two mitral annular regions towards the left ventricular apex
TMAD MP%	The proportional displacement of that midpoint concerning the total length of the left ventricle

TMAD MV1	Displacement of the septal (AP4) or anterior (AP2) annulus towards the apex
TMAD MV2	Displacement of the lateral (AP4) or inferior (AP2) annulus towards the apex

Introduction

Assessment of systolic function is a cornerstone of echocardiographic examination. In conventional echocardiography, fractional shortening (FS) and ejection fraction (EF) are widely used as surrogates for systolic function, despite their limitations. Measurement of both parameters requires good image quality, has sub-optimal test-retest reproducibility, fails to evaluate the longitudinal myocardial contraction, and neither detects regional dysfunction on the left ventricle (Mizuguchi et al. 2008; Zacà et al. 2010; Klaeboe e Edvardsen 2019; Luis et al. 2019).

While FS measures only the heart's circumferential contraction, EF represents longitudinal and circumferential contraction (Hu et al. 2013). However, the longitudinal systolic function is routinely less evaluated on echocardiographic examinations. The contraction of the longitudinal fibers during systole causes a shortening of the left ventricular chamber along its longitudinal axis, promoting the displacement of the atrioventricular plane towards the cardiac apex (Zacà et al. 2010). In humans, their contraction is the primary contributor to left ventricular pumping, representing up to 60% of the total cardiac stroke (Carlsson et al. 2007). Previous studies have demonstrated that longitudinal systolic dysfunction may be apparent before impaired transverse function becomes overt (Luis et al. 2019; Spalla et al. 2019). For this reason, practical and easy-to-apply techniques are sought to assess longitudinal systolic function in cats.

The Mitral Annular Plane Systolic Excursion (MAPSE) is more sensitive than EF to detect early longitudinal fibers abnormalities (Hu et al. 2013). When low, MAPSE and its right counterpart, Tricuspid Annular Plane Systolic Excursion (TAPSE), reveal longitudinal systolic dysfunction in cats with asymptomatic hypertrophic cardiomyopathy (HCM), being even smaller in congestive heart failure (Spalla et al. 2017). The systolic wave S' from tissue Doppler imaging (TDI) is a more sensitive index of global contractility of the left ventricle (LV) than EF, reflecting both longitudinal shortening and torsional deformation (Chetboul et al. 2004; Simpson et al. 2009; Seo et al. 2010). Regrettably, both MAPSE and TDI are angle-dependent (Vinereanu et al. 1999; Chetboul et al. 2004; van Dalen et al. 2009; Zacà et al. 2010; Hu et al. 2013; Aloia et al. 2016; Spalla et al. 2017).

In contrast, speckle-tracking echocardiography (STE) is angle-independent and determines tissue velocities accurately (van Dalen et al. 2009). The longitudinal strain (LSt) has been used to assess the longitudinal systolic function in people (Collier et al. 2017; Trivedi et al. 2019), dogs (Tidholm et al. 2009; Chetboul e Tissier 2012; Zois et al. 2012), and cats (Silva et al. 2013; Spalla et al. 2019; Suzuki et al. 2019a; Caivano et al. 2020). Cats with preclinical HCM have a decrease in LSt (Spalla et al. 2019), highlighting the use of this technique in the early detection of this disease.

Another STE method to estimate the longitudinal function is the Tissue Motion Annular Displacement (TMAD), which measures the systolic displacement of two regions of interest (ROI) located in the mitral annulus, tracking them towards a third ROI at the cardiac apex (Buss et al. 2012). Previous studies observed that TMAD is faster than LSt and requires lower image quality (Buss et al. 2012; Black et al. 2014; Asada et al. 2018). Another advantage of the TMAD concerning the LSt is that the

last one presents a variation in its values according to the software and equipment used, this problem being observed in humans (Bansal et al. 2008; Negishi et al. 2013; Yingchoncharoen et al. 2013; Yang et al. 2015; Ramlogan et al. 2020) and dogs (Santarelli et al. 2019). Finally, TMAD was considered a viable method for rapid assessment of longitudinal systolic function in humans with HCM (Liu et al. 2014). Therefore, TMAD may be useful in the early diagnosis of HCM in cats, although further studies are needed to confirm this supposition.

Our research group was the first to describe the relevance of TMAD to evaluate longitudinal systolic function in dogs, both in healthy animals and those with heart disease (Wolf et al. 2018, 2021). However, no articles reported a study of TMAD in cats on a recent search (January 2022) on two platforms: PubMed and ProQuest. In this study, we aimed to explore the potential applicability of TMAD for the assessment of longitudinal systolic function in healthy cats. Our goal was to clarify whether TMAD is a reliable method compared with LSt and other echocardiographic surrogates in cats. Another objective was to determine whether a correlation exists between TMAD and LSt, and other echocardiographic parameters such as FS, EF, TDI, and MAPSE. Lastly, we investigated whether TMAD alters with age, body surface area (BSA), heart rate (HR), and systemic blood pressure (SBP).

Animals, Materials and Methods

Animals

Client-owned healthy cats were recruited for this prospective, cross-sectional observational study at the cardiology section of a veterinary teaching facility between May and July 2019. The experimental unit was the individual animal. All procedures were previously approved by the Institutional Animal Care and Use Committee

(protocol 014/2019) and complied with the National Institutes of Health Guide for the Care and Use of Laboratory Animals. Written consent from owners allowing their cats to participate in the study was mandatory.

All cats underwent a complete physical examination before enrollment, as well as SBP measurement, electrocardiography (ECG), conventional and speckle-tracking echocardiography. The Doppler technique (Binns et al. 1995) was used to obtain SBP indirectly by a trained observer (GLRT), acquiring at least five reliable values to measure the average. Subsequently, a 2-min recording of a computer-based ECG was performed.

The inclusions criteria were: cats more than one year, considered adults (Quimby et al. 2021), absence of murmur on cardiac auscultation, no previously diagnosed disease, and standard examinations (ECG, SBP, and echocardiography). The SBP before the echocardiogram was considered normal up to 160 mmHg (Acierno et al. 2018). Animals whose SBP exceeded this value were only included if they were patients without a record of arterial hypertension, with at least three normal SBP measurements in the last five years. Free plasma T4 excluded hyperthyroidism in cats over 11 years old or whenever this disease was suspected.

Exclusion criteria were established in an attempt to select only apparently healthy cats, rejecting cats receiving topical or systemic medication and those previously diagnosed with any illness, including chronic systemic hypertension, arrhythmias, acquired or congenital heart disease.

Echocardiography

All cats underwent echocardiographic examinations[1] with electrocardiography monitoring using only gentle restraint and no sedation. Positioning followed the recommendations of the Echocardiography Committee of the Specialty of Cardiology of the American College of Veterinary Internal Medicine (Thomas et al. 1994). The same operator (GLRT) performed all examinations and measurements.

The FS of the left atrium (LA) was estimated based on the minimum and maximum LA diameter from the right parasternal short-axis view image at the aortic valve level, using anatomic M-mode(Abbott e MacLean 2013). The ratio between LA and aorta was measured at the maximum LA diameter, right after the T wave from the ECG, as described before(Rishniw e Erb 2000). A normal relation of LA and aorta (LA/Ao <1.6, at the final of the T wave) was considered evidence of normal diastolic pressure, combined with a normal diastolic pattern defined by the transmitral outflow (E/A>1) and TDI waves (E´/A´>1)(Schober e Chetboul 2015).

The HCM was ruled out after examining the LV in the right and left parasternal long-axis LV outflow view and in the right parasternal short axis view of the left ventricle at the level of the papillary muscles. The M-Mode measurements of the LV at the papillary level were measured before the QRS to characterize the end of diastole as described (Sahn et al. 1978), being 5.5 millimeters the cut-off point for HCM (Häggström et al. 2016).

The left parasternal window allowed the acquisition of apical 4-chamber (AP4) and 2-chamber (AP2) images (Thomas et al. 1994). AP4 was used to measure the TDI velocities (Koffas et al. 2006) and MAPSE from the interventricular septum mitral annulus (MAPSE IVS) and from and free wall (MAPSE FW) as described elsewhere

[1] Philips Affiniti 50 ultrasound system equipped with 12 MHz phased-array transducer

(Mondillo et al. 2006; Spalla et al. 2017). Recording of at least five cardiac cycles of AP4 and AP2 images enabled the offline calculation of all TMAD and LSt values.

Both TMAD and LSt required the measure of the aortic valve closure time from the apical 5-chamber image. It corresponds to the time, in milliseconds, from the beginning of the QRS complex to the end of the aortic valve spectra obtained with the pulsed Doppler gate positioned distal to the aortic valve.

Longitudinal strain

The LSt was measured offline using speckle-tracking software[2] and AP4 and AP2 images containing at least five cardiac cycles obtained from standard echocardiography. To calculate AP4 LSt, three ROIs were defined from the selected frame: the septal and lateral portions of the mitral valve leaflets and the epicardial region of the left ventricular apex (Spalla et al. 2019). The equipment's software automatically tracked the myocardium and calculated longitudinal deformation (Fig. 1a). Manual corrections were made whenever auto-tracking was obviously incorrect. The mean value from three cardiac cycles in the same frame was used for analysis. A similar procedure was used for AP2 images, and the ROIs were defined at the anterior and inferior aspects of the mitral annulus (Fig. 1c).

The average of the LSt values obtained with AP2 and AP4 was assumed as a modified global deformation index (Wolf et al. 2018), as it did not include the apical three-chamber (AP3) view, as follows:

GLS = (AP2 LSt + AP4 LSt) / 2

Tissue motion annular displacement

[2] QLAB Software with automatic cardiac motion quantification (aCMQ)

Mitral annular motion was measured offline as described for LSt, using the same ROIs. The displacement of both annuli towards the apex (in mm) was automatically calculated. The abbreviation MV1 refers to the displacement of the septal (AP4) or anterior (AP2) annulus, while MV2 corresponds to the lateral (AP4) or inferior (AP2) annulus. The software also defined a virtual midpoint (MP) between the two annular ROIs and calculated its displacement (in mm) towards the left ventricular apex, as well as the proportional displacement of that midpoint concerning the total length of the left ventricle (MP%) (Fig. 1b, 1d). The mean values from three cardiac cycles in the same recording were used to calculate the TMAD.

The average of the indices obtained by AP2 and AP4 was called global TMAD values (Wolf et al. 2021), calculated as follows:

Global TMAD MP = (AP2 MP + AP4 MP) / 2

Global TMAD MP% = (AP2 MP% + AP4 MP%) / 2

Figure 1 - Longitudinal strain and tissue motion annular displacement of the mitral annulus in two-chamber and four-chamber apical view

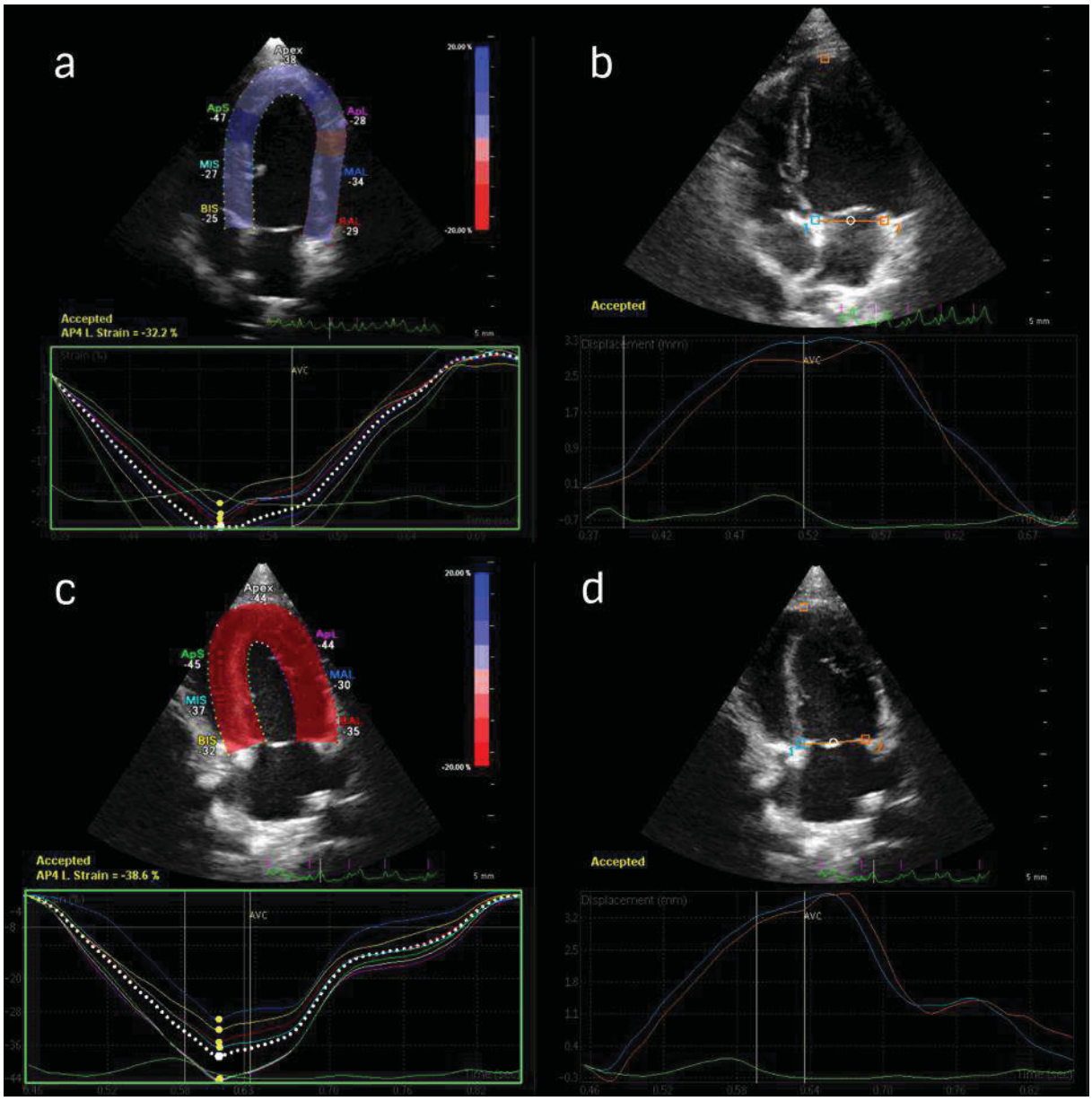

Fig. 1 Above: two apical 4-chamber images demonstrate the longitudinal strain on the left (a) and the tissue motion annular displacement on the right (b). Below: two apical 2-chamber images display the longitudinal strain on the left (c) and the tissue motion annular displace

Intra-observer and inter-observer variability and time requirements

The same observer (GLRT) randomly reassessed the echocardiography of 18 patients at least 30 days after the first evaluation to estimate intra-observer

variability. A co-investigator blinded to the previous results (MW) assessed the same examinations, whose results were used to calculate inter-observer variation.

Different 23 echocardiographic records were selected to calculate the time spent for the offline calculation of the TMAD and LSt.

Age and Body Surface Area categories

Cats were divided into groups according to age and BSA, allowing the investigation of their action on TMAD. The age distribution followed the most recent age classification of cats by the American Animal Hospital Association (AAHA) and the American Association of Feline Practitioners (AAFP) (Quimby et al. 2021): 1-6 years (young adult); 7 to 10 years (mature adult); and 11 years or older (senior). The BSA categories were: less than 0.252 m^2 (<4 kg), 0.253 to 0.292 m^2 (4.01 to 5 kg), 0.293 to 0.330 m^2 (5.1 to 6 kg), and more than 0.330 m^2 (>6.01 kg). The BSA was calculated as described before (Hill e Scott 2004), following the formula:

$$BSA\ (m^2) = 0.1 \times (\text{bodyweight in kg})^{⅔}$$

Statistical analysis

The *Statistica Single User* software version 13.2 performed most of the analyses, with a significant level of 0.05 (P-value <0.05). Descriptive data analysis included mean and standard deviation calculations, minimum and maximum of all quantitative variables, and pure frequencies of qualitative variables. The Shapiro-Wilk test was used to investigate the normality of the data. Group comparison was performed with ANOVA followed by Tukey's or Dunn's posthoc test. The parameters with not normally distributed data were adequate for the Kruskal-Wallis test (LSt and TMAD MP%).

The correlations were investigated using Pearson's correlation coefficient, scaled and ranged from -1 to +1, where 0 indicates no linear association. The relationship gets stronger as the coefficient approaches an absolute value of 1. They were considered weak between 0-1 to 0.39, moderate from 0.40 to 0.69, strong from 0.7 to 0.89, and very strong above 0.9 (Schober e Schwarte 2018).

The intra- and inter-observer agreement analysis was performed using the interclass correlation coefficient (ICC) with its respective 95%CI and standard error of measurement (SEM) (Fleiss 1986; Popovic e Thomas 2017). From the ten different ICC formulas, it was used the two-way mixed-effects model (Koo e Li 2016) defined for the formula:

ICC= MSR−MSE / MSR; where MSR = mean square for rows; MSE= mean square for error

The minimum sample size for using the ICC was calculated with a power of 80%, with a drop of 10%, minimum acceptable reliability of 0.6, and expected reliability of 0.85. Its interpretation was based on a Fleiss study: low for values below 0.40; moderate between 0.40 and 0.75; substantial between 0.75 and 0.90; and excellent greater than 0.90 (Fleiss 1986). The Bland-Altman test was used to better represent non-normal data as it does not necessarily require a normal distribution (Bland e Altman 2010).

Wilcoxon test was used to compare the median time spent to calculate the TMAD and LSt variables on AP4 and AP2.

Results

A total of 193 client-owned cats (1-19 y/2.5-11.8 kg) were recruited for this study (105 females; 56%). The population included crossbred cats (n=172; 89.1%),

Persian (n=10; 5.2%), Siamese (n=6; 3.1%), Angora (n=2; 1%), Maine Coon (n=2; 1%), American Shorthair (n=1; 0.5%), and Bengal (n=1; 0.5%). Most of the cats weighed less than 5 kg, i.e., the BSA category below 0.292 m^2 (n=127; 65.8%). The BSA distribution was as follow: 32.64% (63) less then 0.252 m^2 (< 4 kg), 33.16% (64) between 0.253 to 0.292 m^2 (4.01 to 5 kg), 20.72% (40) between 0.293 to 0.330 m^2 (5.1 to 6 kg), and 13.47% (26) with more than 0.331 m^2 (> 6.01 kg). The age distribution was: 108 (55.96%) young adults; 48 (24.87%) mature adults; 36 (18.65%) seniors, and 1 (0.52%) unknown.

Table 1 displays the TMAD and LSt results for the studied population. Table 2 presents TMAD and LSt results according to BSA categories. From all TMAD variables analyzed, only AP4 MP% differed by BSA. In contrast, all LSt values were lower in heavier cats. The age categories of the animals did not influence LSt and TMAD values, as can be seen in Table 3.

Table 1 - Conventional and speckle-tracking echocardiographic parameters obtained in healthy non-sedated cats

Variables	n	Mean	Min	Max	SD
Age (years)	192	6.6	1	19	4
Weight (kg)	193	4.8	2.5	11.6	1.3
SBP (mmHg)	191	141.1	100	220	19.5
HR (bpm)	193	193.5	145	260	25.9
FS (%)	193	53.2	25.1	68.5	8.1
EF (%)	193	86	68.6	95.7	6.3
MAPSE IVS (mm)	136	4.4	2.3	7.7	0.9
MAPSE FW (mm)	174	4.7	2.2	7.9	0.9
Sep S' (cm/s)	189	7.6	4.1	14.3	1.8
Lat S' (cm/s)	165	7.3	3.9	11.4	1.5
TMAD Parameters					
AP2 MV1 (mm)	104	4.4	2	6.8	0.9
AP2 MV2 (mm)	104	4.8	2.2	8.2	1.1
AP2 MP (mm)	104	4.7	2.5	7.8	1
AP2 MP% (%)	104	18.5	11.3	26.4	3.4
AP4 MV1 (mm)	193	4.0	1.6	6.9	1
AP4 MV2 (mm)	193	4.2	1.8	7.4	1.1
AP4 MP (mm)	193	4.3	1.9	7.5	1
AP4 MP%	193	17.6	8.4	30.6	4
Global MP (mm)	104	4.6	3	7.6	0.8
Global MP%	104	18	12.7	26	2.7
Longitudinal Strain					
AP2 LSt (%)	104	28.9	19.9	45	4.6
AP4 LSt (%)	192	28.3	14.7	45.9	5.1
GLS (%)	104	29.4	20.4	42.3	4.6

SBP: systemic blood pression; HR: hear rate; FS: Fractional Shortening; EF: ejection fraction; MAPSE FW: mitral annular plane systolic excursion from the lateral annulus; MAPSE IVS: mitral annular plane systolic excursion from the septal annulus; Sep S′: systolic myocardium wave from tissular Doppler from the septal annulus; Lat S′: systolic myocardium wave from tissular Doppler from the lateral annulus; TMAD: tissue motion annular displacement; AP2: apical 2-chamber; MV1: point of septal mitral annulus; MV2: point of lateral mitral annulus; MP: displacement of a virtual midpoint between the two mitral annulus towards the left ventricle apex; MP%: percentage value of the midpoint in relation to the total length of the left ventricle; AP4: apical 4-chamber; LSt: longitudinal strain of the left ventricle; GLS: global longitudinal strain n: total number of individuals; Min: minimum; Max: maximum; SD: standard deviation

Table 2 - Tissue motion annular displacement and longitudinal strain obtained in healthy non-sedated cats according to body surface area categories

BAS (m^2)	< 0.252 m		0.253 to 0.292 m2		0.293 to 0.330		> 0.331		P-value*
Bodyweight (kg)	< 4		4.01 to 5		5.01 to 6		> 6.01		
	Mean (n)	SD	Mean (n)	SD	Mean (n)	SD	Mean (n)	SD	
TMAD values									
AP2 MV1 (mm)	4.22 (32)	0.97	4.31 (32)	0.88	4.47 (26)	0.88	4.81 (14)	0.78	0.2099
AP2 MV2 (mm)	4.60 (32)	1.27	4.75 (32)	1.09	4.86 (26)	0.96	5.04 (14)	1.08	0.6261
AP2 MP (mm)	4.59 (32)	1.1	4.64 (32)	0.98	4.82 (26)	0.83	4.99 (14)	0.87	0.5409
AP2 MP%	18.65 (32)	3.73	18.96 (32)	3.72	17.4 (26)	2.26	18.94 (14)	3.46	0.3132
AP4 MV1 (mm)	3.89 (63)	1.00	4.02 (64)	0.94	4.16 (40)	0.89	3.87 (26)	0.94	0.9985
AP4 MV2 (mm)	4.2 (63)	1.22	4.23 (64)	1.08	4.21 (40)	1.00	4.18 (26)	1.04	0.496
AP4 MP (mm)	4.28 (63)	1.05	4.29 (64)	0.98	4.31 (40)	0.91	4.13 (26)	0.87	0.8836
AP4 MP%	18.66[a] (63)	4.61	17.57 (64)	3.99	16.7 (40)	3.1	16.18[b] (26)	3.12	**0.0205**
Global MP (mm)	4.48 (32)	1.01	4.56 (32)	0.75	4.68(26)	0.69	4.62 (14)	0.58	0.8169
Global MP%	18.35 (32)	3.08	18.57 (32)	2.69	17.11 (26)	2.03	17.78 (14)	2.29	0.1706
LSt values (%)									
AP2 LSt	30.25[a] (32)	4.54	30.19 (32)	4.82	26.35[b] (26)	3.08	27.42 (14)	4.41	**0.0013**
AP4 LSt	29.54[a] (63)	5.21	28.80 (63)	4.66	26.42[b] (40)	4.61	27.02 (26)	5.9	**0.0095**
GLS	30.94[a] (32)	4.57	30.27[a] (33)	4.61	26.80[b] (26)	3.81	28.46 (14)	4.18	**0.0025**

*p value<0.05 means a significant difference

a, b: Lowercase letters indicate significant differences between the categories ($p < 0.05$)

BAS: body surface area

AP2: apical 2-chamber; MV1: point of septal mitral annulus; MV2: point of lateral mitral annulus; MP: displacement of a virtual midpoint between the two mitral annulus towards the left ventricle apex; MP%: percentage value of the midpoint in relation to the total length of the left ventricle; AP4: apical 4-chamber; LSt: longitudinal strain of the left ventricle; GLS: global longitudinal strain

n: total number of individuals; SD: standard deviation

Table 3 – Comparison of tissue motion annular displacement (TMAD) values between the age categories

Variables	Age category	n	Mean	SD	*p-valor**
AP4 MP	Young	108	4.32	0.94	0.4700
	Mature	48	4.28	1.03	
	Senior	36	4.09	1.00	
AP4 MP%	Young	108	17.51	3.73	0.9930
	Mature	48	17.53	4.18	
	Senior	36	17.61	4.68	
AP4 MV1	Young	108	4.09	0.92	0.1382
	Mature	48	3.93	1.05	
	Senior	36	3.73	0.89	
AP4 MV2	Young	108	4.30	1.05	0.2647
	Mature	48	4.19	1.16	
	Senior	36	3.96	1.18	

*p value<0.05 means a signifcant diference
AP4: apical 4-chamber; MP: displacement of a virtual midpoint between the two mitral annulus towards the left ventricle apex; MP%: percentage value of the midpoint in relation to the total length of the left ventricle; MV1: point of septal mitral annulus; MV2: point of lateral mitral annulus
n: total number of individuals; SD: standard deviation

Significant correlations between TMAD and echocardiographic variables are shown in Table 4. The scatter plots of the moderate correlations between TMAD and echocardiographic variables are in Figure 2. When comparing all variables, all significant correlations were considered low, such as those with BSA (MAPSE IVS, r= 0.221; TAPSE, r=0.206; AP4 LSt, r= - 0.251; AP2 LSt, r= - 0.341; GLS, r= - 0.286; Lat s', r= 0.161; Sep s', r=0.341), HR (SBP, r= 0.138; FS, r=0.243, EF, r=0.255; Sep s', r= 0.341; Lat s', r= 0.242; TRIV, r= - 0.219), Sep s' (IVRT, r= AP,4) LSt (MAPSE IVS, r= - 0.173; TAPSE, r= - 0.182), AP2 LSt (TAPSE, r= - 0.201), and GLS (TAPSE, r= - 0.256; EF, r= -0.256).

Table 4 - Correlations detected between echocardiographic variables and TMAD indices

Variable	TMAD indices	r	CI	p-valor
Age	AP4 MV1	-0,155	-0,290 to -0,0140	0,0314
	AP2 MP	-0,208	-0,397 to -0,0321	0,0226
	Global MP	-0,208	-0,3838 to -0,0183	0,0321
HR	AP2 MV2	-0,207	-0,3809 to -0,0130	0,0353
	AP2 MP	-0,195	-0,3680 to 0,0020	0,0468
	Global MP	-0,194	-0,3676 to 0,0006	0,0469
BSA	AP4 MP%	-0,200	-0,3313 to -0,0605	0,0052
	Global MP%	-0,209	-0,3828 to -0,0171	0,0322
SBP	AP4 MV1	0,185	-0,1354 to 0,1464	0,0102
	AP4 MV2	0,171	-0,1183 to 0,1633	0,0178
	AP4 MP	0,194	-0,1685 to 0,1131	0,0072
	AP2 MP	0,208	0,0148 to 0,3858	0,0352
MAPSE FW	AP4 MV1	0,192	0,0396 to 0,3261	0,0113
	AP4 MV2	0,278	0,1345 to 0,4089	0,0002
	AP4 MP	0,244	0,0964 to 0,3762	0,0012
	AP2 MV1	0,337	0,1376 to 0,4842	0,0005
	AP2 MV2	0,411	0,0274 to 0,3948	0,0001
	AP2 MP	0,401	0,2139 to 0,5422	0,0001
	AP2 MP%	0,227	0,0274 to 0,3948	0,0213
	Global MP	0,390	0,2058 to 0,5349	0,0001
	Global MP%	0,179	-0,0178 to 0,3543	0,0001
MAPSE IVS	AP4 MV1	0,216	0,0522 to 0,3721	0,0114
	AP2 MV1	0,320	0,1365 to 0,4834	0,0001
	AP2 MV2	0,268	0,0814 to 0,4395	0,0061
	AP2 MP	0,297	0,0769 to 0,4343	0,0024
	AP2 MP%	0,265	0,0769 to 0,4343	0,0064
	Global MP%	0,253	-0,0962 to 0,2837	0,0071
Lat S’	AP4 MV1	0,185	0,03361 to 0,3289	0,0017
	AP4 MV2	0,207	0,0556 to 0,3484	0,0078
	AP4 MP	0,190	0,0385 to 0,3333	0,0144
AP4 LSt	AP4 MP	0,147	0,0048 to 0,2813	0,0422
	AP4 MP%	0,337	0,2054 to 0,4564	0,0001
	AP2 MP%	0,255	0,0628 to 0,4227	0,0091
	Global MP%	0,280	0,0920 to 0,4450	0,0038
AP2 LSt	AP4 MP%	0,242	0,0599 to 0,4203	0,013
	AP2 MP%	0,458	0,2706 to 0,5821	0,00001
	Global MP%	0,444	0,2557 to 0,5715	0,00001
GLS	AP4 MP%	0,209	0,0168 to 0,3825	0,0327
	AP2 MP%	0,285	0,0854 to 0,4412	0,0033
	Global MP%	0,307	0,1140 to 0,4627	0,0014

Figure 2 Scatter plots of the moderate correlations between TMAD and echocardiographic variables

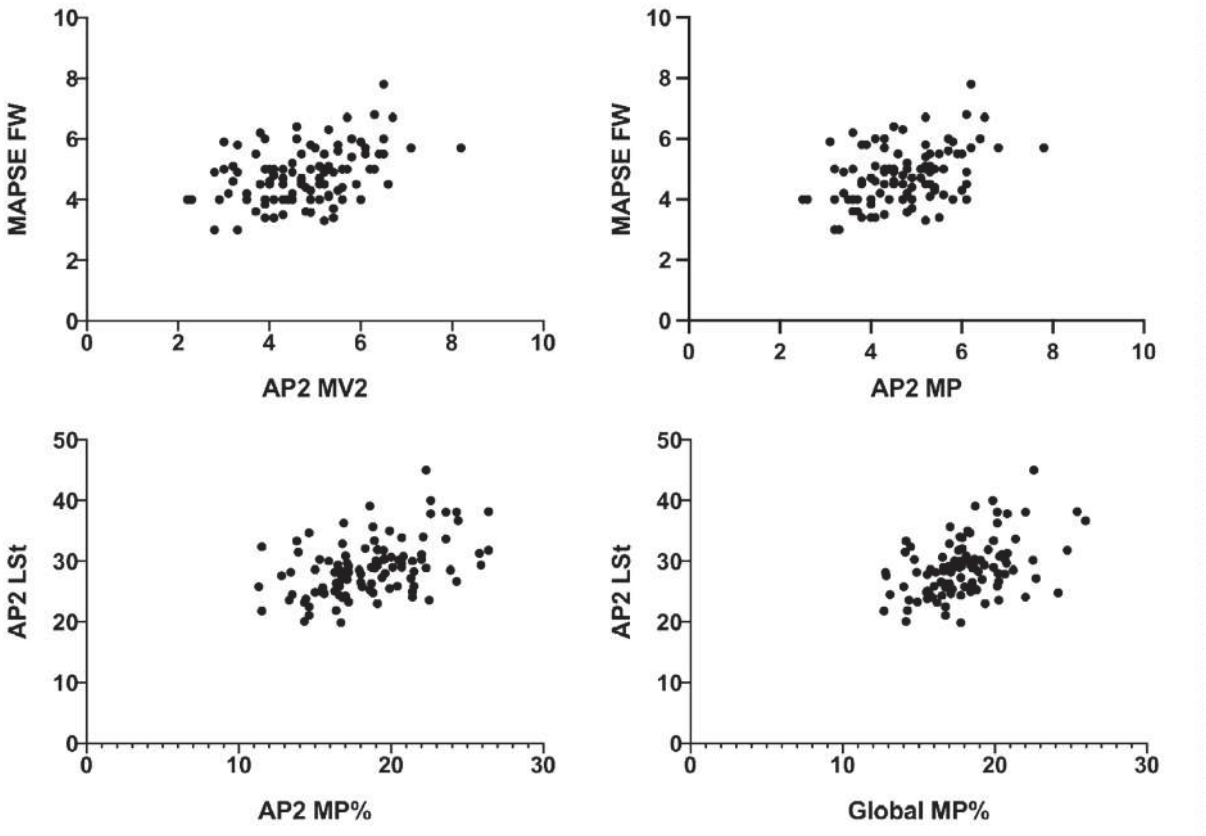

The inter and intra-observer variations are demonstrated in Table 5 for all the TMAD indexes, including the one without normality, TMAD MP%. Figure 3 displays the Bland-Altman graphics for this variable. Most TMAD variables had a moderate agreement, except the interobserver TMAD MP and MP%, which showed a substation correlation.

Figure 3 - Bland-Altmann graphic representing inter and intra-observer agreement for the variable TMAD MP% (a) interobserver variation; (b) intraobserver variation

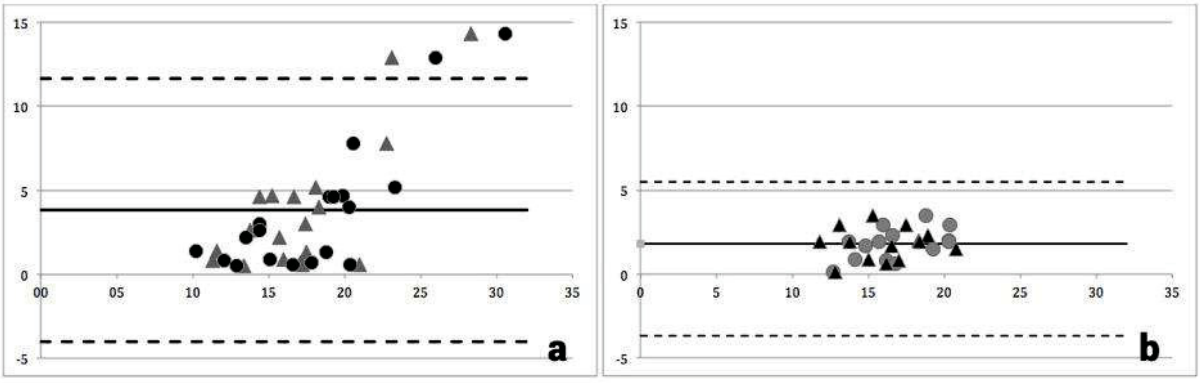

Table 5 – Intra and inter-observer variations for tissue motion annular displacement (TMAD) variables obtained for the apical four-chamber image

Variable	ICC	SEM	M	SD	95%CI
	(0-1)	mm or %			
Intraobserver variation					
TMAD MV1 (mm)	0.72	0.44	3.9	0.8	3.05 - 4.71
TMAD MV2 (mm)	0.55	0.43	3.7	0.6	2.87 - 4.58
TMAD MP (mm)	0.68	0.34	3.9	0.6	3.34 - 4.66
TMAD MP%*	0.71	1.42	16.5	2.6	14.98- 20.53
Interobserver variation					
TMAD MV1 (mm)	0.64	0.65	3.9	1.1	Not calculated
TMAD MV2 (mm)	0.52	0.83	3.8	1.2	Not calculated
TMAD MP (mm)	0.75	0.52	4.0	1.0	Not calculated
TMAD MP%*	0.85	1.78	17.7	4.6	Not calculated

* Variable without normal distribution
ICC: interclass correlation coefficient; SEM: Standard error of measurement; M: mean; SD: Standard deviation; 95%CI: range of 95% confidence interval calculated from the mean value
MV1: point of septal mitral annulus; MV2: point of lateral mitral annulus; MP: displacement of a virtual midpoint between the two mitral annulus towards the left ventricle apex; MP%: percentage value of the midpoint in relation to the total length of the left ventricle

Concerning the time spent, although there was a numerical difference between the median time of AP4 LSt and AP4 TMAD (16.9 and 12.2 s, respectively), it was not significant (p=0.107, Wilcoxon test). The same happened for AP2 LSt and AP2 TMAD (17.46 and 11.8 s, respectively; p= 0.301).

Discussion

This investigation sought to investigate whether TMAD would be a reliable surrogate for systolic function in apparently healthy cats. To date, TMAD has been extensively evaluated in people and proved to be a valuable and reproducible technique (Buss et al. 2012; Black et al. 2014; Asada et al. 2018; Teraguchi et al. 2019; Sharma et al. 2021; Teraguchi et al. 2021). In dogs, we recently evaluated TMAD and demonstrated its correlation with LSt of the left ventricle (Wolf et al.

2018). It was speculated that the results were at least as promising as those observed in the species mentioned above.

Interestingly, most of the mean TMAD values obtained in cats in this investigation were lower than those found in dogs within a comparable weight, between 1.7 and 8.5 kg (Wolf et al. 2018). A reasonable justification was that the mean bodyweight in cats was lower than in dogs, even within a similar weight range. Heavier animals with larger hearts present a more significant absolute mitral displacement towards the apex (Schober e Fuentes 2001).

On the contrary, the mean AP4 LSt in this study was higher than those observed in cats by other authors (Silva et al. 2013; Spalla et al. 2019; Suzuki et al. 2019b; Caivano et al. 2020). An explanation may be using different equipment and software to acquire the LSt, which has been discussed in human medicine lately (Bansal et al. 2008; Negishi et al. 2013; Yingchoncharoen et al. 2013; Yang et al. 2015; Ramlogan et al. 2020). A study with children found that the mean LSt differed between QLAB 10.5 and all other software packages, including contemporary versions of QLAB (Ferraro et al. 2020). Coincidentally, the LSt obtained in dogs using QLAB 10.5 was also higher than the average found by other researchers with different equipment (Kusunose et al. 2013; Wolf et al. 2018), pointing to a tendency of this software to acquire higher LSt indexes. Furthermore, the LSt means obtained in the present study were similar to small dogs (up to 8.5 kg) using the same software version (Wolf et al. 2018). A study with dogs observed significant variability of strain variables obtained using different software, being the GLS the most reproducible measurement (Santarelli et al. 2019). Still, there is a need to standardize the abbreviation GLS in veterinary medicine, which can represent a weighted mean of the regional strains, using a single view (AP4) (Santarelli et al.

2019), or performing the average of the values from two apical images, AP2 and AP4 (Wolf et al. 2018, 2021). A reasonable option would be to follow human medicine, which refers to the GLS as the average of the values obtained from three apical views: AP2, AP3, and AP4 (Johnson et al. 2019).

As observed in children (Asada et al. 2018), the age categories did not influence TMAD values (Table 3). In dogs, although a significant correlation between TMAD and age happened, it disappeared when TMAD was normalized by body surface area (Wolf et al. 2018). Consequently, there is a need for a longitudinal study measuring TMAD values to clarify the effect of age, similarly to what was done previously with strain values, having been detected a reduction in the rate of maximum longitudinal strain during diastole after six years of follow-up (Sugimoto et al. 2021).

Regarding the BSA, a positive correlation existed between BSA and AP4 MP% and Global MP% (Table 4). However, most TMAD parameters did not differ among cats of different BSA categories, the only exception being AP4 MP%, which decreased with the increase in BSA (Table 2). On the contrary, all TMAD variables evaluated in dogs changed following bodyweight, reducing when in percentage (MP%) and increasing when measured in millimeters (Wolf et al. 2018). One possible explanation might be the slight difference between BSA categories in cats compared to dogs. This hypothesis is supported by the fact that dogs showed a much more pronounced decrease in LSt as weight increased, justified by the considerable variation in heart size within this species.

A low correlation appeared between SBP in almost all AP4 TMAD indices, except MP%. Sympathetic activity may explain it, affecting both SBP and contraction force. However, there was no correlation between HR and TMAD indices measured

in AP4. This lack of correlation was also previously reported in children (Asada et al. 2018) and dogs (Wolf et al. 2018). Nevertheless, a negative correlation occurred between HR and AP2 MV2, AP2 MP, and Global MP (Table 4). The contrary would be expected: an increase in HR would raise contraction, called the Bowditch staircase effect (Lakkatta 2004), confirmed by the positive correlation between HR and FS. The arrangement of the myofibrils may explain these contrasting results. It was recently observed that the ventricular mass is organized in a mesh shape with myocytes aggregated in tangential alignment and some obliquely in the wall, with antagonistic function (Lunkenheimer et al. 2004). If this also occurs in the cat's heart, these antagonistic fibers may predominate in the inferior portion of the mitral annulus, corresponding to MV2 from AP2 image, explaining the negative correlations found. However, it is still a conjecture.

Concerning the most commonly used systolic indices, FS and EF, TMAD did not correlate with them, coinciding with the results from dogs (Wolf et al. 2018) and children (Black et al. 2014). A likely explanation for this finding is that both FS and EF acquired from M-mode echocardiography reflect the transversal and circumferential fibers (Kocica et al. 2006; Buss et al. 2012; Trivedi et al. 2019), not the target of TMAD. On the contrary, TMAD strongly correlated with the EF based on magnetic resonance imaging (MRI) in normal children (Black et al. 2014). The same happened in adult humans comparing a TMAD algorithm with EF MRI (Tsang et al. 2010). Future studies can confirm whether TMAD values in cats correlate with EF MRI.

The best correlation between LSt and TMAD occurred in AP2 (Table 4 and Figure 2), obtaining two moderate correlations: LSt with MP%; and LSt with Global MP%. These findings were not surprising since both methods use STE. Nonetheless,

a low correlation was observed between Global MP% and GLS, while studies with people (Asada et al. 2018) and dogs (Wolf et al. 2018) found a moderate one.

Apparently, despite using speckle-tracking technology, TMAD and LSt have some very distinct characteristics. For example, TMAD was not influenced by cardiac rhythm in dogs, while GLS presented higher GLS values in sinus arrhythmia than sinus tachycardia or sinus rhythm (Wolf et al. 2018). The predominant rhythm in cats in hospital settings is tachycardia due to the fear reaction (Abbott 2005), requiring an investigation with sleeping or sedated cats to verify whether the GLS would be higher in sinus arrhythmia or if the mean TMAD values would change in sinus arrhythmia.

There were moderate correlations between TMAD and MAPSE, while in in humans it was observed a strong correlation (Hoit 2017; Mauermann et al. 2020). In cats, the strongest correlations were documented when comparing results obtained at the same mitral annulus, i.e., MV1 (septal) correlated better with MAPSE IVS and MV2 (lateral) with MAPSE FW (Table 4). These results were expected since both techniques follow the displacement of the mitral annulus in the longitudinal plane, except that the angle-independency from STE presumably makes the TMAD more accurate. For this reason, TMAD was also called $MAPSE_{STE}$ by some authors (Mauermann et al. 2020), highlighting that both techniques measure the displacement of the mitral annulus by different methods, M-mode and STE, respectively. Unlike the mentioned authors, who concluded that the TMAD underestimates the MAPSE values in M-mode, the TMAD indices in the present study were quite similar to the MAPSE ones.

Comparing IVS and FW annulus for MAPSE acquisition, it seemed that the first had better performance, obtaining more correlations with the TMAD variables (Table 4). Moreover, FW annulus also presented more correlations with TDI, having

Lat s' correlated with all AP4 variables, except MP%. In humans, a strong correlation was seen with both s' waves (Buss et al. 2012), although others authors have not found it (Teraguchi et al. 2019).

About the inter-and intra-observer variations, most variables presented ICC classified as moderate (Table 4). Surprisingly, two interobserver comparisons were substantial (Fleiss 1986), MP and MP%, achieving better performance than the intraobserver assessment. Nevertheless, the visual interpretation given by the Bland-Altman plot of the MP% variability revealed satisfactory repeatability and reproducibility (Figure 2). Earlier studies with TMAD obtained a satisfactory coefficient of variation in dogs (Wolf et al. 2018) and people (Tsang et al. 2010; Buss et al. 2012; Black et al. 2014; Penk et al. 2018; Teraguchi et al. 2019). The moderate agreement observed in this study may be due to more significant variability in the TMAD indices. An increase in the variability of STE indices was verified by an investigation that compared the left ventricular mechanics of mice, rats, rabbits, dogs, and humans, using strain imaging (Kusunose et al. 2012; Popovic e Thomas 2017). Another unproven possibility is that the HR three times greater than the human could make it difficult to correctly track the myocardium since the software was initially developed for humans.

Nevertheless, the SEM results shown in Table 5 provide an expected random variation in the scores of normal cats, which may be helpful in further studies with cats with HCM and compromised systolic function.

Concerning time, TMAD was faster to obtain in cats (MD=12.2 s) compared to dogs (MD=19.7 s) (Wolf et al. 2018) and slightly longer than reported in humans (8.22 and 10 s, respectively) (Tsang et al. 2010; Buss et al. 2012). Although it takes less than 15 s to be calculated, the real-time spent with TMAD should also compute

the image acquisition for later offline calculation and the time spent selecting the best record. The need for the three measurements to obtain the mean is advisable for most echocardiographic parameters in cats, so it does not count. However, all these mentioned steps also occur to acquire LSt, inherent to the STE. The authors consider that the TMAD calculation does not interfere negatively with the day-to-day exam. In addition, adequate tracking for calculating the TMAD was possible in all images obtained, like dogs (Wolf et al. 2018) and humans (Teraguchi et al. 2019).

Presumably, this was the first study to mention difficulties in obtaining STE in cats due to very low amplitude QRS complexes, even using the maximum magnification to increase ECG sensitivity. In general, the software can automatically detect QRS complexes and select a frame immediately before the ventricular systole, allowing the observer to determine the ROIs. However, sometimes very low QRS complexes resulted in incorrect P or T waves identification instead of QRS, producing unusual TMAD waves and unreliable LSt values. Provided the echocardiographer identifies this problem, TMAD can still be calculated, but failure to recognize this limitation can result in incorrect measurements being recorded.

Some limitations are recognized in this study. First, despite all efforts to include only healthy individuals, asymptomatic comorbidities may not have been identified based on clinical evaluation and ancillary examinations. In addition, the number and variability of cats included in the study may not represent feline populations from other countries, as Brazilian crossbred cats have an average weight of four to five kilograms, lighter than observed elsewhere. Lastly, the technique may have some disadvantages seen in STE, including the necessity of a simultaneous ECG, which can cause more stress depending on the cat's sensibility and the need for offline analysis.

Conclusion

This investigation led us to conclude that TMAD is viable to assess left ventricular longitudinal systolic function in healthy cats, with acceptable repeatability and reproducibility. Since the mitral motion can be easily tracked, TMAD has the advantage of not requiring an image quality as high as LSt, encouraging its application in routine. In addition, TMAD does not present remarkable discrepancies due to the equipment's software as occurs with strain. Even so, like most echocardiographic parameters, the TMAD may not be recommended as a single surrogate, but it complements the use of other parameters in the assessment of systolic function.

Although diastolic dysfunction predominates in cats' cardiomyopathies, little is comprehended about how the impairment of systolic function can contribute to the progression of the disease. Based on the reference values obtained for the species, further investigations may verify whether this technique can early detect systolic dysfunction in cats with subclinical HCM, and how this information could help in the primary care clinic. Another good purpose would be to define a cutoff value to aid in the prognosis of symptomatic patients.

Acknowledgements

The researchers acknowledge the Veterinary Hospital of UPPR for allowing the use of the facilities during the study period and all the staff from the Laboratory of Comparative Cardiology, Department of Veterinary Medicine.

Special gratitude to Vera Hubner, who brought healthy cats and brightened our laboratory with her experience and love for the animals.

Declarations

Funding

None

Conflicts of interest/Competing

The authors do not have any conflicts of interest to declare.

Code or data availability

The datasets generated during and/or analysed during the current study are available from the corresponding author on reasonable request

Authors' Contribution

- Giovana Lais Ruviaro Tuleski, M.Sc: electrocardiographys, echocardiography, blood pressure measurements, analysis of the results, text writing;

- Marcela Wolf, M.Sc: blood pressure measurements, TMAD measurements as co-observer, advice from her practice with TMAD in dogs;

- Maria José Garcia Ribeiro Pscheidt, BSc: animal recruitment, physical examination, blood pressure measurements, literature research;

- Júlio Pereira dos Santos, M.Sc: physical examination, electrocardiographys, blood pressure measurements, research assistance, text revision;

- Marlos Gonçalves Sousa, PhD: research design, guidance, statistical support, analysis of results, final review.

Ethics approval

The study was ethically approved by an established committee as established in the manuscript, protocol number 014/2019 of the Animal Use and Care Committee, and all procedures followed the National Institutes of Health Guide for the Care and Use of Animals of Laboratory.

Consent to participate

Written informed consent was obtained from the owners.

Consent for publication Statement of Animal Ethics

The written consent from owners allowing their cats to participate in the study included permission to publish the echocardiographic images obtained.

References

Abbott JA (2005) Heart rate and heart rate variability of healthy cats in home and hospital environments. J Feline Med Surg 7:195–202. https://doi.org/10.1016/j.jfms.2004.12.003

Abbott JA, MacLean HN (2013) Two-dimensional echocardiographic assessment of the feline left atrium. J Vet Intern Med 20:111–9. https://doi.org/10.1892/0891-6640(2006)20[111:teaotf]2.0.co;2

Acierno MJ, Brown S, Coleman AE, et al (2018) ACVIM consensus statement: Guidelines for the identification, evaluation, and management of systemic hypertension in dogs and cats. J Vet Intern Med 32:1803–1822. https://doi.org/10.1111/jvim.15331

Aloia E, Cameli M, D'Ascenzi F, et al (2016) TAPSE: An old but useful tool in different diseases. Int J Cardiol 225:177–183. https://doi.org/10.1016/j.ijcard.2016.10.009

Asada D, Okumura K, Ikeda K, Itoi T (2018) Tissue Motion Annular Displacement of the Mitral Valve Can Be a Useful Index for the Evaluation of Left Ventricular Systolic Function by Echocardiography in Normal Children. Pediatr Cardiol 39:976–982. https://doi.org/10.1007/s00246-018-1847-2

Bansal M, Cho GY, Chan J, et al (2008) Feasibility and Accuracy of Different Techniques of Two-Dimensional Speckle Based Strain and Validation With Harmonic Phase Magnetic Resonance Imaging. J Am Soc Echocardiogr 21:1318–1325. https://doi.org/10.1016/j.echo.2008.09.021

Binns SH, Sisson DD, Buoscio DA, Schaeffer DJ (1995) Doppler Ultrasonographic, Oscillometric Sphygmomanometric, and Photoplethysmographic Techniques for Noninvasive Blood Pressure Measurement in Anesthetized Cats. J Vet Intern

Med 9:405–414. https://doi.org/10.1111/j.1939-1676.1995.tb03301.x

Black DE, Bryant J, Peebles C, et al (2014) Tissue motion annular displacement of the mitral valve using two-dimensional speckle tracking echocardiography predicts the left ventricular ejection fraction in normal children. Cardiol Young 24:640–648. https://doi.org/10.1017/S1047951113000863

Bland JM, Altman DG (2010) Statistical methods for assessing agreement between two methods of clinical measurement. Int J Nurs Stud 47:931–936. https://doi.org/10.1016/j.ijnurstu.2009.10.001

Buss SJ, Mereles D, Emami M, et al (2012) Rapid assessment of longitudinal systolic left ventricular function using speckle tracking of the mitral annulus. Clin Res Cardiol 101:273–280. https://doi.org/10.1007/s00392-011-0389-x

Caivano D, Rishniw M, Baiona L, et al (2020) Assessment of Longitudinal Left Ventricle Deformation by 2-Dimensional Speckle Tracking Echocardiography Obtained from Different Views in Cats. Vet Sci 7:104. https://doi.org/10.3390/vetsci7030104

Carlsson M, Ugander M, Mosén H, et al (2007) Atrioventricular plane displacement is the major contributor to left ventricular pumping in healthy adults, athletes, and patients with dilated cardiomyopathy. Am J Physiol Circ Physiol 292:H1452–H1459. https://doi.org/10.1152/ajpheart.01148.2006

Chetboul V, Athanassiadis N, Carlos C, et al (2004) Quantification, repeatability, and reproducibility of feline radial and longitudinal left ventricular velocities by tissue Doppler imaging. Am J Vet Res 65:566–572. https://doi.org/10.2460/ajvr.2004.65.566

Chetboul V, Tissier R (2012) Echocardiographic assessment of canine degenerative mitral valve disease. J Vet Cardiol 14:127–148.

https://doi.org/10.1016/j.jvc.2011.11.005

Collier P, Phelan D, Klein A (2017) A Test in Context: Myocardial Strain Measured by Speckle-Tracking Echocardiography. J Am Coll Cardiol 69:1043–1056. https://doi.org/10.1016/j.jacc.2016.12.012

Ferraro AM, Adar A, Ghelani SJ, et al (2020) Speckle tracking echocardiographically-based analysis of ventricular strain in children: an intervendor comparison. Cardiovasc Ultrasound 18:15. https://doi.org/10.1186/s12947-020-00199-x

Fleiss JL (1986) Reliability of Measurement. John Wiley & Sons, Inc

Häggström J, Andersson O, Falk T, et al (2016) Effect of Body Weight on Echocardiographic Measurements in 19,866 Pure-Bred Cats with or without Heart Disease. J Vet Intern Med 30:1601–1611. https://doi.org/10.1111/jvim.14569

Hill RC, Scott KC (2004) Energy requirements and body surface area of cats and dogs. J Am Vet Med Assoc 225:689–694. https://doi.org/10.2460/javma.2004.225.689

Hoit BD (2017) Evaluation of Left Atrial Function: Current Status. Struct Hear 1:109–120. https://doi.org/10.1080/24748706.2017.1353718

Hu K, Liu D, Herrmann S, et al (2013) Clinical implication of mitral annular plane systolic excursion for patients with cardiovascular disease. Eur Heart J Cardiovasc Imaging 14:205–212. https://doi.org/10.1093/ehjci/jes240

Johnson C, Kuyt K, Oxborough D, Stout M (2019) Practical tips and tricks in measuring strain, strain rate and twist for the left and right ventricles. Echo Res Pract 6:R87–R98. https://doi.org/10.1530/ERP-19-0020

Klaeboe LG, Edvardsen T (2019) Echocardiographic assessment of left ventricular systolic function. J Echocardiogr 17:10–16. https://doi.org/10.1007/s12574-018-

0405-5

Kocica MJ, Corno AF, Carreras-Costa F, et al (2006) The helical ventricular myocardial band: global, three-dimensional, functional architecture of the ventricular myocardium. Eur J Cardio-thoracic Surg 29:. https://doi.org/10.1016/j.ejcts.2006.03.011

Koffas H, Dukes-McEwan J, Corcoran BM, et al (2006) Pulsed tissue Doppler imaging in normal cats and cats with hypertrophic cardiomyopathy. J Vet Intern Med 20:65–77. https://doi.org/10.1892/0891-6640(2006)20[65:PTDIIN]2.0.CO;2

Koo TK, Li MY (2016) A Guideline of Selecting and Reporting Intraclass Correlation Coefficients for Reliability Research. J Chiropr Med 15:155–163. https://doi.org/10.1016/j.jcm.2016.02.012

Kusunose K, Penn MS, Zhang Y, et al (2012) How similar are the mice to men? Between-species comparison of left ventricular mechanics using strain imaging. PLoS One 7:. https://doi.org/10.1371/journal.pone.0040061

Kusunose K, Zhang Y, Mazgalev TN, et al (2013) Left ventricular strain distribution in healthy dogs and in dogs with tachycardia-induced dilated cardiomyopathy. Cardiovasc Ultrasound 11:43. https://doi.org/10.1186/1476-7120-11-43

Lakkatta EG (2004) Beyond Bowditch: The convergence of cardiac chronotropy and inotropy. Cell Calcium 35:629–642. https://doi.org/10.1016/j.ceca.2004.01.017

Liu L, Tuo S, Zhang J, et al (2014) Reduction of left ventricular longitudinal global and segmental systolic functions in patients with hypertrophic cardiomyopathy: Study of two-dimensional tissue motion annular displacement. Exp Ther Med 7:1457–1464. https://doi.org/10.3892/etm.2014.1617

Luis SA, Chan J, Pellikka PA (2019) Echocardiographic Assessment of Left Ventricular Systolic Function: An Overview of Contemporary Techniques,

Including Speckle-Tracking Echocardiography. Mayo Clin Proc 94:125–138. https://doi.org/10.1016/j.mayocp.2018.07.017

Lunkenheimer PP, Redmann K, Florek J, et al (2004) The forces generated within the musculature of the left ventricular wall. Heart 90:200–207. https://doi.org/10.1136/hrt.2003.011650

Mauermann E, Bouchez S, Bove T, et al (2020) Rapid, Single-View Speckle-Tracking–Based Method for Examining Left Ventricular Systolic and Diastolic Function in Point of Care Ultrasound. J Ultrasound Med 39:2151–2164. https://doi.org/10.1002/jum.15324

Mizuguchi Y, Oishi Y, Miyoshi H, et al (2008) The Functional Role of Longitudinal, Circumferential, and Radial Myocardial Deformation for Regulating the Early Impairment of Left Ventricular Contraction and Relaxation in Patients With Cardiovascular Risk Factors: A Study With Two-Dimensional Strain Im. J Am Soc Echocardiogr 21:1138–1144. https://doi.org/10.1016/j.echo.2008.07.016

Mondillo S, Galderisi M, Ballo P, Marino PN (2006) Left Ventricular Systolic Longitudinal Function: Comparison Among Simple M-Mode, Pulsed, and M-Mode Color Tissue Doppler of Mitral Annulus in Healthy Individuals. J Am Soc Echocardiogr 19:1085–1091. https://doi.org/10.1016/j.echo.2006.04.005

Negishi K, Lucas S, Negishi T, et al (2013) What is the Primary Source of Discordance in Strain Measurement Between Vendors: Imaging or Analysis? Ultrasound Med Biol 39:714–720. https://doi.org/10.1016/j.ultrasmedbio.2012.11.021

Penk JS, Zaidi SJH, Lefaiver CA, et al (2018) Tissue Motion Annular Displacement Predicts Mortality/Transplant After the Bidirectional Glenn. World J Pediatr Congenit Heart Surg 9:171–176. https://doi.org/10.1177/2150135117742650

Popovic ZB, Thomas JD (2017) Assessing observer variability: A user's guide. Cardiovasc Diagn Ther 7:317–324. https://doi.org/10.21037/cdt.2017.03.12

Quimby J, Gowland S, Carney HC, et al (2021) 2021 AAHA/AAFP Feline Life Stage Guidelines. J Feline Med Surg 57:51–72. https://doi.org/10.5326/JAAHA-MS-7189

Ramlogan S, Aly D, France R, et al (2020) Reproducibility and Intervendor Agreement of Left Ventricular Global Systolic Strain in Children Using a Layer-Specific Analysis. J Am Soc Echocardiogr 33:110–119. https://doi.org/10.1016/j.echo.2019.08.004

Riffel JH, Mereles D, Emami M, et al (2015) Prognostic significance of semiautomatic quantification of left ventricular long axis shortening in systemic light-chain amyloidosis. Amyloid 22:45–53. https://doi.org/10.3109/13506129.2014.992515

Rishniw M, Erb HN (2000) Evaluation of four 2-dimensional echocardiographic methods of assessing left atrial size in dogs. J Vet Intern Med 14:429–435. https://doi.org/10.1111/j.1939-1676.2000.tb02252.x

Sahn DJ, DeMaria A, Kisslo J, Weyman A (1978) Recommendations regarding quantitation in M-mode echocardiography: Results of a survey of echocardiographic measurements. Circulation 58:1072–1083. https://doi.org/10.1161/01.CIR.58.6.1072

Santarelli G, Baron Toaldo M, Bouvard J, et al (2019) Variability among strain variables derived from two-dimensional speckle tracking echocardiography in dogs by use of various software. Am J Vet Res 80:347–357. https://doi.org/10.2460/ajvr.80.4.347

Schober KE, Chetboul V (2015) Echocardiographic evaluation of left ventricular diastolic function in cats: Hemodynamic determinants and pattern recognition. J

Vet Cardiol 17:S102–S133. https://doi.org/10.1016/j.jvc.2015.02.002

Schober KE, Fuentes VL (2001) Mitral annulus motion as determined by M-mode echocardiography in normal dogs and dogs with cardiac disease. Vet Radiol Ultrasound 42:52–61. https://doi.org/10.1111/j.1740-8261.2001.tb00904.x

Schober P, Schwarte LA (2018) Correlation coefficients: Appropriate use and interpretation. Anesth Analg 126:1763–1768. https://doi.org/10.1213/ANE.0000000000002864

Seo J-S, Kim D-H, Kim W-J, et al (2010) Peak systolic velocity of mitral annular longitudinal movement measured by pulsed tissue Doppler imaging as an index of global left ventricular contractility. Am J Physiol Heart Circ Physiol 298:H1608-15. https://doi.org/10.1152/ajpheart.01231.2009

Sharma JB, Deora S, Choudhary R, Kaushik A (2021) Comparison of mitral annular displacement and global longitudinal strain imaging for predicting significant coronary atherosclerotic disease in patients of chronic stable angina pectoris. Int J Cardiovasc Imaging 37:861–870. https://doi.org/10.1007/s10554-020-02058-2

Silva AC, Muzzi RAL, Oberlender G, et al (2013) Longitudinal strain and strain rate by two-dimensional speckle tracking in non-sedated healthy cats. Res Vet Sci 95:1175–1180. https://doi.org/10.1016/j.rvsc.2013.07.020

Simpson KE, Gunn-Moore DA, Shaw DJ, et al (2009) Pulsed-wave Doppler tissue imaging velocities in normal geriatric cats and geriatric cats with primary or systemic diseases linked to specific cardiomyopathies in humans, and the influence of age and heart rate upon these velocities. J Feline Med Surg 11:293–304. https://doi.org/10.1016/j.jfms.2008.08.003

Spalla I, Boswood A, Connolly DJ, Luis Fuentes V (2019) Speckle tracking echocardiography in cats with preclinical hypertrophic cardiomyopathy. J Vet

Intern Med 33:1232–1241. https://doi.org/10.1111/jvim.15495

Spalla I, Payne JRR, Borgeat K, et al (2017) Mitral Annular Plane Systolic Excursion and Tricuspid Annular Plane Systolic Excursion in Cats with Hypertrophic Cardiomyopathy. J Vet Intern Med 31:691–699. https://doi.org/10.1111/jvim.14697

Sugimoto K, Aoki T, Fujii Y (2021) Longitudinal evaluation of cardiovascular function in six healthy cats aged 1–8 years. J Feline Med Surg 23:98–104. https://doi.org/10.1177/1098612X20932255

Suzuki R, Mochizuki Y, Yoshimatsu H, et al (2019a) Layer-specific myocardial function in asymptomatic cats with obstructive hypertrophic cardiomyopathy assessed using 2-dimensional speckle-tracking echocardiography. J Vet Intern Med 33:37–45. https://doi.org/10.1111/jvim.15339

Suzuki R, Mochizuki Y, Yuchi Y, et al (2019b) Assessment of myocardial function in obstructive hypertrophic cardiomyopathy cats with and without response to medical treatment by carvedilol. BMC Vet Res 15:1–8. https://doi.org/10.1186/s12917-019-2141-0

Teraguchi I, Hozumi T, Emori H, et al (2021) Prognostic value of tissue-tracking mitral annular displacement by speckle-tracking echocardiography in asymptomatic aortic stenosis patients with preserved left ventricular ejection fraction. J Echocardiogr 19:95–102. https://doi.org/10.1007/s12574-020-00490-w

Teraguchi I, Hozumi T, Takemoto K, et al (2019) Assessment of decreased left ventricular longitudinal deformation in asymptomatic patients with organic mitral regurgitation and preserved ejection fraction using tissue-tracking mitral annular displacement by speckle-tracking echocardiography. Echocardiography 36:678–686. https://doi.org/10.1111/echo.14290

Thomas WP, Gaber CE, Jacobs GJ, et al (1994) Recommendations for Standards in Transthoracic Two-Dimensional Echocardiography in the Dog and Cat. Vet Radiol Ultrasound 35:173–178. https://doi.org/10.1111/j.1740-8261.1994.tb01588.x

Tidholm A, Ljungvall I, HÃ¶glund K, et al (2009) Tissue Doppler and Strain Imaging in Dogs with Myxomatous Mitral Valve Disease in Different Stages of Congestive Heart Failure. J Vet Intern Med 23:1197–1207. https://doi.org/10.1111/j.1939-1676.2009.0403.x

Trivedi SJ, Altman M, Stanton T, Thomas L (2019) Echocardiographic Strain in Clinical Practice. Hear Lung Circ 28:1320–1330. https://doi.org/10.1016/j.hlc.2019.03.012

Tsang W, Ahmad H, Patel AR, et al (2010) Rapid Estimation of Left Ventricular Function Using Echocardiographic Speckle-Tracking of Mitral Annular Displacement. J Am Soc Echocardiogr 23:511–515. https://doi.org/10.1016/j.echo.2010.03.003

van Dalen BM, Bosch JG, Kauer F, et al (2009) Assessment of Mitral Annular Velocities by Speckle Tracking Echocardiography versus Tissue Doppler Imaging: Validation, Feasibility, and Reproducibility. J Am Soc Echocardiogr 22:1302–1308. https://doi.org/10.1016/j.echo.2009.08.004

Vinereanu D, Khokhar A, Fraser AG (1999) Reproducibility of pulsed wave tissue Doppler echocardiography. J Am Soc Echocardiogr 12:492–499. https://doi.org/10.1016/S0894-7317(99)70086-6

Wolf M, Lucina SB, Silva VBC, et al (2021) Assessment of longitudinal systolic function using tissue motion annular displacement in dogs with degenerative mitral valve disease. J Vet Cardiol 38:44–58.

https://doi.org/10.1016/j.jvc.2021.10.004

Wolf M, Lucina SBSB, Brüler BCBC, et al (2018) Assessment of longitudinal systolic function using tissue motion annular displacement in healthy dogs. J Vet Cardiol 20:. https://doi.org/10.1016/j.jvc.2018.04.004

Yang H, Marwick TH, Fukuda N, et al (2015) Improvement in Strain Concordance between Two Major Vendors after the Strain Standardization Initiative. J Am Soc Echocardiogr 28:642–648.e7. https://doi.org/10.1016/j.echo.2014.12.009

Yingchoncharoen T, Agarwal S, Popović ZB, Marwick TH (2013) Normal Ranges of Left Ventricular Strain: A Meta-Analysis. J Am Soc Echocardiogr 26:185–191. https://doi.org/10.1016/j.echo.2012.10.008

Zacà V, Ballo P, Galderisi M, Mondillo S (2010) Echocardiography in the assessment of left ventricular longitudinal systolic function: current methodology and clinical applications. Heart Fail Rev 15:23–37. https://doi.org/10.1007/s10741-009-9147-9

Zois NE, Tidholm A, Nägga KM, et al (2012) Radial and Longitudinal Strain and Strain Rate Assessed by Speckle-Tracking Echocardiography in Dogs with Myxomatous Mitral Valve Disease. J Vet Intern Med 26:1309–1319. https://doi.org/10.1111/j.1939-1676.2012.01017.x

CAPÍTULO 2 - **Influência da solução oftálmica de timolol 0,5% na função cardíaca de gatos saudáveis**

Giovana L. R. Tuleski[a], M.Sc.; Maria Jose Garcia Ribeiro Pscheidt[b], B.Sc.; Júlio Pereira dos Santos[a], M.Sc.; Marlos Gonçalves Sousa[a], Ph.D.

[a]Laboratory of Comparative Cardiology, Department of Veterinary Medicine, Federal University of Paraná (UFPR), Rua dos Funcionários, 1540, CEP 80035-050, Curitiba, Paraná, Brazil.

[b]Autonomous veterinarian, Curitiba, Paraná, Brazil

Corresponding author name: Giovana Lais Ruviaro Tuleski, MSc - ORCID 0000-0002-0817-3470

Contact details: Phone number 55 41 99669-5473, e-mail: gtuleski@yahoo.com.br

Publicado na Revista *Journal of Feline Medicine and Surgery* no dia 26 de abril de 2022, cidtado a seguir:

Tuleski, Giovana LR, et al. "Timolol 0.5% ophthalmic solution influences cardiac function in healthy cats." Journal of Feline Medicine and Surgery (2022): 1098612X221083372.

Abstract

Objectives: Ascertain the effect of a drop of timolol ophthalmic solution 0.5% on the systolic function of the left ventricle (LV) and left atrium (LA). Confirm if timolol helps the diastolic function appraisal by reducing the heart rate and separating the transmitral outflow waves from tissue Doppler imaging (TDI).

Methods: A total of 41 client-owned healthy cats underwent two echocardiograms 20 minutes apart. The timolol group (33 cats) received a drop of timolol solution after the first exam. Standard and speckle-tracking echocardiography evaluated the LV and LA function of both groups at the two-time points evaluated.

Results: Timolol reduced HR (19%), fractional shortening from LV (20.3%) and LA (16.6%). The septal S' decreased 51% (7.7 to 5.2 cm/s) and the lateral S’ dropped 43.1% (7.3 to 5.1 cm/s). Most longitudinal techniques did not change after timolol, as the mitral annular plane systolic excursion from the interventricular annulus (MAPSE IVS), tricuspid annular plane systolic excursion (TAPSE), LV longitudinal strain, and LV tissue motion annular displacement. The isovolumic relaxation time increased by 15.2% (54 to 64.6 ms), with most cats presenting this variable above the reference (> 60 ms). Timolol did not support diastolic assessment, enabling evaluation in only two of eleven cats when using lateral TDI and one from nine cats using septal TDI. Regarding side effects, miosis occurred in 18 cats (54.5%).

Conclusions and relevance: Timolol reduced systolic function, decreasing standard echocardiographic variables. As for the diastolic evaluation, although timolol decreased the HR, it did not separate the mitral diastolic waves as expected.

Keywords: beta-blocker, tissue motion annular displacement, speckle tracking, atrial function

Introduction

An echocardiogram in cats usually activates the fear response, causing an increase in heart rate (HR)[1,2], systemic blood pressure (SBP)[3] and respiratory rate. Tachycardia is an undesirable consequence of stress, as it can impede or complicate the diastolic evaluation[4]. At lower HR, there are two transmitral outflow waves: the E wave, which corresponds to the filling of the left ventricle (LV) in early diastole, followed by the A wave, the peak resulting from the atrial systole[5,6]. In most cats with normal diastolic function, E is greater than A (E/A>1). An HR above 170-180 bpm during echocardiography in cats leads to fusion of the mitral outflow waves (EAfus). The same occurs with tissue Doppler imaging (TDI), the summation of waves with tachycardia (E'A'fus). This technique reflects the myocardial velocity instead of the blood movement by placing the Doppler gate at the mitral annulus (IVS or FW). The E' wave, called early diastolic mitral annular velocity, is produced during the early diastole of the LV, while A' reflects the annulus movement during the left atrium contraction[5]. Normally, E' is expected to be greater than A', although a slightly inverted ratio (E'/A' between 0.8 and 1.0) can be considered normal in cats with high HR[4].

Fused waves do not allow diastolic assessment, which is essential for diagnosis, as the most prevalent heart diseases in cats, cardiomyopathies with hypertrophic or restrictive phenotypes, start with impairment of diastolic function[4,7,8]. It is highly recommended to evaluate the diastolic function and classify its pattern using a combination of spectral Doppler and TDI. Precocious detection of dysfunction can help diagnose early-stage disease. In cats that have already developed signs of congestive heart failure or arterial thromboembolism, that is, those classified as stage C, diastolic information helps establish a prognosis[9].

An alternative to avoid summation and enable the diastolic assessment is applying a vagal manoeuvre at the time of mitral outflow Doppler or TDI acquisition[10]. It requires the presence of an assistant to perform the parasympathetic stimulation correctly at the appropriate moment. Another option is to administer timolol ophthalmic solution to block the sympathetic tone and decrease the HR, separating the transmitral and TDI waves[11]. The topical application of timolol has a systemic absorption[12,13], reducing the HR when administered in cats alone[11] or associated with topically applied carbonic anhydrase inhibitors, such as dorzolamide or brinzolamide[14].

Timolol maleate is the most frequently used drug in managing open-angle glaucoma[15], although long-term treatment may have adverse effects in humans, such as low systolic or diastolic blood pressure[16]. A nonselective beta-adrenergic antagonist such as timolol may reduce the heart´s contraction force[17,18], compromising the commonly used systolic variables. In consequence, it may also modify the left atrium (LA) activity, directly affected by the LV[19].

This study assumed that timolol would alter cardiac function in cats undergoing an echocardiogram. In this case, the objective was to determine how much a single drop of timolol interferes with the systolic variables obtained by standard and speckle-tracking echocardiography. Furthermore, it was expected that the echocardiographic indices of the control group would not change after twenty minutes of waiting and second handling, even though it could be stressful for the cats.

Materials and Methods

Animals

This prospective longitudinal observational study recruited client-owned healthy cats between May and July 2019. Before enrollment, all cats underwent a thorough physical examination, SBP measurement with Doppler, electrocardiography (ECG), and standard transthoracic echocardiography.

The Institutional Animal Care and Use Committee (protocol 014/2019) previously approved all the procedures complied with the National Institutes of Health Guide for the Care and Use of Laboratory Animals. Owners were required to formally agree to participate in this research by signing the informed consent form.

Age limitation was adopted to avoid possible changes in drug metabolism in young or old animals, excluding animals younger than one year or older than 14 years. Cats with elevated SBP prior to the first echocardiogram (>160 mmHg) did not participate, as did any cat with a history or signs of heart disease or other chronic illness or who had received any treatment in the past six months.

Echocardiography

All cats underwent two echocardiographic examinations with only gentle restraint and no sedation. Positioning followed the recommendations of the Echocardiography Committee of the Specialty of Cardiology of the American College of Veterinary Internal Medicine[20]. The same operator (G.L.R.T.) performed all exams and measurements.

A drop of 0.5% timolol ophthalmic solution containing approximately 0.17 mg of timolol (1 millimetre = 30 drops) was instilled at the left eye immediately after the first echocardiogram (Control Timolol). A second echocardiogram (Timolol) was

performed twenty minutes later, following the same protocols mentioned. The control group consisted of 8 cats not receiving the timolol eyedrop, submitted to two echocardiograms with 20 minutes between them: "Control 1" and "Control 2", respectively.

Left ventricle systolic function

LV M-mode measurements at the papillary level were determined as described by other authors[21], allowing the calculation of the most common systolic variables, such as fractional shortening (FS) and ejection fraction (EF). The end-diastolic and end-systolic LV diameters were measured using a leading edge-to-leading edge technique, with a simultaneous ECG permitting to exactly distinguish the cardiac phases. The cutoff point for hypertrophic cardiomyopathy (HCM) was considered to be 5.5 mm for any image of the LV[22], including the IVS thickness in the left ventricular outflow tract view from the right parasternal window.

Evaluating the longitudinal systolic function of the LV required the acquisition of apical 4-chamber (AP4) and 2-chamber (AP2) images obtained from the left parasternal window. At least five cardiac cycles were recorded to allow off-line calculation of the tissue motion annular displacement (TMAD) measures and the longitudinal strain (LSt) values, considering the mean of AP4 and AP2 values as global indices. In addition, AP4 was applied to measure the mitral annular plane systolic excursion (MAPSE) from the interventricular septum (IVS) annulus and free wall (FW) annulus, the tricuspid annular plane systolic excursion (TAPSE), and the mitral annular velocities with the gate of investigation on the IVS and FW annulus, as described elsewhere[5,23].

Both LV TMAD and LV LSt required the aortic valve closure time, measured from the apical 5-chamber image. It corresponds to the time, in milliseconds, from the beginning of the QRS complex to the end of the aortic valve spectra obtained with the pulsed Doppler gate positioned distally to the valve[24].

The hinge points of mitral valve leaflets (septal and lateral) and the LV apex epicardial region were the three regions of interest (ROIs) used to calculate the LV LSt[25] (Figure 1a), which was measured automatically by the equipment software (QLAB ACMQ - Auto Cardiac Motion Quantification). Manual corrections were made whenever the automatic myocardial tracking was obviously incorrect. For LV TMAD, the same three ROIs were defined (Figure 1b). The displacement of both annuli towards the apex (in mm) was automatically calculated. Also, the software defined a virtual midpoint between the two annular ROIs (LV MP TMAD) and calculated its displacement towards the LV apex (in mm), as well as the proportional displacement of that midpoint concerning the total length of the LV (LV MP% TMAD).

Left atrium function

The LA FS was estimated based on the minimum and maximum LA diameter from the right parasternal short-axis view image at the aortic valve level, using anatomic M-mode[26]. The ratio between LA and aorta was measured at the maximum LA diameter, right after the T wave from the ECG, as described before[27]. The AP4 was the image used to measure LA dimensions at three different moments based on the LA cycle: before P wave, before QRS complex, and after T wave, enabling later calculation of the passive (pEF), active (aEF), and complete (cEF) LA ejection fraction (EF) as detailed elsewhere[28].

To calculate LA LSt and LA TMAD, the first two ROIs had the same position as the LV at the mitral leaflet hinge points, while the third ROI was defined at the cranial inner edge of the LA. The total displacement (LA D TMAD) between the maximal negative and positive positions was the average of the displacements documented individually for each of the two annular points. The systolic displacement (LA S TMAD) was the average movements of the two ROIs between diastasis and the maximal positive position. In humans, diastasis is easily recognized by a plateau wave[29] (Figure 1c). However, as the mean HR in cats is approximately three times higher, a plateau phase might not happen. In these cases, it is possible to determine the diastasis based exclusively on the simultaneous ECG, pausing the marker immediately before the P wave (Figure 1d).

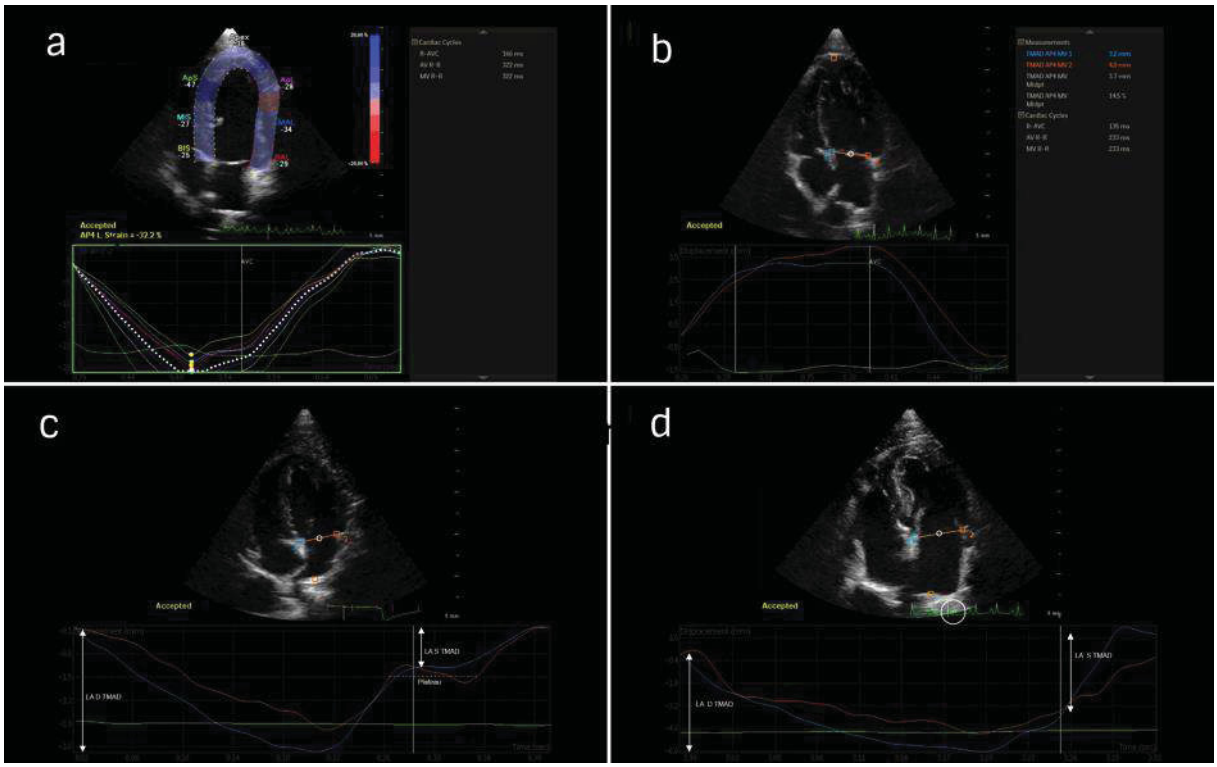

Apical four-chamber (AP4) images demonstrating (a) longitudinal strain of the left ventricle (LV); (b) tissue motion annular displacement of the LV; (c) tissue motion annular displacement of the left atrium (LA) in a patient with low heart rate (150 bpm) and a visible plateau (dashed line); and (d) tissue motion annular displacement of the LA in a cat with faster heart rate (186 bpm), with diastasis determined by pausing the electrocardiogram (ECG) cursor just before the P wave on the ECG (white circle). Tissue motion annular displacement (TMAD) AP4 MV1 (in blue) describes the displacement of mitral septal annulus towards the LV apex; TMAD AP4 MV2 (in orange) is the displacement of mitral lateral annulus towards the LV apex; TMAD AP4 MV midpt (in white) signifies the displacement of a virtual point determined in between the septal and lateral hinge points of mitral annulus towards the LV apex. In (c) and (d), the larger arrows designate the total displacement of the mitral annulus towards the farthest point of the LA (LA D TMAD); the shorter ones represent systolic displacement to the same point (LA S TMAD)

Statistical analysis

The study aimed to determine whether timolol would cause differences in the cats' echocardiographic variables after its ophthalmic application. The same group of animals was compared before and after application (paired quantitative variable). The sample size was calculated using GPower 3.1.9.4[30] with an expected effect of 80%, a sampling power of 95% and an error of 5% for quantitative measurements

and using two dependent samples, reaching the total number of 23 cats for the Timolol group.

Analysis was conducted in R 4.0.5 (R Core Team 2021)[31]. Initially, a descriptive analysis of the data was accomplished with an estimate of the mean, median, standard deviation, minimum, maximum, and interquartile range of the quantitative variables and simple and relative frequencies of the qualitative variables.

The Shapiro-Wilk normality test was performed to determine the parametric and non-parametric approaches to evaluate the quantitative variables. For variables with normal distribution, the difference between two independent groups was verified with Student's t-test or paired t-test for dependent groups (cross-over). For variables without normal distribution, this difference was verified using the Mann-Withney or Wilcoxon U test. P values lower than 0.05 were considered significantly different. Finally, Spearman's correlation was adopted to analyze the relationship between HR and body weight (BW) for both timolol and control groups.

Results

Forty-one client-owned healthy cats enrolled in the study. The timolol's group was composed of thirty-three cats (6.1 y [1-13y]; 5.1 kg [2.1-11 kg]; 18 females). It included Persian (n=2), Maine coon (n=1), Siamese (n=1), and mixed breed cats (n=29). Eight mixed breed cats participated as control group (8.8 y [3-13y]; 4.5 kg [2.1-7.6 kg]; 6 females).

Most data were normally distributed, except BW, HR, LA and aorta measurements at the right transversal image, isovolumic relaxation time (IVRT), TDI velocities, MAPSE IVS, MAPSE FW and TAPSE.

The mean SBP of the control groups (Control Timolol and Control 1) did not differ significantly between them, presenting a mean of 140 mmHg. All animals had normal sinus rhythm on ECG recording.

The echocardiographic indices of the control group presented no significant differences between the two exams performed after a twenty-minute interval (Control 1 and Control 2). On the contrary, the echocardiogram of cats after timolol administration showed differences in many indices, as shown in Table 1 and Figure 2. Figure 3 displays the variations in some of the variables affected by timolol (Control timolol and timolol).

Table 1 - Standard and speckle-tracking echocardiographic variables in the Timolol Group, before the drug administration (Timolol Control) and after (Timolol), and in the Control Group, before (Control 1) and after (Control 2) the twenty-minutes interval

Parameters	Control Timolol		Timolol		p-value* Control timolol x Timolol	Control 1		Control 2		p-value* Control 1 x Control 2
	M	SD	M	SD		M	SD	M	SD	
HR	**190,8**	26,1	**160,3**	18	**<0,001**	212,5	20,7	210,6	25,7	0,832
LAD	12,9	1,5	13,3	1,5	0,251	13,1	<	13,4	1	0,637
LA FS	**35,2**	7	**30,2**	5,3	**0,02**	34,1	6,7	38	4,3	0,225
IVSd	3,3	0,7	3,5	0,6	0,34	3,7	0,8	3,4	0,6	0,445
LVIDd	15,5	2,1	16,4	2	0,093	15,5	1,5	14,3	1,9	0,139
LVPWd	3,7	0,8	3,8	0,7	0,9	3,6	0,7	3,6	0,5	0,939
IVSs	6,2	1,4	5,8	1,3	0,374	7,1	1,4	6,4	1	0,4
LVIDs	**7,6**	1,6	**9,4**	1,4	**<0,001**	6,6	1,1	6,1	1,3	0,101
LVPWs	6,1	1,1	5,9	1,2	0,567	6,4	0,9	6,3	0,6	1
FS	**51**	7,8	**42,4**	5,6	**<0,001**	60,4	9,3	58,3	6,4	0,944
EF	**83,3**	6,5	**76,4**	5,8	**<0,001**	89,7	3,3	90,1	3,4	0,288
A flow	**89,9**	17,1	**74,1**	13,6	**<0,001**	92,2	20,8	97,3	12,9	0,637
P flow	**83,8**	16,6	**65,9**	15,2	**<0,001**	82	18,1	78	8,1	0,843
Sep S'	**7,7**	2	**5,1**	0,9	**<0,001**	8,3	1,4	7,9	1,4	0,554
Lat S'	**7,3**	1,7	**5,1**	0,6	**<0,001**	7,1	0,7	6,9	1,2	0,64
IVRT	**54,8**	8,5	**64,6**	9,5	**0,001**	54	8,7	54,5	5,8	0,932
MAPSE FW	**4,5**	0,7	**4,1**	0,7	**0,01**	4,9	1,4	4,6	1	0,621
MAPSE IVS	4,4	1	3,9	0,9	0,064	4,7	0,8	4,5	0,8	0,546
TAPSE	8	1,8	7,5	2,1	0,362	8,8	0,7	8,6	1,5	0,742
Parameters from AP4										
4C LV LSt	29,6	5,2	28,3	5,9	0,325	24,4	4,3	25,4	4,1	0,723
4C LV MP TMAD	4	0,9	4	0,8	0,855	4,3	0,6	4	0,8	0,335
4C LV MP% TMAD	17,2	3,4	16,1	3,1	0,236	17,3	3	16,2	2,4	0,363
4C LA LSt	**36,2**	6,6	**33,1**	6,9	**0,052**	33,7	7,2	37,2	7,5	0,261
4C LA D TMAD	2.5	1.2	2.2	1.1	0.618	2.7	1.3	2.3	1.1	0.880
4C LA S TMAD	2.5	1.7	2	1.3	0,415	2.5	1.3	3.2	2.3	0,47
4C LA cEF	**57,8**	6,3	**52,8**	6,4	**0,011**	65,1	4,8	62,2	4,8	0,283
4C LA aEF	43	7,6	39,4	7,6	0,094	43,5	31,1	50,4	9,1	0,812
4C LA pEF	25,8	8,4	21,8	8,4	0,194	21,9	5,9	22,7	10,2	0,893
Parameters from AP2										
2C LV LSt	31,5	5,5	30,7	7,5	0,616	27,1	3	24,6	4,1	0,096
2C LV MP TMAD	4,2	1	4,2	1	0,858	4,6	0,8	4	0,5	0,169
2C LV MP% TMAD	17,6	4,3	17	4,1	0,492	18,2	2,5	15,7	3	0,155
2C LA LSt	**37,2**	7,6	**32,9**	7,7	**0,049**	38,3	7,6	35,7	7	0.536
2C LA D TMAD	3,8	1,1	4	1,2	0,397	4	1,1	4,8	1,7	0.303
2C LA S TMAD	2.3	1.3	2.5	1.1	0.188	3.2	1,7	2.6	0.6	0.234
2C LA cEF	**56,8**	5	**51,7**	6,4	**0,001**	63	4,5	60,8	4,9	0,074
2C LA aEF	44	8.4	40.7	8.9	0.006	52.7	7.5	48.7	8.1	0.594
2C LA pEF	22,3	8	21,1	10,6	1	25,8	5,1	21,6	10,8	0,296
Global parameters										
Global LV LSt	33,9	3,9	31,8	5,4	0,092	25,7	2,7	25	3,3	0,686
Global LV MP TMAD	4,1	0,8	4,1	0,7	0,918	4,4	0,4	4	0,4	0,076
Global LV MP% TMAD	17,5	3	16,6	2,9	0,287	17,8	2,3	15,9	2,1	0,167
Global LA LSt	**36,9**	4,4	**32,9**	6,1	**0,004**	36,4	6,5	36,5	4,2	0,971
Global LA D TMAD	2,4	0,6	2,4	0,7	0.885	4,2	0,9	4,4	1,1	0,876
Global LA S TMAD	4	0,8	4,1	0,8	0.747	2,7	1,6	1,9	0,4	0.239
Global LA cEF	**57,4**	4,6	**52,7**	4,2	**0,001**	64	3,5	61,5	4,5	0,132
Global LA aEF	43,5	5,9	39	5,5	0,006	46,7	14,9	49,9	7,5	0,594
Global LA pEF	24,2	7,4	22,3	6,5	0,434	23,8	3	22,1	9,8	0,716

*P-value<0.05

HR = heart rate; LAD = left atrium diameter; LA FS = left atrium fractional shortening; IVSd = interventricular septum thickness end diastole; LVIDd = left ventricular internal dimension at end-diastole;

LVPWd = left ventricular posterior wall thickness at end-diastole; IVSs = interventricular septum thickness at end-systole; LVIDs = left ventricular internal dimension at end-systole; LVPWs = left ventricular posterior wall thickness at end-systole; FS = fractional shortening; EF = ejection fraction; IVRT = isovolumic relaxation time; MAPSE = mitral annular plane systolic excursion; FW = free wall; IVS = intraventricular septum; TAPSE = tricuspid annular plane systolic excursion; AP4 = apical four-chamber; LV = left ventricle; LSt = longitudinal strain; MP = midpoint (virtual midpoint determined between the septal and lateral points of the mitral annulus); TMAD = tissue motion annular displacement; LA D TMAD = total displacement of the mitral annulus towards the farthest point of the left atrium; LA S TMAD = systolic displacement of the mitral annulus towards the farthest point of the left atrium; LA = left atrium; cEF = complete ejection fraction; aEF = active ejection fraction; pEF = passive ejection fraction; AP2 = apical two-chamber

Figure 2 - Percentage of change in echocardiographic indices significantly affected by timolol administration

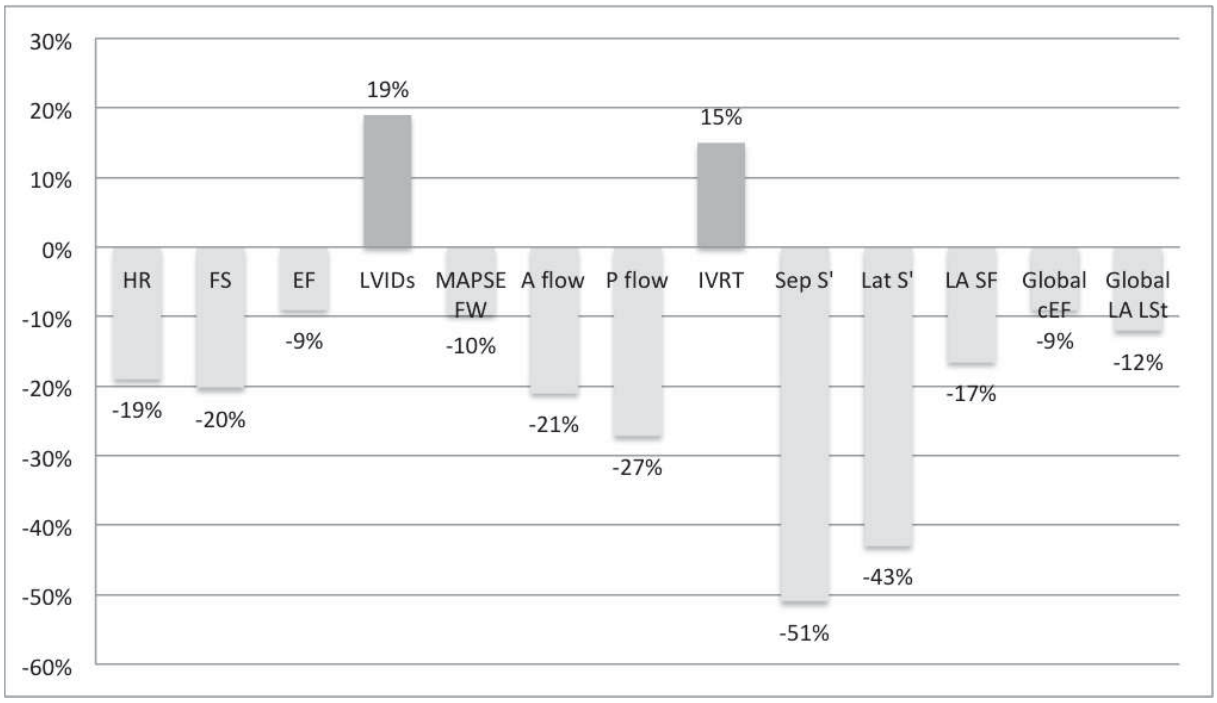

HR= heart rate; FS=fractional shortening of the left ventricle; EF= ejection fraction of the left ventricle; LVIDs= left ventricular internal dimension at end-systole; MAPSE FW= mitral annular plane systolic excursion measured at the free wall annulus; A flow= peak velocity of aortic valve flow; P flow = peak velocity of pulmonary valve flow; Sep S'= peak velocity of systolic mitral annular motion as determined by pulsed wave Doppler at the septal annulus; Lat S'= peak velocity of systolic mitral annular motion as determined by pulsed wave Doppler at the lateral annulus; LA FS= shortening fraction of the left atrium; Global cEF= complete ejection fraction of the left atrium; Global LA LSt= global longitudinal strain of the left atrium

Figure 3 - Boxplots representing echocardiographic indices altered significantly after timolol administration. Comparison between the first and second echocardiograms in the timolol group (control timolol and timolol) and the control group (control 1 and control 2).

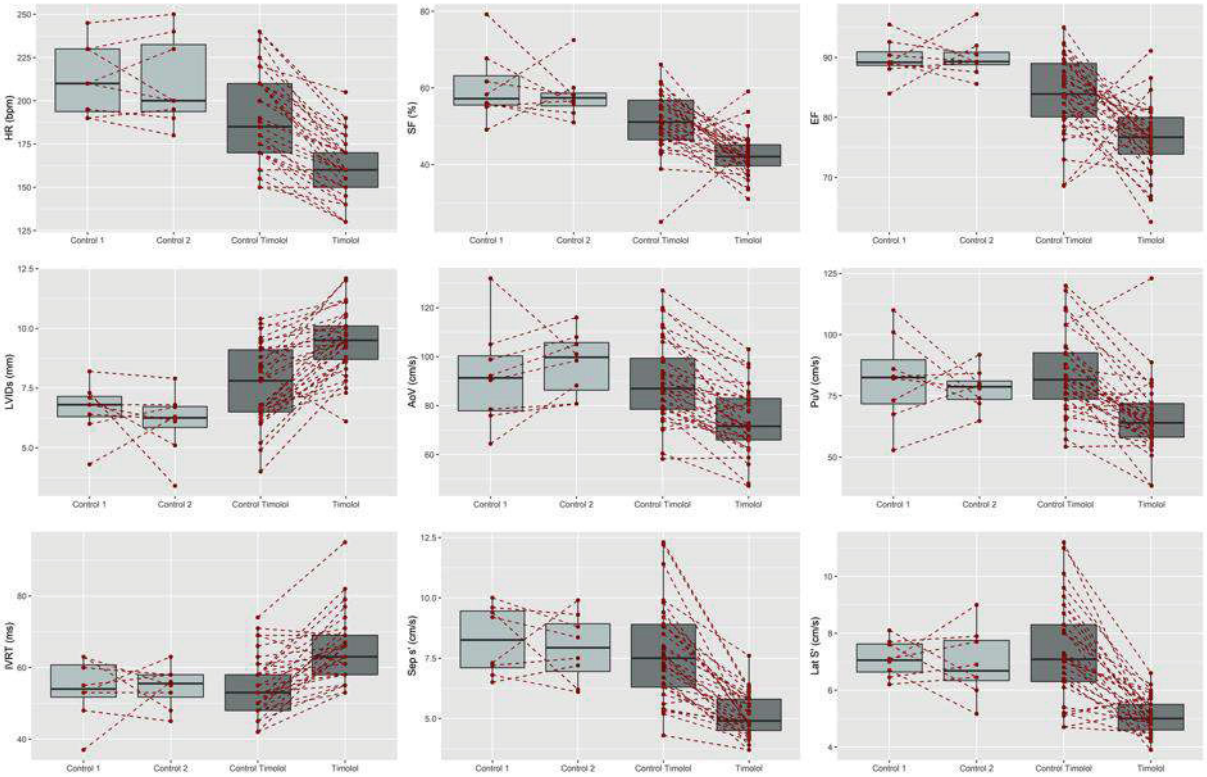

HR = heart rate; bpm = beats per min; SF = shortening fraction; EF = ejection fraction; LVIDs = left ventricle internal diameter in systole; AoV = aortic outflow velocity; PuV = pulmonary outflow velocity; IVRT = isovolumic relaxation time

Table 2 presents the assessment results of the left ventricular filling pattern before and after timolol. The lower HR resulted in an increase in IRVT by 15.2% (54.8 to 64.6 ms), with most cats having such variable above the reference range (> 60 ms)[4] after drug administration. Out of 33 cats, only 11 (24.4%) presented fused transmitral waves before timolol administration. Similarly, few diastolic TDI waves were fused on the control echocardiogram (Control Timolol), only five when measured at the IVI annulus (15.1%), and eight at FW annulus (24.2%). The

"impossibility of diastolic assessment" described in the table refers to the fusion of mitral waves or TDI waves preventing diastolic interpretation, as it requires the presence of unfused waves in both techniques.

Table 2 - Echocardiographic diastolic alterations before and after timolol administration

Diastolic alteration	Control (n=33)		Timolol (n=33)		
	n	%	n	%	*p-value*
Enlarged IVRT (>60 ms)	**8**	24.2	**20**	60.6	**0.003**
EAfus	8	24.2	8	24.2	0.613
E'A'fus FW	**8**	24.2	**2**	6	**0.041**
Impossibility of diastolic assessment (FW)	11	33.3	8	24.2	0.552
E'A'fus IVI	5	15.1	5	15.1	0.500
Impossibility of diastolic assessment (IVI)	9	27.3	8	24.2	0.625

Data are n (%)
IVRT = isovolumetric relaxation time; EAfus = fused E and A outflow mitral waves; E'A'fus FW = peak velocity of summated E' and A' waves from the the tissue Doppler measured at the free wall mitral annulus; FW = free wall; E'A'fus IVI = peak velocity of summated E' and A' waves from the tissue Doppler measured at the interventricular septum mitral annulus; IVS = interventricular septum

Spearman's test revealed a moderate negative correlation between HR and BW (R = -0.290 and -0.393, respectively) for both Control and Timolol groups, with evidence of statistical significance for the Timolol group (p = 0.025).

Concerning the LA TMAD results, most graphs in cats did not show a plateau phase (Fig. 1d). A horizontal line during the left atrial diastasis similar to the human's diagram[29] (Fig. 1c) occurred in a few cats: three in the first echocardiogram of the control group (Control 1) and two in the second (Control 2). In the timolol group, four cats showed a plateau phase on the first echocardiogram (Control Timolol), increasing to eight on the second (Timolol), without statistical significance.

Regarding side effects, miosis occurred in 18 cats (54%) and lasted an average of 18 hours, eventually reaching up to 80 hours in one cat. A contralateral effect on pupil diameter was not seen in the non-treated eye, ending in anisocoria (Figure 4). Short-lived ptyalism (<3 min) was observed immediately after timolol application in 4/33 cats (12%).

Figure 4 - Left eye of the cat with miosis due to timolol resulting in anisocoria

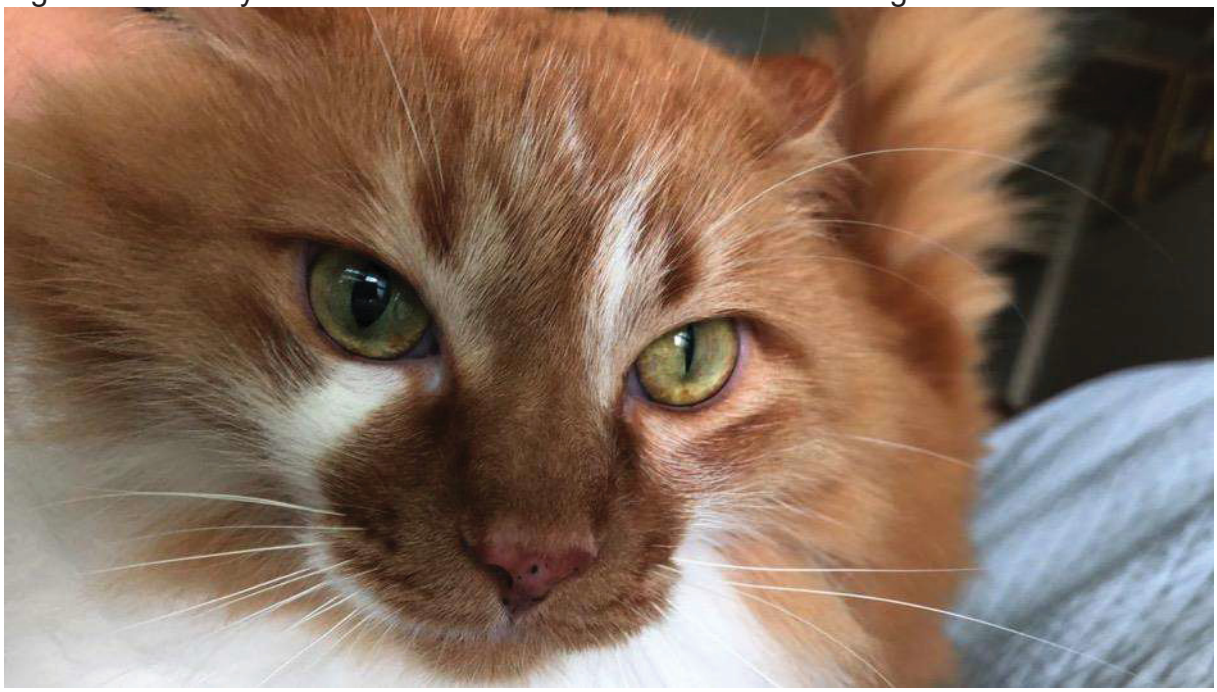

Discussion

This investigation sought to assess whether timolol administered in eye drops interferes with cardiac variables assessed by echocardiography. In general, cats are more sensitive to stressful conditions, although they may hide signs of stress due to their survival strategy[32]. Continued restraining during echocardiography exacerbates sympathetic activation, resulting in tachycardia and changes in several variables to assess cardiac function. The administration of a beta-blocker could lead to a condition closer to physiological, reflecting what the cat was before the sympathetic

activation, or it could pass to the other side, i.e., a parasympathetic predomination. Probably the second option occurred, given the high number of significantly altered variables (17 of 46) in the second echocardiogram of the timolol group (Table 1). On the contrary, in the control group no significant differences were observed between the variables from the two echocardiographs performed. Hence, handling twice for echocardiograms and the waiting period in a hospital environment did not stress sufficiently to raise HR and affect the indices.

Although timolol has its maximum effect in cats between six and twelve hours after administration[12], we chose to repeat the echocardiogram 20 minutes later to follow the same protocol for the diastolic assessment detailed before[11], which coincides with the onset of its action after topical administration. As already mentioned, timolol applied topically to the eyes has systemic effects, being the HR reduction the easiest to observe. Timolol effectively decreased HR by 19%, from ~190 to ~160 bpm. The mean decrease of 30 bpm was close to previously described (25 bpm)[11]. Interestingly, another research group observed that a drop of timolol gel-forming solution did not affect HR four and eight hours later[33], suggesting the bradycardic effect may not last long.

As there was a difference in BW between the animals, the dose of assimilated timolol was not the same, which may have influenced the variations observed. One drop of timolol contains approximately 0.17 mg, with most cats receiving around 0.033 mg/kg, considering an average BW of 5.1 kg. The dose that the lightest animal (2 kg) received was 5.6 times that of the heaviest cat (11 kg), 0.085 and 0.015 mg/kg, respectively. The difference in dosage may justify the non-alteration of HR between the two echocardiograms of the heaviest animal, remaining 150 bpm, already a low HR for the species. However, excluding this outlier cat, the others

weighed a maximum of 7.5 kg, and all showed a significant drop in HR after timolol. Moreover, Spearman's test showed a significant negative correlation between HR and BW after timolol, amplifying a tendency already pointed by the control group, although without significance. The control's group correlation presumably would also be significant in a larger sample, as previously observed in healthy cats[22], with HR decreasing as BW increases.

Comparing the results from timolol administration and the vagal manoeuvre previously investigated is challenging. Their advantages and limitations are pretty balanced, being difficult to determine which is more suitable. Timolol required a twenty-minute waiting interval and the HR reduction lasted all echocardiographic exam. The vagal manoeuvre produced a more pronounced HR reduction (42 bpm) within a few seconds[10], lasting a maximum of 15 seconds, allowing systolic assessment with usual HR. Still, about one-quarter of animals submitted to vagal stimulation had an inadequate response (HR reduction <20 bpm). Although the cited investigation did not observe it, a paradoxical tachycardia might result from the oculocardiac reflex[34]. Besides, to separate both the spectral and TDI waves, it might be necessary to repeat the stimuli, with the risk of reducing the intensity of the decrease in HR due to fatigue, as reported in children[35]. Finally, the timolol instillation seems to be less invasive and more suitable for stressed cats. They may resent the mechanical procedures summed to the restrain for the echocardiogram. In dogs, fear and pain may be associated with the procedure, being potential reasons for a paradoxical HR elevation or absence of response after the manoeuvre[10].

Most systolic surrogates decreased with the use of timolol, such as the fractional shortening (FS) and the ejection fraction (EF) (Table 1). The FS, a classical echocardiographic variable used to evaluate the radial systolic function, reduced by

20.3% (from 51 to 42.4%), coinciding with previously reported[11]. However, post-timolol FS was still within the reference range for cats, i.e. between 39 and 51%[22]. At least in normal cats, timolol is not likely to impair the interpretation of the echocardiogram. Nonetheless, in cats with HCM, the reduction in FS was already demonstrated to be a prognostic surrogate[9,36]. Mean FS of 42.4% is much closer to what was seen in cats with heart failure due to HCM than healthy cats[37].

Interestingly, the variables known to assess longitudinal ventricular systolic function, including LV LSt, MAPSE IVS, and TMAD, were less impaired by timolol. A possible explanation would be a more potent action of timolol on the transversal myocardial fibres. In humans, transverse cardiomyocytes showed to be significantly more sensitive to beta-blockers, with studies suggesting a physiological balance of antagonism between myocytes[38,39]. Another explanation relays on the HR variation itself, witch affects the radial fibres more pronouncedly than the longitudinal ones, as previously described[40] .

A surprising result was the significant reduction of MAPSE FW after timolol by 9.8%, while MAPSE IVS did not. This finding reinforces the perception that MAPSE does not behave likewise when measured on the FW or the IVS annulus, being the IVS annulus somehow affected by the right ventricle as already mentioned[41]. A previous study with HCM cats concluded that the MAPSE IVS was the only factor predicting pleural effusion on multivariable regression model[42], pointing to the influence of the right ventricle on this index. The researchers assumed that the IVS mitral annulus acts differently from the FW, and changes in its longitudinal function could lead to pleural effusion rather than pulmonary oedema. In any case, the MAPSE FW decrease pointed that timolol may also have influenced longitudinal

fibres, although not sufficiently to change other longitudinal indices previously discussed.

It was interesting to note that many LA variables changed significantly after instillation. Considerable LA area measures obtained from AP2 and AP4 images increased on the second echocardiogram of the timolol group, affecting LA cEF from both 4AP and 2AP. The reductions in LA FS (17%), Global LA LSt (12%), and Global LA cEF (9%) suggest a compromise in atrial function once timolol was used. On the contrary, the LA TMAD values did not change between exams, requiring more understanding of this LA assessment technique to justify its non-alteration. Despite presenting potential advantages, such as not demanding high-quality images, the use of TMAD to evaluate the LA function has not been validated in cats, being previously applied by only one research group in humans[29]. Curiously, the HR reduction promoted by timolol was insufficient to significantly increase the number of graphics with a plateau phase signalling the diastasis of the LA, as occurred in humans' LA TMAD, suggesting a need for an even lower HR.

Out of the seventeen variables that changed after timolol (Table 1), the one that presented the most remarkable change was the peak systolic mitral annular velocity as determined by tissue Doppler (S'). The S' obtained from the interventricular annulus reduced by 51% (7.7 to 5.2 cm/s) and 43.1% from the free wall (7.3 to 5.1 cm/s). Consequently, timolol lowered the S' velocity to less than 5.2 cm/s, below the reference range[5]. Similar results on S' velocity were documented before[5,8]. There is a positive relationship between the S' wave and the HR; however, it is impossible to delimit how much the HR reduction may have played a role in such a marked decline. It seems that a combination of factors contributed, such as a systolic impairment evidenced by the lower FS. Of note, cats with HCM are known to

have lower S' wave velocity[5,23]. In such patients, timolol might difficult the echocardiogram interpretation as the cardiologist will not settle if a reduced myocardial velocity is a result of the illness or the drug.

The pulmonary and aortic outflow velocities also decreased (27.2 and 21.3%, respectively) with timolol. This reduction seems to be a consequence of the HR reduction. A previous study with dogs concluded that an increase in HR leads to a faster aortic and pulmonary flow velocity[44], insinuating a directly proportional relationship between them.

Regrettably, a low frequency of fused mitral outflow waves was documented in the first echocardiogram (Table 2). We speculate that having the cats undergo a series of procedures (auscultation, hair clip, ECG, and SBP measurement) before the echocardiogram might have contributed to their adaptation to the environment. Also, timolol did not separate most EAfus and E'A'fus, which impaired the left ventricular filling pressure assessment. In those cats where fused mitral or TDI waves were observed (11/33, using TDI IVS; 33,33%), timolol produced the desired separation in a few (3/11; 10,1%). In a previous study with timolol, 13/20 cats had a transmitral fusion, and the successful separation was achieved in 8 (62%)[11]. The investigation with vagal manoeuvres had better results, effectively separating 71% of the fused transmitral flows and 72% of the TDI velocity[10].

The fusion of transmitral waves may be due to increased HR, as mentioned so far, or indicate diastolic impairment. A previous study found that cats with HCM tend to have more EAfus at lower HR than healthy cats, suggesting that summation may indicate diastolic impairment[5]. However, since the present study aimed to evaluate healthy cats, a more likely explanation for the low success of timolol might be the combination of factors: an insufficient reduction on HR, few animals with fused waves

on the control echocardiogram (Control Timolol), and the separation of only one variable (mitral outflow or TDI), not both simultaneously.

A noteworthy result was the increase in IVRT post-timolol (Table 2). It is a diastolic variable influenced by the HR, lasting longer as the HR decreases[4]. Combined with other variables, an enlarged IVRT reveals a diastolic dysfunction[45]. Eight cats in the timolol group had increased TRIV (>60 ms) before instillation (24%), which were maintained in the experiment because they did not manifest alterations in any other variable and had an HR low enough to justify an increase in this index. However, enlarged IVRT more than doubled after using the drug, rising to 20 (60.6%). Consequently, the timolol administration might lead to a misinterpretation of the cat´s echocardiogram since the enlarged IVRT in these cases reflects the beta-blocker action and is not associated with a diastolic impairment.

The administration of timolol ophthalmic solution was initially proposed to assist in the early diagnosis of HCM[11] since diastolic dysfunction secondary to hypertrophy is characteristic of this disease[46]. However, timolol might not be indicated in cats with HCM since it increases IVRT and interferes negatively with the systolic function of LV and LA. The instillation would likely make the diagnosis of subclinical HCM more challenging. In patients already diagnosed, a low LA FS, a classical indicator of poor prognostic[9,36], could be due to timolol action and not to the disease itself. Besides, there is no data about the effect of timolol in cats in advanced stages of cardiomyopathy.

The ideal would be to adopt a technique to assess diastolic function independent of preload and HR. One method that meets this requirement is assessing the flow velocity profiles of the left anterior descending coronary artery through transesophageal echocardiography[47]. Another more promising relaxation

index is the velocity of propagation of the mitral flow (Vp) [48], obtained during transthoracic echocardiography. It measures the rapid filling phase determined by M-mode colour Doppler echocardiography, being its application reported in humans with HCM[49] and dogs with dilated cardiomyopathy[50]. A recent study in HCM cats concluded that the decline in Vp is correlated associated with the degree of increase in LA, which is significantly associated with the progression of diastolic dysfunction in HCM[45].

Interesting, two cats appeared much calmer on the second echocardiogram. Their HR decreased slightly more than the mean, from 240 to 185 bpm (22.9%) and from 180 to 140 bpm (22.3%). Hence, it is plausible that the observed relaxation resulted from a beta-blocker anxiolytic effect[51], not from the reduction in HR itself. Behavioural assessment was not part of the experimental design, and the tranquillizing effect may have been present in other cats and gone unnoticed. Although this relaxation was not perceived in the control group, it is not possible to exclude the cat's acclimatization in reducing anxiety.

In this investigation, a drop of timolol did not cause any clinically relevant adverse. All the cats likely had miosis on the eye that received the drug (Figure 4), but it was observed in only 18 of the 33 cats (54.5%), resulting in anisocoria since the contralateral non-treated eye was not affected[11,33]. A previous study with the administration of timolol in normotensive eyes in healthy cats reported a reduction of pupil diameter of 38.7% at 30 minutes after treatment in all cats[12]. Despite going unnoticed by a significant part of the owners, anisocoria was disturbing for some of them, who reported non-specific behavioural changes, such as hiding or inactivity, both common alterations in cats exposed to a hospital environment.

Considering that only healthy cats were included, some possible side effects were not observed, such as bronchoconstriction[52], an important reason to contraindicate timolol for cats with feline asthma[15]. This eye solution might also be avoided in elderly cats, as its continued use has been linked to syncope[53], postprandial head-drops[54] and atrioventricular block[55] in older people. Many articles do not recommend timolol for long-term treatment of glaucoma in cats with cardiac diseases[15,56], but nothing is known about the effect of a single administration in cats with advanced heart failure. On the other hand, some researchers even hypothesize that the negative inotropic effect of timolol may help to elucidate the patient's response to beta-blockade, particularly in cats with obstructive cardiomyopathy[11]. In the cited study, all the six cats with evidence of dynamic obstruction or hypertrophic obstructive cardiomyopathy on baseline echocardiogram had relief of that obstruction after timolol administration.

Moreover, some episodes of ptyalism were reported in this study, which is in line with preliminary data[11]. This excess salivation was not an action of timolol but simply a normal cat response to the bad taste of the eye solution that passed through the tear duct to the back of the throat. However, since this reaction was short-lived, it may have gone unnoticed in most cats, as they usually waited for the second echocardiogram in the crate.

Some limitations were present in this study. Firstly, despite all efforts to select only healthy individuals, occult cardiomyopathies might not have been identified. Another limitation was the variation in the dose administered, which could be resolved by choosing only cats with similar BW or manipulating the ophthalmic solution to administer a similar dose for all. The small number of cats with EAfus and E'A'fus biased the evaluation of timolol as a facilitator in assessing LV filling

pressure. In this case, the owner's awareness that the cat would undergo two echocardiograms may have discouraged them from bringing stressed cats to hospital environments, with only calmer cats participating in the experiment. A less pronounced fear response would result in a control echocardiogram with a lower HR and separate transmitral flow. Lately, an intraocular pressure measurement after the second echocardiogram could have added relevant information connecting the heart effect and eye pressure reduction.

Conclusion

A drop of timolol ophthalmic solution 0.5% reduced HR and interfered negatively with the LV and LA systolic function in healthy cats. It affected many variables commonly used in standard echocardiography, such as FS and EF. All the cited changes are not desirable in evaluating cats with suspected cardiomyopathy, with a risk of misinterpretation. The influence of timolol was milder in the echocardiographic indexes known to assess the longitudinal systolic function of the LV, such as TAPSE, MAPSE IVS, LSt, and TMAD. The MAPSE FW and de S' wave were two exceptions, both decreasing significantly after the instillation.

Lastly, despite not being the objective of the present study, it was found that the diastolic evaluation was not benefited by timolol since the decrease in HR was not enough to separate the transmitral waves. On the contrary, the drug significantly enlarged the IVRT, used applied to classify the diastolic function.

Conflicts of Interest

The authors do not have any conflicts of interest to declare. All co-authors have seen and agree with the contents of the manuscript and there is no financial interest to

report. We certify that the submission is original work and is not under review at any other publication.

Funding

The authors received no financial support for the research, authorship, and/or publication of this article.

Ethical approval

This work involved the use of non-experimental animals (owned or unowned) and procedures that differed from established internationally recognised high standards ('best practice') of veterinary clinical care *for the individual patient*. The study therefore had ethical approval from an established committee as stated in the manuscript.

Informed consent

Informed consent (either verbal or written) was obtained from the owner or legal custodian of all animal(s) described in this work (either experimental or nonexperimental animals) for the procedure(s) undertaken (either prospective or retrospective studies). No animals or humans are identifiable within this publication, and therefore additional informed consent for publication was not required.

References

1. Rodan I. Understanding Feline Behavior and Application for Appropriate Handling and Management. *Top Companion Anim Med* 2010; 25: 178–188.
2. Abbott JA. Heart rate and heart rate variability of healthy cats in home and hospital environments. *J Feline Med Surg* 2005; 7: 195–202.
3. Belew AM, Barlett T, Brown SA. Evaluation of the White-Coat Effect in Cats. *J Vet Intern Med* 1999; 13: 134.
4. Schober KE, Chetboul V. Echocardiographic evaluation of left ventricular diastolic function in cats: Hemodynamic determinants and pattern recognition. *J Vet Cardiol* 2015; 17: S102–S133.
5. Koffas H, Dukes-McEwan J, Corcoran BM, et al. Pulsed tissue Doppler imaging in normal cats and cats with hypertrophic cardiomyopathy. *J Vet Intern Med* 2006; 20: 65–77.
6. Galiuto L, Ignone G, DeMaria AN. Contraction and relaxation velocities of the normal left ventricle using pulsed-wave tissue Doppler echocardiography. *Am J Cardiol* 1998; 81: 609–614.
7. Nagueh SF, Bachinski LL, Meyer D, et al. Tissue Doppler imaging consistently detects myocardial abnormalities in patients with hypertrophic cardiomyopathy and provides a novel means for an early diagnosis before and independently of hypertrophy. *Circulation* 2001; 104: 128–30.
8. SUGIMOTO K, FUJII Y, SUNAHARA H, et al. Assessment of left ventricular longitudinal function in cats with subclinical hypertrophic cardiomyopathy using tissue Doppler imaging and speckle tracking echocardiography. *J Vet Med Sci* 2015; 77: 1101–1108.
9. Luis Fuentes V, Abbott J, Chetboul V, et al. ACVIM consensus statement

guidelines for the classification, diagnosis, and management of cardiomyopathies in cats. *J Vet Intern Med* 2020; 1–16.

10. Smith DN, Schober KE. Effects of vagal maneuvers on heart rate and Doppler variables of left ventricular filling in healthy cats. *J Vet Cardiol* 2013; 15: 33–40.
11. Gunther-Harrington CT, Ontiveros ES, Hodge TE, et al. Effects of 0.5% Timolol Maleate Ophthalmic Solution on Heart Rate and Selected Echocardiographic Indices in Apparently Healthy Cats. *J Vet Intern Med* 2016; 30: 733–740.
12. Wilkie DA, Latimer CA. Effects of topical administration of timolol maleate on intraocular pressure and pupil size in cats. *Am J Vet Res* 1991; 52: 436–40.
13. Willis AM. Ocular hypotensive drugs. *Vet Clin North Am - Small Anim Pract* 2004; 34: 755–776.
14. Slenter IJM, Djajadiningrat-Laanen SC, Elders DJ, et al. The effects of topical dorzolamide 2% and brinzolamide 1%, either alone or combined with timolol 0.5%, on intraocular pressure, pupil diameter, and heart rate in healthy cats. *Vet Ophthalmol* 2019; 1–9.
15. McLellan GJ, Teixeira LBC. Feline Glaucoma. *Vet Clin North Am - Small Anim Pract* 2015; 45: 1307–1333.
16. Chen L, Zeng X, Huang X. Efficacy and safety of intraocular pressure-lowering agents bimatoprost and timolol maleate in glaucoma. *Int J Pharmacol* 2018; 14: 179–186.
17. Riesen SC, Schober KE, Cervenec RM, et al. Comparison of the Effects of Ivabradine and Atenolol on Heart Rate and Echocardiographic Variables of Left Heart Function in Healthy Cats. *J Vet Intern Med* 2011; 25: 469–476.
18. Gorre F, Vandekerckhove H. Beta-blockers: focus on mechanism of action Which beta-blocker, when and why? *Acta Cardiol* 2010; 65: 565–570.

19. Barbier P, Solomon SB, Schiller NB, et al. Left atrial relaxation and left ventricular systolic function determine left atrial reservoir function. *Circulation* 1999; 100: 427–436.

20. Thomas WP, Gaber CE, Jacobs GJ, et al. Recommendations for Standards in Transthoracic Two-Dimensional Echocardiography in the Dog and Cat. *Vet Radiol Ultrasound* 1994; 35: 173–178.

21. Sahn DJ, DeMaria A, Kisslo J, et al. Recommendations regarding quantitation in M-mode echocardiography: Results of a survey of echocardiographic measurements. *Circulation* 1978; 58: 1072–1083.

22. Häggström J, Andersson O, Falk T, et al. Effect of Body Weight on Echocardiographic Measurements in 19,866 Pure-Bred Cats with or without Heart Disease. *J Vet Intern Med* 2016; 30: 1601–1611.

23. Spalla I, Payne JRR, Borgeat K, et al. Mitral Annular Plane Systolic Excursion and Tricuspid Annular Plane Systolic Excursion in Cats with Hypertrophic Cardiomyopathy. *J Vet Intern Med* 2017; 31: 691–699.

24. Wolf M, Lucina SBSB, Brüler BCBC, et al. Assessment of longitudinal systolic function using tissue motion annular displacement in healthy dogs. *J Vet Cardiol*; 20. Epub ahead of print 2018. DOI: 10.1016/j.jvc.2018.04.004.

25. Spalla I, Boswood A, Connolly DJ, et al. Speckle tracking echocardiography in cats with preclinical hypertrophic cardiomyopathy. *J Vet Intern Med* 2019; 33: 1232–1241.

26. Abbott JA, MacLean HN. Two-dimensional echocardiographic assessment of the feline left atrium. *J Vet Intern Med* 2013; 20: 111–9.

27. Rishniw M, Erb HN. Evaluation of four 2-dimensional echocardiographic methods of assessing left atrial size in dogs. *J Vet Intern Med* 2000; 14: 429–

435.

28. Piotrowski G, Goch A, Wlazłowski R, et al. Non-invasive methods of atrial function evaluation in heart diseases. *Med Sci Monit* 2014; 6: 827–39.
29. Strachinaru M, Annis C, Catez E, et al. The mitral annular displacement by two-dimensional speckle tracking. *J Cardiovasc Med* 2016; 17: 344–353.
30. Faul F, Erdfelder E, Lang A-G, et al. G*Power 3: a flexible statistical power analysis program for the social, behavioral, and biomedical sciences. *Behav Res Methods* 2007; 39: 175–91.
31. R Core Team. R: a language and environment for statistical computing. Vienna: R Foundation for Statistical Computing, 2021, https://www.r-project.org/.
32. Horwitz DF, Rodan I. Behavioral awareness in the feline consultation: Understanding physical and emotional health. *J Feline Med Surg* 2018; 20: 423–436.
33. Kiland JA, Voss AM, McLellan GJ. Effect of timolol maleate gel-forming solution on intraocular pressure, pupil diameter, and heart rate in normal and glaucomatous cats. *Vet Ophthalmol* 2016; 19: 91–96.
34. Arnold RW. The oculocardiac reflex: A review. *Clin Ophthalmol* 2021; 15: 2693–2725.
35. Blanc VF, Hardy JF, Milot J, et al. The oculocardiac reflex: a graphic and statistical analysis in infants and children. *Can Anaesth Soc J* 1983; 30: 360–369.
36. Payne JR, Borgeat K, Connolly DJ, et al. Prognostic indicators in cats with hypertrophic cardiomyopathy. *J Vet Intern Med* 2013; 27: 1427–1436.
37. Visser LC, Sloan CQ, Stern JA. Echocardiographic Assessment of Right

Ventricular Size and Function in Cats With Hypertrophic Cardiomyopathy. *J Vet Intern Med* 2017; 31: 668–677.

38. Lunkenheimer PP, Redmann K, Cryer CW, et al. Beta-blockade at low doses restoring the physiological balance in myocytic antagonism. *Eur J Cardio-thoracic Surg* 2007; 32: 225–230.
39. Schmitt B. Accelerated whole-heart 3D CSPAMM reveals impact of beta-blocker therapy on myocardial architecture. *J Cardiovasc Magn Reson* 2010; 12: 3.
40. Simpson KE, Gunn-Moore DA, Shaw DJ, et al. Pulsed-wave Doppler tissue imaging velocities in normal geriatric cats and geriatric cats with primary or systemic diseases linked to specific cardiomyopathies in humans, and the influence of age and heart rate upon these velocities. *J Feline Med Surg* 2009; 11: 293–304.
41. Hu K, Liu D, Herrmann S, et al. Clinical implication of mitral annular plane systolic excursion for patients with cardiovascular disease. *Eur Heart J Cardiovasc Imaging* 2013; 14: 205–212.
42. Spalla I, Payne JR, Borgeat K, et al. Prognostic value of mitral annular systolic plane excursion and tricuspid annular plane systolic excursion in cats with hypertrophic cardiomyopathy. *J Vet Cardiol* 2018; 20: 154–164.
43. Kiatsilapanan A, Surachetpong SD. Assessment of left atrial function in feline hypertrophic cardiomyopathy by using two- dimensional speckle tracking echocardiography. *BMC Vet Res* 2020; 16: 1–10.
44. Kirberger RM, Bland-vanden Berg P, Grimbeek RJ. DOPPLER ECHOCARDIOGRAPHY IN THE NORMAL DOG: PART II: Factors Influencing Blood Flow Velocities And a Comparison between Left and Right Heart Blood

Flow. *Vet Radiol Ultrasound* 1992; 33: 380–386.

45. Sugimoto K, Kawase N, Aoki T. Assessment of diastolic function using mitral flow propagation velocity in cats. *Can J Vet Res* 2020; 84: 124–130.
46. Abbott JA. Feline hypertrophic cardiomyopathy: An update. *Vet Clin North Am - Small Anim Pract* 2010; 40: 685–700.
47. Tomochika Y, Tanaka N, Wasaki Y, et al. Assessment of flow profile of left anterior descending coronary artery in hypertrophic cardiomyopathy by transesophageal pulsed Doppler echocardiography. *Am J Cardiol* 1993; 72: 1425–1430.
48. Garcia MJ, Thomas JD, Klein AL. New doppler echocardiographic applications for the study of diastolic function. *J Am Coll Cardiol* 1998; 32: 865–875.
49. Nishihara K, Mikami T, Takatsuji H, et al. Usefulness of early diastolic flow propagation velocity measured by color M-mode Doppler technique for the assessment of left ventricular diastolic function in patients with hypertrophic cardiomyopathy. *J Am Soc Echocardiogr* 2000; 13: 801–808.
50. O'Sullivan ML, O'Grady MR, Minors SL. Assessment of diastolic function by Doppler echocardiography in normal Doberman Pinschers and Doberman Pinschers with dilated cardiomyopathy. *J Vet Intern Med* 2014; 21: 81–91.
51. Carabine UA, Milligan KR, Moore JA. Adrenergic modulation of preoperative anxiety: A comparison of temazepam, clonidine, and timolol. *Anesth Analg* 1991; 73: 633–637.
52. Shiuey Y, Eisenberg MJ. Cardiovascular effects of commonly used ophthalmic medications. *Clin Cardiol* 1996; 19: 5–8.
53. Müller ME, Van Der Velde N, Krulder JWM, et al. Syncope and falls due to timolol eye drops. *Br Med J* 2006; 332: 960–961.

54. Bin Waqar SH, Rehan A, Zammam M. Postprandial Head-drops: Insight into Systemic Effects of Ocular Timolol Preparation in Elderly. *Cureus*; 11. Epub ahead of print 30 de maio de 2019. DOI: 10.7759/cureus.4780.

55. Wang Z, Denys I, Chen F, et al. Complete atrioventricular block due to timolol eye drops: a case report and literature review. *BMC Pharmacol Toxicol* 2019; 20: 73.

56. McLellan GJ, Miller PE. Feline glaucoma-a comprehensive review. *Vet Ophthalmol* 2011; 14: 15–29.

CAPÍTULO 3 – **Efeitos comportamentais e cardiovasculares da gabapentina ou melatonina em dose única em gatos: estudo randomizado, duplo-cego e controlado por placebo**

Giovana Lais Ruviaro Tuleski[a]; M.Sc; Matheus Folgearini Silveira[a], M.Sc; Rodrigo Franco Bastos[a], DVM; Maria Jose Garcia Ribeiro Pscheidt, DVM; Wiliam da Silva Prieto, DVM; Marlos G. Sousa[a], PhD.

[a] Laboratory of Comparative Cardiology, Department of Veterinary Medicine, Federal University of Paraná (UFPR), Rua dos Funcionários, 1540, CEP 80035-050, Curitiba, Paraná, Brazil

Corresponding author name: Giovana Lais Ruviaro Tuleski, MSc - ORCID 0000-0002-0817-3470

Contact details: Phone number +55 41 99669-5473, e-mail: gtuleski@yahoo.com.br

Artigo será submetido à revista *Journal of Feline Medicine and Surgery* com o título: **Behavioural and cardiovascular effects of single-dose gabapentin or melatonin in cats: a randomized, double-blind, placebo-controlled trial**

As figuras e tabelas estão disposta no final do texto do artigo, sendo colocado [insert Figure] ou [insert Table] no local onde ficariam esses elementos, conforme as normas da revista (https://journals.sagepub.com/author-instructions/JFM)

Abstract

Objectives: Verify whether a single oral dose of gabapentin (100 mg per cat) or melatonin (3 mg per cat) given sixty minutes before a cardiac evaluation would reduce anxiety without interfering with heart rate (HR), systemic blood pressure (SBP), electrocardiography (ECG), and echocardiographic indexes.

Methods: Seventy-five client-owned healthy cats underwent two sets of cardiac assessments 60 minutes apart. The animals were randomly divided into gabapentin, melatonin, and placebo groups. The interval between the drug administration and the second ECG and SBP was 60 minutes and 70 minutes for the echocardiography. Standard and Speckle-tracking techniques were applied. A compliance score (CS) classified the behaviour, focusing on the easiness of handling. Sedation was defined as a more profound relaxation with compromise on environment perception and ataxia, being classified by a sedation score (SS).

Results: Gabapentin's mean dose was 19.6 mg/kg (SD=5.3; 14.3-24.9 mg/kg), while melatonin' was 0.7 mg/kg (SD=0.2; 0.5-0.9 mg/kg). Most variables did not change between the exams, with the placebo group showing more significant changes (SBP, Tricuspid annular plane systolic excursion -TAPSE, HR during echocardiography, aortic flow velocity, S' wave from lateral mitral annulus), followed by gabapentin (E-wave velocity, A'-wave from the lateral mitral annulus, and the interventricular septum thickness during diastole) and melatonin (HR during ECG, LA:Aorta ratio). No alteration was considered haemodynamically relevant. Gabapentin and melatonin significantly decreased the CS of the cats. Eight cats presented mild sedation, seven from the gabapentin group and one from melatonin, a significant difference between the treatments. No major side effects were observed.

Conclusions and relevance: Gabapentin and melatonin relaxed the cats given 60 minutes before ECG and SBP measurement and 70 minutes before echocardiography, without interfering with systolic echocardiographic indexes. Gabapentin achieved sedation in more animals. Both substances were considered safe pre-appointment drugs for cats.

Keywords: gabapentin, melatonin, compliance score, pre-appointment drug, TMAD, longitudinal strain

Introduction

Cardiomyopathies are frequently diagnosed in cats, although overt clinical signs may be absent until the advanced stage[1,2]. Thus, preventive cardiac evaluation is often indicated, especially in older animals or those of increased risk breeds[1]. Domestic cats frequently react aggressively or fearfully in veterinary settings[3], not allowing echocardiography or SBP measurement handling. The stress generated by physical restraint often leads veterinarians to be suspicious of SBP measures, speculating whether an elevated SBP value is only due to a sympathetic response, the white-coat effect, or evidence of an actual disease[4]. In this context, previous use of a substance to reduce anxiety without compromising cardiac assessment is convenient because it does not confound the exams' interpretation, increases the cat's welfare, and provides better veterinary care.

Gabapentin is a drug known to facilitate both transport and examination of cats[5,6]. Recently, its oral administration two hours before echocardiography proved to be effective in tranquilization, although it decreased some systolic echocardiographic parameters[7]. In feline medicine, melatonin is best known for acting in the reproductive field[8], effectively and reversibly inhibiting endogenous ovarian activity[9], often recommended to suppress estrus in cats administered orally[10] or as an implant[10,11]. Unlike gabapentin, melatonin has not been indicated as a pre-appointment substance for veterinary use, based on a recent search on two medical database platforms (PubMed and ProQuest). However, a meta-analysis reported that melatonin has an anxiolytic effect in humans, with high-grade quality of evidence, reducing preoperative anxiety[12]. In veterinary medicine, melatonin provided a beneficial calming effect for doubtful dogs 90 minutes after administration and reduced the required dose of propofol for anaesthesia induction in trustful dogs[13].

Both gabapentin and melatonin have matching time to maximum plasma concentration (T_{max}) around one hour[9,14], which permitted studying them in the same trial. Based on this time, the objective of this investigation was to ascertain whether a single dose of gabapentin or melatonin would reduce anxiety without interfering with heart rate (HR), systemic blood pressure (SBP), electrocardiography (ECG) parameters, and echocardiographic indices. Also, despite the maximum effect of gabapentin being reached at approximately two hours after oral administration[15], we sought to investigate if a shorter interval would be enough to tranquillize the cats for cardiac examinations.

Materials and Methods

This study was designed as a prospective, randomized, double-blind, placebo-controlled investigation and was carried out between July and December 2020 at a Veterinary Teaching facility. All procedures were previously approved by the Institutional Animal Care and Use Committee (protocol 014/2019) and complied with the National Institutes of Health Guide for the Care and Use of Laboratory Animals.

Animals

Client-owned cats were recruited for the study after a complete physical examination was performed. Inclusion criteria comprised a young or mature adult cat (one to 10 years old)[16], normal auscultation and an ECG trace without arrhythmias. Also, cardiac diseases were ruled out by standard transthoracic echocardiography, which required a normal myocardial thickness during diastole[17], and normal-sized cardiac chambers, systolic indices within reference values and normal diastolic function parameters[1].

Exclusion criteria were established to select only cats that appeared healthy after checking their medical history and performing a physical examination. Animals previously diagnosed with a disease or receiving any medication were not admitted.

Procedures

The algorithm in Figure 1 describes the procedures from the baseline SBP, ECG, echocardiography and behaviour evaluation with the CS, and the subsequent randomization, drug administration, waiting period, and the second set of SBP, ECG, echocardiography and behaviour evaluation. The schedule was rigorous in terms of exactitude, allowing a maximum of five minutes delays. Most of the exams were performed during the mornings.

[insert Figure 1]

The Doppler technique indirectly measured the SBP[18], being repeated five times and averaged (baseline SBP). Subsequently, a 2-minutes recording of a computer-based ECG was performed (baseline ECG). The ECG variables evaluated were the HR, mean cardiac axis, QT interval and T wave polarity. On the sequence, the first echocardiography was performed (baseline echo). Both ECG recording and SBP measurements were conducted in a single room, whereas echocardiography was executed in another, which required transporting the cats between them.

The cats were randomly assigned to receive a manipulated capsule containing 100 mg of gabapentin (Mdn= 20 mg/kg), 3 mg of melatonin (Mdn = 0.65 mg/kg) or a placebo (lactose powder). Locked randomization was used to ensure a balance between the groups according to the predetermined 1:1:1 ratio, producing groups of

the same size[19]. All capsules had the same shape and size, packaged in numbered bottles (1, 2 and 3). One of the authors (MFS) selected the drugs unaware of the capsule's contents, randomly varying the order of treatments each examination day, avoiding biases regarding the moment the cat was examined (the first or the last one of a sequence). The oral capsule was administered immediately after the baseline echocardiography, flushing 2 mL of water with a syringe to help the swallow. The cat was kept in a silent, dark room between the two sets of procedures.

Sixty minutes later, the same operator (GLRT) carried out SBP measurements (drug SBP) and ECG recording (drug ECG). The second echocardiography (drug echo) was performed precisely seventy minutes after the drug administration. One of the authors (MJGRP) assessed the behaviour during echocardiography.

Echocardiography

Both echocardiographs were performed by the same operator (GLRT) with the cat positioned following the recommendations of the Echocardiography Committee of the Specialty of Cardiology of the American College of Veterinary Internal Medicine[20].

The echocardiographic evaluation included the variables from the right transversal parasternal view: the M-Mode measurements of the left ventricle, the left atrium and aorta ratio (LA:Ao) measured at the maximum LA diameter[21], and the fractional shortening of the left atrium (LA FS) using anatomic M-mode[22]. The maximum diameter of the left atrium (LAD) was measured right after the T wave using right parasternal long-axis four-chamber images[23].

The mitral annular plane systolic excursion from the free wall and interventricular septum (MAPSE FW and IVS, respectively), the tricuspid annular

plane systolic excursion (TAPSE), and the mitral annular velocities were obtained as described elsewhere[24,25].

Two speckle-tracking echocardiography (STE) variables were applied to assess the left ventricle's systolic function: longitudinal strain (LSt) and tissue motion annular displacement (TMAD). Either parameter was measured at AP2 and AP4 images, requiring the aortic valve closure time calculated from the beginning of the QRS complex to the end of the aortic valve spectra[26].

The offline calculation of LSt required selecting three regions of interest (ROIs) by the operator: the septal and lateral mitral valve annulus and the LV apex's epicardial region[27]. Myocardial tracking was automatically performed by the equipment software (QLAB Software - Auto Cardiac Motion Quantification, aCMQ). Manual corrections were made whenever the automatic tracking was obviously incorrect.

The TMAD measurement required the selection of the same three ROIs already described for LSt[28]. The software automatically tracked the displacement of the two points at the mitral ring towards the apex (mm). Also, a virtual midpoint between the two annular ROIs was automatically created, and its displacement towards the left ventricular apex was tracked (TMAD MP). Lastly, the proportional displacement of this midpoint to the total length of the LV was calculated (TMAD MP%).

Compliance score and sedation score

For behavioral assessment, we followed the adherence score (CS) as previously described[5] (Table 1), focusing on reducing signs of stress and aggression and increasing adherence in cats during echocardiographic examination. Although

the terms "tranquillizer" and "sedative" are often used interchangeably, the present study adopted a differentiation between them. *Tranquilization* was defined as an anxiety reduction, while *sedation* has more potent central nervous system (CNS) depression, compromising performance and environment perception[29]. When observed, sedation was classified according to a score developed for cats[30], being described as sedation score (SS) (Table 1).

[insert Table 1]

Statistical analysis

A priori power analysis was conducted to determine the minimum sample size needed to ensure adequate power to detect a clinically significant effect. The sample size calculation was executed in GPower 3.1[31] with 30% of expected effect, 80% of sample power, and 10% error. Based on these assumptions, the sample size necessary for detecting a medium effect was 25 for each experimental group (gabapentin, melatonin and placebo).

Analysis was conducted in R 4.0.5 (R Core Team 2021)[32]. Statistical analysis was conducted to test the null hypothesis that there would be no difference between therapies with gabapentin, melatonin and placebo concerning the assessment of CS, SS, measurements of SBP, ECG, HR and echocardiographic indices.

Firstly, a descriptive analysis of the data was carried out with an estimate of simple and relative frequency and a 95% confidence interval for all qualitative variables. The mean, median, standard deviation, interquartile interval and 95% confidence interval were calculated for all quantitative variables. The Shapiro-Wilk normality test examined whether quantitative variables followed a normal distribution.

The difference between two independent groups was verified with paired t-test for variables with normal distribution, while the Wilcoxon test was applied for those without it. A significant level of 0.05 was adopted (P-value <0.05).

The analysis of the CS before and after the drugs was performed with Fisher's exact test. The sedation was evaluated by classifying the animals as "sedated" and "non-sedated", using a corrected chi-square.

Results

A total of 75 cats were enrolled in the study. Of these, 42 (56%) were female, and 33 (44%) were male; the majority were mixed breed (96%), 2 Persians (2.7%) and 1 Bengal (1.3%). The mean age was 5.1 years (SD=2.5; 1-10 years). The heavier cat (11 kg) was considered an outlier, but it did not affect the average body weight (BW), which was 4.76 kg (SD=1.3; 2.5-11 Kg) with him, and 4.68 kg (SD=1.1; 2.5-7.4 kg) without it. The same occurred with the BSA: 0.281 m2 (SD=0.051; 184-0.495 m2) when including all the animals and 0.278 m2 (SD=0.045; 184-0.380 m2) without the outlier.

Demographic data between the groups are summarized in Table 2. Without adding the heavier cat, the mean BW of the gabapentin group would drop from 5.1 to 4.8 kg (SD= 0.97), increasing the mean dose from 19.7 to 20,7 mg/kg.

[insert Table 2]

The distribution of sex between groups was similar: gabapentin had fourteen females (56%), melatonin thirteen (52%), and placebo fifteen (60%). The three purebred cats were randomly assigned to receive gabapentin.

The continuous variables from the two sets of exams in each group are shown in Table 3. Most of them did not present a normal distribution (23/42). Figure 2 displays the graphic distribution of the variables that significantly altered after treatment: five from the placebo group (SBP, Tricuspid annular plane systolic excursion -TAPSE, HR during echocardiography, aortic flow velocity, S' wave from lateral mitral annulus), three from the gabapentin treatment (E-wave velocity, septal A'-wave, and the interventricular septum thickness during diastole - IVSd), and two from the melatonin (HR during ECG and the ratio between LA and aorta- LA/Ao).

[insert Table 3]

[insert Figure 2]

The behaviour assessment using CS before and after the treatment is displayed in Table 4. No cat was categorised as a 3 score, i.e. extreme struggling with or without urination or defecation. According to the CS results, gabapentin was the only substance that managed to drop it from 2 to 0 in 4/25 cats (16%), bypassing the intermediate score between them. Only eight cats were considered sedated, i.e., they produced sufficient CNS depression to cause muscle relaxation and an apparent unawareness of the environment[29]. even belonged to the gabapentin group (28%), including the Bengal and the 11 kg outlier cat, and one to the melatonin group (4%). Therefore, gabapentin significantly provoked more sedation than other treatments (P=0.004). Finally, the sedation in all patients was considered mild (SS score 1, Table 1).

[insert Table 4]

Side effects were only documented in cats given gabapentin. Mydriasis was observed in one cat (4%), whereas nine cats (36%) presented drowsiness at home. Of note, a single cat treated with gabapentin changed the polarity of the T wave on the ECG trace (negative to positive), whereas most of them maintained the baseline polarity.

Discussion

The restraint in a veterinary environment generates stress, fear and anxiety and may activate two important pathways: the sympathoadrenal (SA) and the hypothalamic-pituitary-adrenal (HPA)[33]. SA is characterised by the epinephrine and norepinephrine release from the adrenal gland and subcortical areas of the brain. It is the classic fight, flight, or freeze response, enabling the animal to respond physiologically with increased cardiac output and HR. The activation of the HPA by the amygdala results in glucocorticoid secretion, with multiple systems redirecting energy resources to satisfy existing demands. Gabapentin and melatonin interact in both pathways, although their mechanisms of action are distinct [34–37].

Gabapentin binds and blocks the calcium channel alpha2-delta protein[38], decreasing the release of excitatory neurotransmitters and peptide neuromodulators, lowering anxiety and pain and controlling seizures. In humans, gabapentin can also reduce cortisol[39] and inhibit the sympathetic system[37]. Melatonin also operates on both stress routes. Its synthesis by the pineal gland is controlled by the hypothalamic suprachiasmatic nucleus, which stimulates its production at night and inhibits it by daylight. Once secreted into the blood and cerebrospinal fluid, melatonin modulates

pituitary cellular activities[34] and has analgesic, anti-inflammatory, antioxidant, and circadian rhythm effects[12,34–36,40,41]. Such a variety of actions makes it difficult to determine how an anxiolytic result is achieved, and the interaction of many of them is likely to cause relaxation[12].

Minimal cardiovascular effects were observed after administering either gabapentin, melatonin or placebo to cats in a hospital environment. Interestingly, there were more changes in the second set of exams of the placebo group than in those receiving an active substance (Table 3, Figure 2). Nonetheless, these differences have no haemodynamic implications that could impair the characterization of cardiac function.

Although changes in the placebo group were deemed irrelevant to cardiovascular function, it is worthy to speculate why they occurred. They must be a consequence of the procedures performed, including the interval between the two sets of exams. Interesting, SBP significantly decreased on the second measurement, suggesting that waiting in a dark silent room can relax cats and decrease sympathetic tone. Additionally, a dark-stimulated melatonin release could have contributed to this finding. In rats, long-term exposure to continuous darkness for ten days led to an increase in serum melatonin[42], but little is known about the consequence of only one hour in a dark room during daytime.

On the contrary, most of the changes on the second echocardiography of placebo evidenced a sympathetic tone predominance (Figure 2). The transportation of the animals from one room to another may have triggered a stress response, increasing HR during echocardiography, aortic flow velocity, and the systolic annular velocity (S' wave). Since these cats were not on any tranquillizer, this group might

have shown better the nuisance of being carried, taken in and out of the cat carrier, handled, and restrained repetitively.

Fewer variables altered significantly after administering gabapentin, and none was directly related to systolic function. Gabapentin caused an increase in the interventricular septum thickness during diastole (IVSd) and the mitral E wave velocity and a decrease in the mitral annular A' wave velocity (Figure 2). As already mentioned, these insubstantial changes have no implications for overall cardiac assessment. In contrast, a previous study with a much longer interval between drug administration and the subsequent echocardiography (120 minutes) observed a modest reduction in systolic function in healthy cats, highlighted by an increment in the left ventricle diameter during systole (LVIDs) and a decrease in the two-dimensional fractional shortening[7]. In our investigation, the contraction force was preserved, emphasised by STE, with the longitudinal strain (LSt) and TMAD keeping their values after the drug was given. It is possible that the smaller interval adopted, almost half of the previous one, contributed to preserving systolic function. As documented previously, gabapentin maintained all parameters within the reference range for healthy cats[7].

Melatonin was the substance that less interfered with cardiovascular physiology (Table 3). An acute soporific effect of melatonin given in daytime was observed in humans, independently of the time of application[43]. Due to the darkness, endogenous melatonin may also have been secreted. The summation of endogenous and exogenous melatonin induced these cats into a deeper drowsy state. The sudden withdrawal from the dark environment may have activated sympathetic tone[44], increasing ECG-derived HR. Subsequently, HR dropped to its normal range in a hospital environment, despite being higher than the one observed

at home[45]. The other significant difference observed was a minor decrease in the LA/Aorta ratio (from1.3 to 1.2) on the second echocardiography, which was also observed in dogs with mitral myxomatous degeneration after four weeks of melatonin supplementation (2mg/kg)[46].

Regarding the behavioural assessment, we chose to perform it during the echocardiography because this exam requires more prolonged restraint than SBP measurement or ECG recording. The search to reduce anxiety aims to allow better echocardiographic images, enabling the diagnosis. The CS was chosen for the evaluation because the goal is to have greater compliance. Another alternative to classifying behaviour would be the seven-level cat stress score (CSS)[47], based on the cat's assessment score[48], and designed to interpret the cat's behaviour without manipulation. Despite being widely used, there is no evidence that the CSS is more effective in stress analysis, as there is no correlation between its scores and the urinary cortisol/creatinine ratio (C:Cr)[49]. Furthermore, the CS classification was a straightforward way to assess the cats since it has only four levels (Table 1).

Interestingly, all cats tended to be more relaxed in the second set of exams, even when treated with a placebo (Figure 3). As already speculated, a dark-induced melatonin secretion may have helped tranquillize the cats in the placebo group. However, only the gabapentin and melatonin groups significantly reduced SC (Table 4). Unfortunately, most cats were already easy to handle at baseline (score 0). A sample with more animals classified with higher CS might have helped differentiate the effects of the two substances. Still, gabapentin as a pre-appointment medication had already been amply proven. Regarding melatonin, its use in dogs before anaesthesia reduced the induction dose of propofol1[13]. Additionally, melatonin's

action may be more potent with a longer interval, higher dose[50], combined with gabapentin[51], or with a preceding administration.

The proportion of sedated cats after gabapentin was given was lower than in previous investigations (7/25, 28%). Recently, a study demonstrated sedation in 5/10 (50%) of the cats 60 minutes after oral administration of a higher dose of gabapentin (27.9 ± 2.6 mg/kg) [7]. Another investigation mentioned sedation as an at-home side effect observed by the owners in 12/20 (60%) cats[5]. On the contrary, an experiment comparing gabapentin (50 mg and 100 mg) and placebo in community cats kept in cages without handling found no difference in sedation scores between treatments, even though there were variable signs of relaxation[15]. It is worth mentioning that many papers use the terms sedation and tranquillization as synonymous, which might have influenced the conclusions mentioned upward. Additionally, there is still no consensus on whether gabapentin really causes sedation, although some cats became ataxic and slower, but not overtly sedated as they would be with a combination of acepromazine and butorphanol, or acepromazine, butorphanol, and ketamine[52].

Melatonin achieved mild sedation in only one cat. As already mentioned, it is not expected that neither gabapentin nor melatonin would cause proper sedation in animals when administered alone. However, melatonin-induced sleep provided an alternative to conventional sedation in human pediatric patients (<4 years) submitted to magnetic resonance imaging, causing 65% of them to sleep when given 30 minutes before the procedure[53]. Another investigation described melatonin-induced sleep as an excellent alternative to sedation, especially in children younger than three years[54]. Therefore, it is more liable that the cat of the present study was not under actual sedation but was almost asleep.

Our study's interval between drug administration and the CS classification was based on T_{max}. In rats, gabapentin readily crosses the blood-brain barrier (BBB) and concentrates in brain tissue via an active transport process, achieving maximum brain interstitial fluid concentration at approximately one hour[55]. It accumulates intracellularly in brain tissue and has a low degree of binding to plasma proteins (3%), resulting in similar drug concentrations in cerebrospinal fluid and blood plasma[56]. Therefore, this drug's pharmacokinetics/ pharmacodynamics relationships might explain why the sedation is achieved coincidently with its T_{max}. However, the T_{max} of oral gabapentin in cats varies across publications, ranging from 63 minutes[14] to 100 minutes[57] after an oral dose of 10 mg/kg. The variation can be explained by higher bioavailability or differences in sampling sites and times[57]. Coincidentally, a previous study with gabapentin proved that 60 minutes was enough to reach its maximum sedation, while the highest stress reduction was only achieved after two hours[15]. In our experiment, the opposite occurred, with most cats tranquillizing 70 minutes after gabapentin and only a few exhibiting sedation. Of note, the excessive handling and transport from the ECG room to the echocardiography room might have interfered with the degree of CNS depression.

The amphiphilic nature of melatonin allows it to easily cross cellular and morphophysiological barriers, including BBB[58], which would justify considering that its maximum tranquillizer effect would coincide with its T_{max}. The brain has abundant melatonin receptors, permitting it to exert multiple effects[59]. However, little is known about melatonin's pharmacokinetics in cats, and the investigation available focuses on its reproductive action[9]. For this reason, it is impossible to specify the moment tranquilization will take place precisely. In dogs, oral melatonin administration required 90 minutes to calm them in preoperative circumstances[13].

The cats of this research well tolerated the tested substances, and no notable side effects were documented. Drowsiness was the only alteration reported by owners during the day of gabapentin treatment, as seen in people[60] and cats[6]. Also, mydriasis was noticed in one cat during the second echocardiography. The pupillary diameter was unchanged in dogs given gabapentin orally for three days[61], and mydriasis is recognized as a rare side effect in human beings, being considered a psychophysical indicator of CNS depression[62].

An interesting finding was the change in T wave polarity between the ECG tracings of a cat receiving gabapentin. A previous investigation with dexmedetomidine, another sedative drug, also showed inversion on T wave polarity in 2/11 (18%) cats[63]. Drug-induced T-wave inversion is uncommon, and its explanation is unclear[64]. Although this modification is not alarming in this species since positive, biphasic, or negative T waves are considered normal[65], its clinical importance warrants further understanding.

The limitations of this study need to be acknowledged. The adopted CS classification is not widely validated concerning behavioural assessment. Compliance is a categorical variable, most likely to be biased and might require larger samples. Most of the included cats accepted handling already in the first echocardiography, and none of them was classified with the maximum CS. Whether the CS level had been higher, the effects of the treatments might have been even more evident, or one substance might have overlapped the other. Consequently, the experiment could not clarify whether the tested substances would allow the management of extreme struggling cats. Finally, melatonin is not subject to the same standardization required for approved drugs, which may interfere with future results.

Conclusions

Oral gabapentin or melatonin given to cats 70 minutes before echocardiography effectively reduced CS without causing substantial changes in HR, SBP, ECG and most echocardiographic variables, including surrogates for systolic function. The shorter interval adopted for gabapentin is a considerable advantage, as most studies with this drug advise waiting 120 minutes to achieve maximum effect. Our findings facilitate the practice of feline cardiology, allowing the administration of gabapentin in the hospital once the waiting interval is briefer than previously recommended.

Although melatonin improved compliance with fewer changes in echocardiographic variables than other treatments, this was the first study of its use as a pre-appointment medication. According to evidence-based medicine, further investigations should be conducted to confirm the present findings. If confirmed, melatonin has the benefit of being an over-the-counter nutraceutical in most countries, making it easier to obtain and less harmful.

Conflicts of Interest

The authors do not have any conflicts of interest to declare. All co-authors have seen and agree with the contents of the manuscript and there is no financial interest to report. We certify that the submission is original work and is not under review at any other publication.

Funding

The authors received no financial support for the research, authorship, and/or publication of this article.

Ethical approval

This work involved the use of non-experimental animals (owned or unowned) and procedures that differed from established internationally recognised high standards ('best practice') of veterinary clinical care *for the individual patient*. The study therefore had ethical approval from an established committee as stated in the manuscript.

Informed consent

Informed written consent was obtained from the owner or legal custodian of all animal(s) described in this work (either experimental or nonexperimental animals) for the procedure(s) undertaken (either prospective or retrospective studies). No animals or humans are identifiable within this publication, and therefore additional informed consent for publication was not required.

References

1. Luis Fuentes V, Abbott J, Chetboul V, et al. ACVIM consensus statement guidelines for the classification, diagnosis, and management of cardiomyopathies in cats. *J Vet Intern Med* 2020; 1–16.
2. Fox PR, Keene BW, Lamb K, et al. Long-term incidence and risk of noncardiovascular and all-cause mortality in apparently healthy cats and cats with preclinical hypertrophic cardiomyopathy. *J Vet Intern Med* 2019; 33: 2572–2586.

3. Rodan I. Understanding Feline Behavior and Application for Appropriate Handling and Management. *Top Companion Anim Med* 2010; 25: 178–188.
4. Belew AM, Barlett T, Brown SA. Evaluation of the White-Coat Effect in Cats. *J Vet Intern Med* 1999; 13: 134.
5. Van Haaften KA, Forsythe LRE, Stelow EA, et al. Effects of a single preappointment dose of gabapentin on signs of stress in cats during transportation and veterinary examination. *J Am Vet Med Assoc* 2017; 251: 1175–1181.
6. Kruszka M, Graff E, Medam T, et al. Clinical evaluation of the effects of a single oral dose of gabapentin on fear-based aggressive behaviors in cats during veterinary examinations. *J Am Vet Med Assoc* 2021; 259: 1–7.
7. Allen ME, LeBlanc NL, Scollan KF. Hemodynamic, Echocardiographic, and Sedative Effects of Oral Gabapentin in Healthy Cats. *J Am Anim Hosp Assoc* 2021; 57: 278–284.
8. Goericke-Pesch S, Wehrend A, Georgiev P. Suppression of fertility in adult cats. *Reprod Domest Anim* 2014; 49: 33–40.
9. Graham LH, Swanson WF, Wildt DE, et al. Influence of oral melatonin on natural and gonadotropin-induced ovarian function in the domestic cat. *Theriogenology* 2004; 61: 1061–1076.
10. Faya M, Carranza A, Priotto M, et al. Long-term melatonin treatment prolongs interestrus, but does not delay puberty, in domestic cats. *Theriogenology* 2011; 75: 1750–1754.
11. Gimenez F, Stornelli MC, Tittarelli CM, et al. Suppression of estrus in cats with melatonin implants. *Theriogenology* 2009; 72: 493–499.
12. Madsen BK, Zetner D, Møller AM, et al. Melatonin for preoperative and

postoperative anxiety in adults. *Cochrane Database Syst Rev*; 2020. Epub ahead of print 8 de dezembro de 2020. DOI: 10.1002/14651858.CD009861.pub3.

13. Niggemann JR, Tichy A, Eberspächer-Schweda MC, et al. Preoperative calming effect of melatonin and its influence on propofol dose for anesthesia induction in healthy dogs. *Vet Anaesth Analg* 2019; 46: 560–567.
14. Adrian D, Papich MG, Baynes R, et al. The pharmacokinetics of gabapentin in cats. *J Vet Intern Med* 2018; 32: 1996–2002.
15. Pankratz KE, Ferris KK, Griffith EH, et al. Use of single-dose oral gabapentin to attenuate fear responses in cage-trap confined community cats: a double-blind, placebo-controlled field trial. *J Feline Med Surg* 2018; 20: 535–543.
16. Quimby J, Gowland S, Carney HC, et al. 2021 AAHA/AAFP Feline Life Stage Guidelines. *J Feline Med Surg* 2021; 57: 51–72.
17. Häggström J, Andersson O, Falk T, et al. Effect of Body Weight on Echocardiographic Measurements in 19,866 Pure-Bred Cats with or without Heart Disease. *J Vet Intern Med* 2016; 30: 1601–1611.
18. Binns SH, Sisson DD, Buoscio DA, et al. Doppler Ultrasonographic, Oscillometric Sphygmomanometric, and Photoplethysmographic Techniques for Noninvasive Blood Pressure Measurement in Anesthetized Cats. *J Vet Intern Med* 1995; 9: 405–414.
19. Lim CY, In J. Randomization in clinical studies. *Korean J Anesthesiol* 2019; 72: 221–232.
20. Thomas WP, Gaber CE, Jacobs GJ, et al. Recommendations for Standards in Transthoracic Two-Dimensional Echocardiography in the Dog and Cat. *Vet Radiol Ultrasound* 1994; 35: 173–178.

21. Rishniw M, Erb HN. Evaluation of four 2-dimensional echocardiographic methods of assessing left atrial size in dogs. *J Vet Intern Med* 2000; 14: 429–435.

22. Abbott JA, MacLean HN. Two-dimensional echocardiographic assessment of the feline left atrium. *J Vet Intern Med* 2013; 20: 111–9.

23. Schober KE, Wetli E, Drost WT. Radiographic and echocardiographic assessment of left atrial size in 100 cats with acute left-sided congestive heart failure. *Vet Radiol Ultrasound* 2014; 55: 359–367.

24. Koffas H, Dukes-McEwan J, Corcoran BM, et al. Pulsed tissue Doppler imaging in normal cats and cats with hypertrophic cardiomyopathy. *J Vet Intern Med* 2006; 20: 65–77.

25. Spalla I, Payne JRR, Borgeat K, et al. Mitral Annular Plane Systolic Excursion and Tricuspid Annular Plane Systolic Excursion in Cats with Hypertrophic Cardiomyopathy. *J Vet Intern Med* 2017; 31: 691–699.

26. Wolf M, Lucina SBSB, Brüler BCBC, et al. Assessment of longitudinal systolic function using tissue motion annular displacement in healthy dogs. *J Vet Cardiol*; 20. Epub ahead of print 2018. DOI: 10.1016/j.jvc.2018.04.004.

27. Spalla I, Boswood A, Connolly DJ, et al. Speckle tracking echocardiography in cats with preclinical hypertrophic cardiomyopathy. *J Vet Intern Med* 2019; 33: 1232–1241.

28. Buss SJ, Mereles D, Emami M, et al. Rapid assessment of longitudinal systolic left ventricular function using speckle tracking of the mitral annulus. *Clin Res Cardiol* 2012; 101: 273–280.

29. KLERMAN GL, DIMASCIO A, HAVENS LL SJ. Sedation and Tranquilization: a Comparison of the Effects of a Number of Psychopharmacologic Agents upon

Normal Human Subjects. *Arch Gen Psychiatry* 1960; 3: 4–13.

30. Steagall PVM, Taylor PM, Rodrigues LCC, et al. Analgesia for cats after ovariohysterectomy with either buprenorphine or carprofen alone or in combination. *Vet Rec* 2009; 164: 359–363.
31. Erdfelder E, FAul F, Buchner A, et al. Statistical power analyses using G*Power 3.1: Tests for correlation and regression analyses. *Behav Res Methods* 2009; 41: 1149–1160.
32. R Core Team. R: a language and environment for statistical computing. Vienna: R Foundation for Statistical Computing, 2021, https://www.r-project.org/.
33. Levine ED. Feline Fear and Anxiety. *Vet Clin North Am - Small Anim Pract* 2008; 38: 1065–1079.
34. Ciani E, Haug TM, Maugars G, et al. Effects of Melatonin on Anterior Pituitary Plasticity: A Comparison Between Mammals and Teleosts. *Front Endocrinol (Lausanne)* 2021; 11: 1–20.
35. Rivara S, Pala D, Bedini A, et al. Therapeutic uses of melatonin and melatonin derivatives: A patent review (2012 - 2014). *Expert Opin Ther Pat* 2015; 25: 425–441.
36. Rios ERV, Venâncio ET, Rocha NFM, et al. Melatonin: Pharmacological Aspects and Clinical Trends. *Int J Neurosci* 2010; 120: 583–590.
37. Behuliak M, Bencze M, Polgárová K, et al. Hemodynamic response to gabapentin in conscious spontaneously hypertensive rats the role of sympathetic nervous system. *Hypertension* 2018; 72: 676–685.
38. Belliotti TR, Capiris T, Ekhato IV, et al. Structure-activity relationships of pregabalin and analogues that target the α2-δ protein. *J Med Chem* 2005; 48:

2294–2307.

39. Karbić VO, Škoda M, Antončić D, et al. Gabapentin-induced changes of plasma cortisol level and immune status in hysterectomized women. *Int Immunopharmacol* 2014; 23: 530–536.
40. Barrenetxe J, Delagrange P, Martínez JA. Physiological and metabolic functions of melatonin. *J Physiol Biochem* 2004; 60: 61–72.
41. Salavati S, Mogheiseh A, Nazifi S, et al. The effects of melatonin treatment on oxidative stress induced by ovariohysterectomy in dogs. *BMC Vet Res* 2021; 17: 1–8.
42. Farhadi N, Gharghani M, Farhadi Z. Effects of long-term light, darkness and oral administration of melatonin on serum levels of melatonin. *Biomed J* 2016; 39: 81–84.
43. Cajochen C, Kräuchi K, Wirz-Justice A. The Acute Soporific Action of Daytime Melatonin Administration: Effects on the EEG during Wakefulness and Subjective Alertness. *J Biol Rhythms* 1997; 12: 636–643.
44. Taylor KS, Murai H, Millar PJ, et al. Arousal from Sleep and Sympathetic Excitation during Wakefulness. *Hypertension* 2016; 68: 1467–1474.
45. Abbott JA. Heart rate and heart rate variability of healthy cats in home and hospital environments. *J Feline Med Surg* 2005; 7: 195–202.
46. Pongkan W, Piamsiri C, Dechvongya S, et al. Short-term melatonin supplementation decreases oxidative stress but does not affect left ventricular structure and function in myxomatous mitral valve degenerative dogs. *BMC Vet Res* 2022; 18: 1–11.
47. Kessler M., Turner DC. Stress and adaptation of cats (Felis silvestris catus) housed singly, in pairs and in groups in boarding catteries. *Anim Welf* 1997; 6:

243–254.

48. Mccune S. *Temperament and the welfare of caged cats*. University of Cambridge, 1992. Epub ahead of print 1992. DOI: 10.13140/RG.2.1.4799.4644.

49. McCobb EC, Patronek GJ, Marder A, et al. Assessment of stress levels among cats in four animal shelters. *J Am Vet Med Assoc* 2005; 226: 548–555.

50. Lotfy M, Ayaad M. Preoperative oral melatonin can reduce preoperative anxiety and postoperative analgesia in a dose-dependent manner. *Ain-Shams J Anesthesiol* 2021; 13: 13–32.

51. Costa R, Karas A, Borns-Weil S. Chill Protocol to Manage Aggressive & Fearful Dogs. *Clin Br* 2019; 63–65.

52. Ward JL, Schober KE, Fuentes VL, et al. Effects of sedation on echocardiographic variables of left atrial and left ventricular function in healthy cats. *J Feline Med Surg* 2012; 14: 678–685.

53. Johnson K, Page A, Williams H, et al. The use of melatonin as an alternative to sedation in uncooperative children undergoing an MRI examination. *Clin Radiol* 2002; 57: 502–506.

54. Schmidt CM, Knief A, Deuster D, et al. Melatonin is a useful alternative to sedation in children undergoing brainstem audiometry with an age dependent success rate - A field report of 250 investigations. *Neuropediatrics* 2007; 38: 2–4.

55. Welty DF, Schielke GP, Vartanian MG, et al. Gabapentin anticonvulsant action in rats: disequilibrium with peak drug concentrations in plasma and brain microdialysate. *Epilepsy Res* 1993; 16: 175–181.

56. Chappell M, Payne S. The Central Nervous System. *Biosyst Biorobotics* 2020;

24: 141–152.

57. Siao KT, Pypendop BH, Ilkiw JE. Pharmacokinetics of gabapentin in cats. *Am J Vet Res* 2010; 71: 817–821.

58. Alavijeh MS, Chishty M, Qaiser MZ, et al. Drug metabolism and pharmacokinetics, the blood-brain barrier, and central nervous system drug discovery. *NeuroRx* 2005; 2: 554–571.

59. Ng KY, Leong MK, Liang H, et al. Melatonin receptors: distribution in mammalian brain and their respective putative functions. *Brain Struct Funct* 2017; 222: 2921–2939.

60. Calandre EP, Rico-Villademoros F, Slim M. Alpha2delta ligands, gabapentin, pregabalin and mirogabalin: a review of their clinical pharmacology and therapeutic use. *Expert Rev Neurother* 2016; 16: 1263–1277.

61. Shukla AK, Pinard CL, Flynn BL, et al. Effects of orally administered gabapentin, tramadol, and meloxicam on ocular variables in healthy dogs. *Am J Vet Res* 2020; 81: 973–984.

62. Peterson BL. Prevalence of gabapentin in impaired driving cases in Washington State in 2003-2007. *J Anal Toxicol* 2009; 33: 545–549.

63. Carvalho ER, Champion T, D'Otaviano Vilani RGC, et al. Sedative and electrocardiographic effects of low dose dexmedetomidine in healthy cats. *Pesqui Vet Bras* 2019; 39: 142–147.

64. Malik M. Drug-induced changes in the T-wave morphology. *Drug Saf* 2009; 32: 613–617.

65. Roberto Santilli, Sidney Moïse, Romain Pariaut MP. *Electrocardiography of the dog and cat. Diagnosis of arrhythmias.* 2nd Ed. Florida : Edra Pulishing, 2018.

Figures

Figure 1 - Algorithm describing the sequence of procedures, starting with baseline exams (electrocardiography, systemic blood pressure measurement and echocardiography), followed by the drug administration, interval, and second set of exams

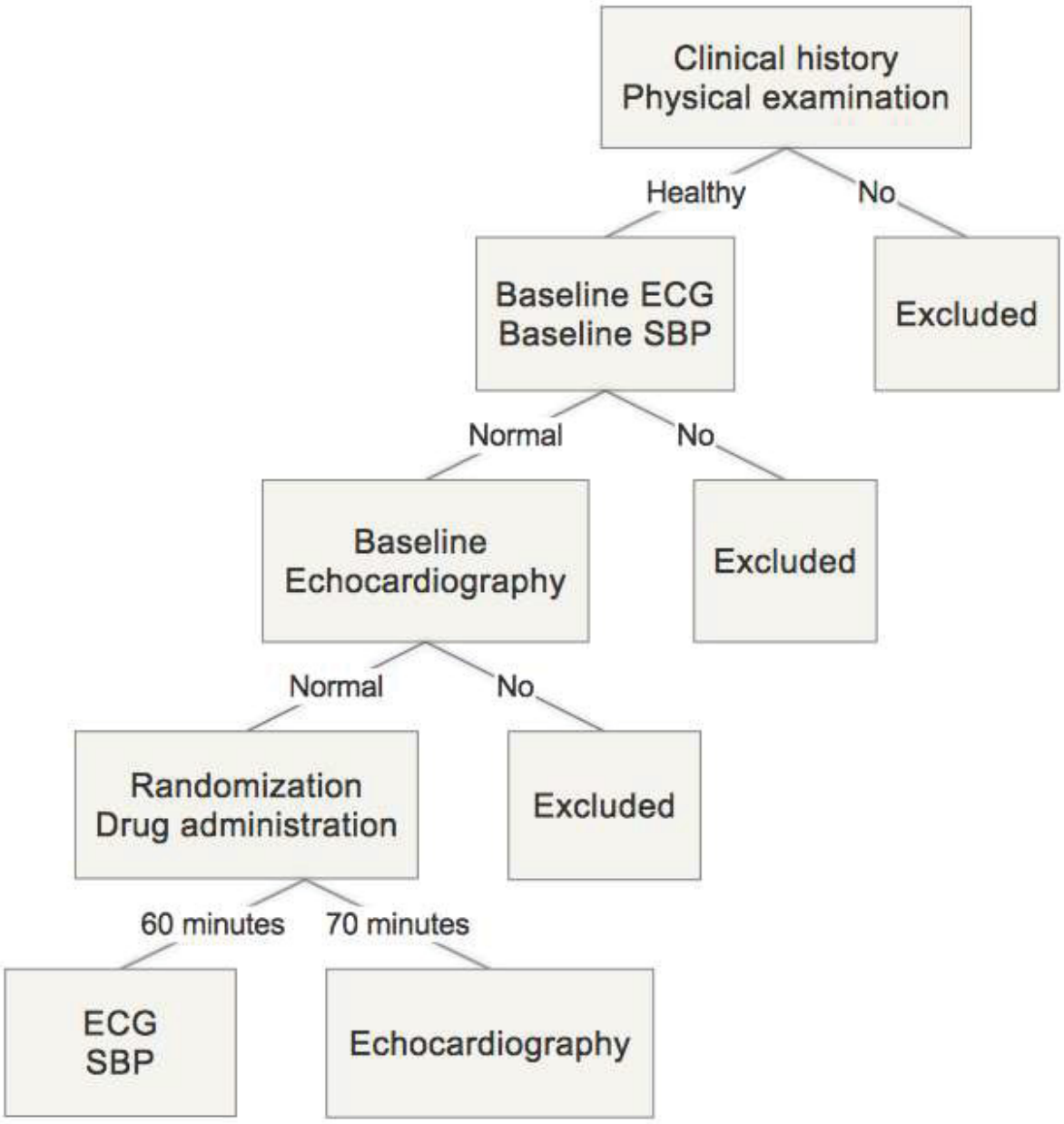

ECG: electrocardiography; SBP: systemic blood pressure measurement

Figure 2 - Boxplots representing cardiovascular variables with significant difference after treatment

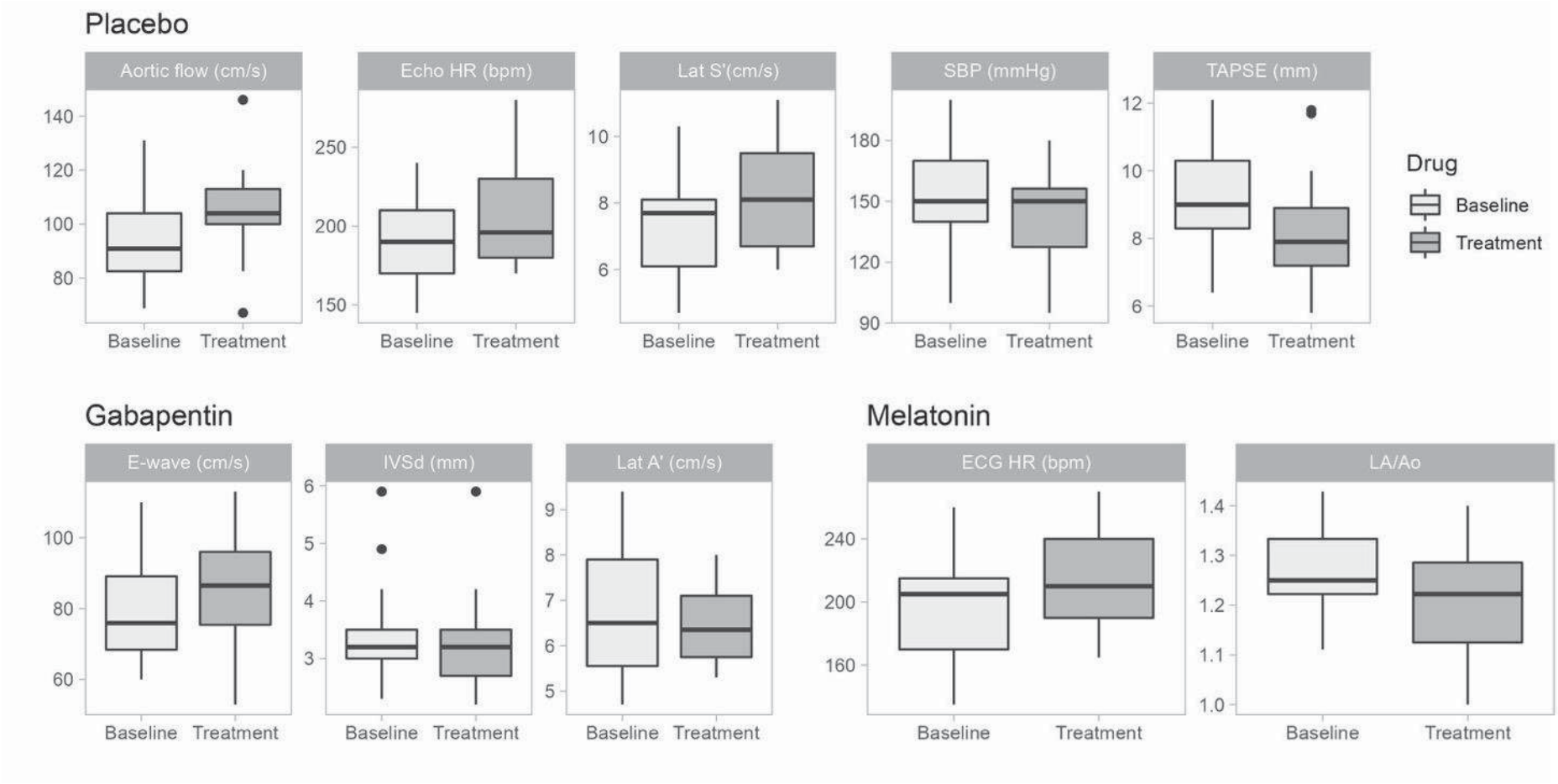

Tables

Talbe 1 – Compliance score (CS) and sedation score (SS)

Score	CS[1]	Score	SS[2]
0	No resistance to handling	0	No sedation
1	Minimally resistant to handling	1	Standing but unstable
2	Struggling and difficult to handle	2	Sternal recumbency
3	Extreme struggling with or without urination or defecation	3	Can lift head
		4	Asleep or unresponsive to clap

1: van Haaften et al, 2017; 2: Steagall et al, 2009

Table 2 – Means of age, body weight, body surface area and drug doses in gabapentin, melatonin and placebo treatments

Variable	Gabapentin			Melatonin			Placebo		
	Mean (SD)	Min	Max	Mean (SD)	Min	Max	Mean	Min	Max
Age (years)	4.8 (2.4)	1	9	5.3 (2.3)	1	10	5.1 (2.7)	1	10
BW (kilos)	5.1 (1.6)	3.05	11.0	4,7 (1.2)	2.5	7.4	4.5 (1.3)	2.9	7.3
BSA (m^2)	0.293 (0.057)	0.210	0.348	0.278 (0.047)	0.184	0.380	0.272 (0.049)	0.203	0.376
Dose (mg/kg)	19.6 (5.3)	9.09	32.79	0.7 (0.2)	0.41	1.20	-	-	-

BW: body weight; BSA: body surface area; SD: standard deviation; Min: minimum value; Max: maximum value

Table 3 - Means and standard deviations of systemic blood pressure measurements and variables from electrocardiography and echocardiography, before (baseline) and after treatment

	Gabapentin					Melatonin					Placebo				
	Baseline		Treatment			Baseline		Treatment		p-	Baseline		Treatment		
Variables	Mean	SD	Mean	SD	p-value†	Mean	SD	Mean	SD	value†	Mean	SD	Mean	SD	p-value†
SBP (mmHg)	148.1	21	151.2	18.5	0.391	148	20.9	158.2	28.1	0.053	**152.9**	**24.4**	**144**	**22.9**	**0.027**
Electrocardiographic indexes															
ECG Axis (º)	35	80.5	31.2	79.6	0.349	52.7	69.4	39.6	77.8	0.6	39.2	57.8	39.7	59.6	1.000
ECG HR (bpm)	206.8	22.7	206.4	33.9	0.714	**198.2**	**34.4**	**212.5**	**30.3**	**0.012**	195.4	26.3	202.7	30.1	0.109
QT (s)	0.149	0.015	0.151	0.018	0.745	0.1468	0.024	0.149	0.018	0.774	0.155	0.018	0.149	0.018	0.097
Echocardiographic standard indexes															
Echo HR (bpm)	201.4	29.9	208.7	29.4	0.102	202	25.7	205.6	31.9	0.452	**190.6**	**25.7**	**206**	**31.9**	**<0.001**
LA (mm)	11.0	1.7	11	1.6	0.715	11	1.2	10.8	1.3	0.588	10.9	1.2	10.8	1.4	0.811
Ao (mm)	9.0	1.2	8.7	1.1	0.172	8.7	0.9	8.9	0.8	0.318	8.8	1.1	9.0	1.3	0.616
LA/Ao	1.2	0.1	1.3	0.1	0.141	**1.3**	**0.1**	**1.2**	**0.1**	**0.035**	1.2	0.1	1.2	0.1	0.519
LA FS (%)	33.9	5.2	35.8	6.6	0.201*	37.2	6.7	35.8	6.0	0.436*	33.9	5.9	36.7	7.0	0.818*
LA diameter (mm)	13.1	1.5	13.1	1.3	0.748*	12.8	1.3	12.6	1.1	0.544*	12.8	1.1	12.8	1.1	0.916*
IVSd (mm)	**3.2**	**0.7**	**3.4**	**0.8**	**0.035**	3.2	0.6	3.2	0.6	1.0	3.3	0.5	3.3	0.5	0.807
LVIDd (mm)	16.1	2.2	16	1.7	0.892*	15.9	2.2	16	2.0	0.938*	15.4	1.5	15.5	1.9	0.893*
LVPWd (mm)	3.7	0.7	4	1.2	0.081*	3.8	0.6	3.5	0.8	0.135*	3.6	0.7	3.6	0.7	1.000*
IVSs (mm)	6.4	1.4	6.6	1.3	0.746	6.5	1.1	6.6	1.4	0.819	6.4	1.3	6.4	1.5	0.909
LVIDs (mm)	7.6	1.8	7.6	1.5	0.891*	7.3	1.6	7.2	1.4	0.867*	7.1	1.3	7.4	1.7	0.474*
LVPWs (mm)	6.1	1.1	6.4	1.3	0.251*	6.1	1.1	6.0	0.8	0.734*	6.2	1.1	6.3	1.1	0.801*
FS (%)	52.9	6.6	52.6	8.8	0.853*	55.1	7.1	54.6	7.5	0.805*	52.2	8.9	53.2	6.8	0.659*
EF (%)	86.2	4.7	85.2	6.8	0.423*	87.7	5.2	87.3	5.6	0.787*	84.9	6.8	86	5.2	0.509*
Aortic Flow (cm/s)	96.9	21.8	101.7	17.8	0.095*	97.8	19.8	103.2	14.7	0.320*	**93.2**	**16.4**	**104.6**	**14.7**	**0.023***
Pulmonar Flow (cm/s)	86.1	15.2	86.2	13.4	0.953*	87.2	14.4	90.8	14.8	0.383*	86.8	16.5	93.5	12.8	0.184*
Mitral E-wave (cm/s)	**78.6**	**14.5**	**86.5**	**14.5**	**0.039**	83.3	15.9	83.8	17.3	0.943	79.2	17.3	82.4	16.3	0.146
Mitral A-wave (cm/s)	61.6	14.1	69.4	19.7	0.562	61.4	8.4	60.1	15.6	0.82	60	9.8	66.1	12.9	0.233
E/A ratio	1.2	0.2	1.2	0.2	0.687	1.2	0.2	1.2	0.3	0.496	1.2	0.3	1.1	0.2	0.151

Septum S' (cm/s)	8.0	2.0	8.8	2.2	0.130*	8.2	1.7	8.8	2.0	0.371*	7.7	1.7	8.4	1.9	0.129*
Septum E' (cm/s)	9.5	2.8	10.9	3.1	0.071*	9.8	2.5	9.7	2.8	0.872*	8.5	2.7	9.6	3.4	0.271*
Septum A' (cm/s)	**7.2**	**2.6**	**6.8**	**1.4**	**0.005***	7.3	2.3	7.3	1.9	0.821*	6.9	1.8	7.3	1.4	0.957*
Lateral S’ (cm/s)	7.6	1.7	7.7	1.8	0.821*	7.6	1.4	7.7	1.8	0.761*	**7.3**	**1.5**	**8.2**	**1.7**	**0.047***
Lateral E’ (cm/s)	10.5	3.2	11.2	2.6	0.237*	10.6	2.4	10.3	3.0	0.742*	10	2.6	10.5	2.8	0.521*
Lateral A’ (cm/s)	6.7	1.5	6.5	1.2	0.485*	8	1.8	7.2	1.5	0.585*	7.3	1.3	7.1	1.9	0.708*
IVRT (s)	52.6	5.1	54.4	7.6	0.248*	51.1	6.4	50.7	8.2	0.846*	50	7.4	52.3	8.4	0.342*
MAPSE FW (mm)	4.7	0.8	4.8	1.0	0.822*	4.9	1	5.1	1.0	0.626*	4.9	0.9	4.7	0.5	0.303*
MAPSE IVS (mm)	4.3	0.9	4.3	0.9	0.956*	4.5	0.7	4.4	1.0	0.881*	4.5	1.0	4.5	0.7	0.878*
TAPSE (mm)	8.4	2.8	8.5	1.5	0.162	8.6	1.4	8.7	1.3	0.903	**9.2**	**1.5**	**8.2**	**1.5**	**0.010**
Speckle-tracking echocardiographic indexes															
AP2 LSt (%)	28	3.1	28.7	4.3	0.459	29.3	4.7	28.2	4.9	0.174	28.6	5.0	27.4	4.0	0.178
AP2 TMAD MP (mm)	4.8	1.1	5.0	1.2	0.209*	5.0	0.7	4.6	1.0	0.254*	5.1	1.0	4.8	0.9	0.192*
AP2 TMAD MP%	18.2	2.9	18.7	3.7	0.470*	19.1	3.1	17.8	3.2	0.147*	19.3	3.6	18.1	4.0	0.214*
AP4 LSt (%)	27.4	2.6	29.1	5.6	0.191	28.5	4.7	27.1	3.9	0.225	27.2	4.9	27.7	4.8	0.457
AP4 TMAD MP (mm)	4.7	0.8	4.8	1.2	0.931	4.6	1.0	4.5	0.8	0.474	4.6	0.9	4.7	1.1	0.399
AP4 TMAD MP%	17.9	2.3	18.4	4.4	0.647	18	4.2	17.6	3.3	0.542	17.7	3.0	18.1	3.6	0.767
Global LSt (%)	27.7	2.3	28.9	4.4	0.215	28.9	4.1	27.7	4.0	0.142	27.9	4.6	27.6	3.8	0.811
Global TMAD MP (mm)	4.8	0.9	4.9	1.0	0.406*	4.8	0.7	4.6	0.8	0.284*	4.9	0.8	4.8	0.9	0.827*
Global TMAD MP%	18.1	2.2	18.5	3.5	0.477*	18.5	3.0	17.7	2.6	0.233*	18.5	2.7	18.2	3.1	0.626*

[†]p-value< 0.05 is statistically significant

*Normal distibution (paired t-test)

SBP: systolic blood pressure; ECG: electrocardiography; HR: heart rate; QT: time from the beginning of the QRS complex to the end of the T wave; Echo duration: time spent to perform the echocardiography; LA: left atrium; Ao: Aorta; LA FS: fractional shortening of the left atrium; LA diameter: diameter of the LA at the right parasternal longitudinal four-chamber view; IVSd: interventricular septum thickness at end-diastole; LIVDd: left ventricular internal dimension at end-diastole; LVPWd: left ventricular posterior wall thickness at end-diastole; IVSs: interventricular septum thickness at end-systole; LIVDs: left ventricular internal dimension at end- systole; LVPWs: left ventricular posterior wall thickness at end- systole; FS: fractional shortening; EF: ejection fraction; S’: mitral annular peak systolic velocity; E´: mitral annular peak velocity at early diastole; A’: mitral annular peak velocity at late diastole; IVRT: isovolumic relaxation time; MAPSE FW: mitral annular plane systolic excursion obtained at the free wall annulus; MAPSE IVS: mitral annular plane systolic excursion obtained at the interventricular septum annulus; TAPSE: tricuspid annular plane systolic excursion; AP2: Apical two-chamber image; LSt: longitudinal strain; TMAD MP: displacement arof a virtual midpoint between the septal and lateral hinge points of mitral annulus towards the LV apex; TMAD MP%: fractional displacement of the midpoint towards the left ventricular apex in relation to the total length of the left ventricle; AP4: Apical four-chamber image

Table 4 - Behavioural assessment using the compliance score (CS) in gabapentin, melatonin and placebo groups before and after the treatment

CS	Control		Drug		p-value*
	N	%	N	%	
Gabapentin					
0	10	40%	19	76%	
1	9	36%	3	11%	**0.037**
2	6	24%	3	11%	
Melatonin					
0	13	52%	18	72%	
1	10	40%	3	12%	**0.049**
2	2	8%	4	16%	
Placebo					
0	11	44%	16	64%	
1	10	40%	8	32%	0.374
2	4	16%	1	4%	

*p-value< 0.05 is statistically significant

CONSIDERAÇÕES FINAIS

O TMAD é viável para avaliar a função sistólica longitudinal do ventrículo esquerdo em gatos saudáveis, com repetibilidade e reprodutibilidade aceitáveis. Como o anel mitral pode ser facilmente identificado, essa técnica tem a vantagem de não requerer imagens de qualidade tão alta quanto o LSt. Comparado ao MAPSE, o TMAD se destaca por ser ângulo independente, sendo chamado de $MAPSE_{STE}$ por alguns autores.

A solução oftálmica de timolol a 0,5%, reduziu indices comumente usados, como a fração de encurtamento do VE e AE, a fração de ejeção do VE, o MAPSE FW e a onda S' do Doppler tecidual. Além disso, o timolol não facilitou a avaliação diastólica, pois a diminuição da FC não foi suficiente para separar as ondas transmitrais. Além disso, o droga ampliou significativamente o tempo de relaxamento isovolumétrico (TRIV), estando esse índice acima do valor de referência espécie (60 ms) na maioria dos gatos após tratamento.

Por último, tanto a gabapentina como a melatonina administradas 60 minutos antes do ECG e aferição da PAS, e 70 minutos antes da ecocardiografia, tiveram ação calmante sem alterar a maioria das variáveis observadas, incluindo os índices sistólicos. Clínicos e cardiologistas poderão aguardar menos tempo de ação da gabapentina para obter a tranquilização. Embora tenha mostrado efeito ansiolítico menos evidentes que a gapapentina, a melatonina também diminuiu o escore de comportamento, tendo a vantagem de ser mais facilmente adquirida pelos proprietários por ser considerada um nutracêutico.

REFERÊNCIAS

Abbott JA (2005) Heart rate and heart rate variability of healthy cats in home and hospital environments. J Feline Med Surg 7:195–202. https://doi.org/10.1016/j.jfms.2004.12.003

Abbott JA (2010) Feline hypertrophic cardiomyopathy: An update. Vet Clin North Am - Small Anim Pract 40:685–700. https://doi.org/10.1016/j.cvsm.2010.04.004

Abbott JA, MacLean HN (2013) Two-dimensional echocardiographic assessment of the feline left atrium. J Vet Intern Med 20:111–9. https://doi.org/10.1892/0891-6640(2006)20[111:teaotf]2.0.co;2

Acierno MJ, Brown S, Coleman AE, et al (2018) ACVIM consensus statement: Guidelines for the identification, evaluation, and management of systemic hypertension in dogs and cats. J Vet Intern Med 32:1803–1822. https://doi.org/10.1111/jvim.15331

Adrian D, Papich MG, Baynes R, et al (2018) The pharmacokinetics of gabapentin in cats. J Vet Intern Med 32:1996–2002. https://doi.org/10.1111/jvim.15313

Alavijeh MS, Chishty M, Qaiser MZ, Palmer AM (2005) Drug metabolism and pharmacokinetics, the blood-brain barrier, and central nervous system drug discovery. NeuroRx 2:554–571. https://doi.org/10.1602/neurorx.2.4.554

Allen ME, LeBlanc NL, Scollan KF (2021) Hemodynamic, Echocardiographic, and Sedative Effects of Oral Gabapentin in Healthy Cats. J Am Anim Hosp Assoc 57:278–284. https://doi.org/10.5326/jaaha-ms-7081

Aloia E, Cameli M, D'Ascenzi F, et al (2016) TAPSE: An old but useful tool in different diseases. Int J Cardiol 225:177–183. https://doi.org/10.1016/j.ijcard.2016.10.009

Arnold RW (2021) The oculocardiac reflex: A review. Clin Ophthalmol 15:2693–2725. https://doi.org/10.2147/OPTH.S317447

Asada D, Okumura K, Ikeda K, Itoi T (2018) Tissue Motion Annular Displacement of the Mitral Valve Can Be a Useful Index for the Evaluation of Left Ventricular Systolic Function by Echocardiography in Normal Children. Pediatr Cardiol 39:976–982. https://doi.org/10.1007/s00246-018-1847-2

Bansal M, Cho GY, Chan J, et al (2008) Feasibility and Accuracy of Different Techniques of Two-Dimensional Speckle Based Strain and Validation With Harmonic Phase Magnetic Resonance Imaging. J Am Soc Echocardiogr 21:1318–1325. https://doi.org/10.1016/j.echo.2008.09.021

Barbier P, Solomon SB, Schiller NB, Glantz SA (1999) Left atrial relaxation and left ventricular systolic function determine left atrial reservoir function. Circulation 100:427–436. https://doi.org/10.1161/01.CIR.100.4.427

Barrenetxe J, Delagrange P, Martínez JA (2004) Physiological and metabolic functions of melatonin. J Physiol Biochem 60:61–72. https://doi.org/10.1007/BF03168221

Behuliak M, Bencze M, Polgárová K, et al (2018) Hemodynamic response to gabapentin in conscious spontaneously hypertensive rats the role of sympathetic nervous system. Hypertension 72:676–685. https://doi.org/10.1161/HYPERTENSIONAHA.118.09909

Belew AM, Barlett T, Brown SA (1999) Evaluation of the White-Coat Effect in Cats. J Vet Intern Med 13:134. https://doi.org/10.1892/0891-6640(1999)013<0134:EOTWCE>2.3.CO;2

Belliotti TR, Capiris T, Ekhato IV, et al (2005) Structure-activity relationships of pregabalin and analogues that target the α2-δ protein. J Med Chem 48:2294–110

2307. https://doi.org/10.1021/jm049762l

Bin Waqar SH, Rehan A, Zammam M (2019) Postprandial Head-drops: Insight into Systemic Effects of Ocular Timolol Preparation in Elderly. Cureus 11:. https://doi.org/10.7759/cureus.4780

Binns SH, Sisson DD, Buoscio DA, Schaeffer DJ (1995) Doppler Ultrasonographic, Oscillometric Sphygmomanometric, and Photoplethysmographic Techniques for Noninvasive Blood Pressure Measurement in Anesthetized Cats. J Vet Intern Med 9:405–414. https://doi.org/10.1111/j.1939-1676.1995.tb03301.x

Black DE, Bryant J, Peebles C, et al (2014) Tissue motion annular displacement of the mitral valve using two-dimensional speckle tracking echocardiography predicts the left ventricular ejection fraction in normal children. Cardiol Young 24:640–648. https://doi.org/10.1017/S1047951113000863

Blanc VF, Hardy JF, Milot J, Jacob JL (1983) The oculocardiac reflex: a graphic and statistical analysis in infants and children. Can Anaesth Soc J 30:360–369. https://doi.org/10.1007/BF03007858

Bland JM, Altman DG (2010) Statistical methods for assessing agreement between two methods of clinical measurement. Int J Nurs Stud 47:931–936. https://doi.org/10.1016/j.ijnurstu.2009.10.001

Buss SJ, Mereles D, Emami M, et al (2012) Rapid assessment of longitudinal systolic left ventricular function using speckle tracking of the mitral annulus. Clin Res Cardiol 101:273–280. https://doi.org/10.1007/s00392-011-0389-x

Caivano D, Rishniw M, Baiona L, et al (2020) Assessment of Longitudinal Left Ventricle Deformation by 2-Dimensional Speckle Tracking Echocardiography Obtained from Different Views in Cats. Vet Sci 7:104. https://doi.org/10.3390/vetsci7030104 111

Cajochen C, Kräuchi K, Wirz-Justice A (1997) The Acute Soporific Action of Daytime Melatonin Administration: Effects on the EEG during Wakefulness and Subjective Alertness. J Biol Rhythms 12:636–643. https://doi.org/10.1177/074873049701200619

Calandre EP, Rico-Villademoros F, Slim M (2016) Alpha2delta ligands, gabapentin, pregabalin and mirogabalin: a review of their clinical pharmacology and therapeutic use. Expert Rev Neurother 16:1263–1277. https://doi.org/10.1080/14737175.2016.1202764

Carabine UA, Milligan KR, Moore JA (1991) Adrenergic modulation of preoperative anxiety: A comparison of temazepam, clonidine, and timolol. Anesth Analg 73:633–637. https://doi.org/10.1213/00000539-199111000-00021

Carlsson M, Ugander M, Mosén H, et al (2007) Atrioventricular plane displacement is the major contributor to left ventricular pumping in healthy adults, athletes, and patients with dilated cardiomyopathy. Am J Physiol Circ Physiol 292:H1452–H1459. https://doi.org/10.1152/ajpheart.01148.2006

Carvalho ER, Champion T, D'Otaviano Vilani RGC, et al (2019) Sedative and electrocardiographic effects of low dose dexmedetomidine in healthy cats. Pesqui Vet Bras 39:142–147. https://doi.org/10.1590/1678-5150-PVB-5823

Chappell M, Payne S (2020) The Central Nervous System. Biosyst Biorobotics 24:141–152. https://doi.org/10.1007/978-3-030-39705-0_10

Chen L, Zeng X, Huang X (2018) Efficacy and safety of intraocular pressure-lowering agents bimatoprost and timolol maleate in glaucoma. Int J Pharmacol 14:179–186. https://doi.org/10.3923/ijp.2018.179.186

Chetboul V, Athanassiadis N, Carlos C, et al (2004) Quantification, repeatability, and reproducibility of feline radial and longitudinal left ventricular velocities by tissue 112

Doppler imaging. Am J Vet Res 65:566–572. https://doi.org/10.2460/ajvr.2004.65.566

Chetboul V, Tissier R (2012) Echocardiographic assessment of canine degenerative mitral valve disease. J Vet Cardiol 14:127–148. https://doi.org/10.1016/j.jvc.2011.11.005

Ciani E, Haug TM, Maugars G, et al (2021) Effects of Melatonin on Anterior Pituitary Plasticity: A Comparison Between Mammals and Teleosts. Front Endocrinol (Lausanne) 11:1–20. https://doi.org/10.3389/fendo.2020.605111

Collier P, Phelan D, Klein A (2017) A Test in Context: Myocardial Strain Measured by Speckle-Tracking Echocardiography. J Am Coll Cardiol 69:1043–1056. https://doi.org/10.1016/j.jacc.2016.12.012

Costa R, Karas A, Borns-Weil S (2019) Chill Protocol to Manage Aggressive & Fearful Dogs. Clin Br 63–65

Erdfelder E, FAul F, Buchner A, Lang AG (2009) Statistical power analyses using G*Power 3.1: Tests for correlation and regression analyses. Behav Res Methods 41:1149–1160. https://doi.org/10.3758/BRM.41.4.1149

Farhadi N, Gharghani M, Farhadi Z (2016) Effects of long-term light, darkness and oral administration of melatonin on serum levels of melatonin. Biomed J 39:81–84. https://doi.org/10.1016/j.bj.2015.09.003

Faul F, Erdfelder E, Lang A-G, Buchner A (2007) G*Power 3: a flexible statistical power analysis program for the social, behavioral, and biomedical sciences. Behav Res Methods 39:175–91. https://doi.org/10.3758/bf03193146

Faya M, Carranza A, Priotto M, et al (2011) Long-term melatonin treatment prolongs interestrus, but does not delay puberty, in domestic cats. Theriogenology 75:1750–1754. https://doi.org/10.1016/j.theriogenology.2011.01.015 113

Ferraro AM, Adar A, Ghelani SJ, et al (2020) Speckle tracking echocardiographically-based analysis of ventricular strain in children: an intervendor comparison. Cardiovasc Ultrasound 18:15. https://doi.org/10.1186/s12947-020-00199-x

Fleiss JL (1986) Reliability of Measurement. John Wiley & Sons, Inc

Fox PR, Keene BW, Lamb K, et al (2019) Long-term incidence and risk of noncardiovascular and all-cause mortality in apparently healthy cats and cats with preclinical hypertrophic cardiomyopathy. J Vet Intern Med 33:2572–2586. https://doi.org/10.1111/jvim.15609

Galiuto L, Ignone G, DeMaria AN (1998) Contraction and relaxation velocities of the normal left ventricle using pulsed-wave tissue Doppler echocardiography. Am J Cardiol 81:609–614. https://doi.org/10.1016/S0002-9149(97)00990-9

Garcia MJ, Thomas JD, Klein AL (1998) New doppler echocardiographic applications for the study of diastolic function. J Am Coll Cardiol 32:865–875. https://doi.org/10.1016/S0735-1097(98)00345-3

Gimenez F, Stornelli MC, Tittarelli CM, et al (2009) Suppression of estrus in cats with melatonin implants. Theriogenology 72:493–499. https://doi.org/10.1016/j.theriogenology.2009.04.004

Goericke-Pesch S, Wehrend A, Georgiev P (2014) Suppression of fertility in adult cats. Reprod Domest Anim 49:33–40. https://doi.org/10.1111/rda.12301

Gorre F, Vandekerckhove H (2010) Beta-blockers: focus on mechanism of action Which beta-blocker, when and why? Acta Cardiol 65:565–570. https://doi.org/10.1080/ac.65.5.2056244

Graham LH, Swanson WF, Wildt DE, Brown JL (2004) Influence of oral melatonin on natural and gonadotropin-induced ovarian function in the domestic cat. Theriogenology 61:1061–1076. 114 https://doi.org/10.1016/j.theriogenology.2003.05.004

Gunther-Harrington CT, Ontiveros ES, Hodge TE, et al (2016) Effects of 0.5% Timolol Maleate Ophthalmic Solution on Heart Rate and Selected Echocardiographic Indices in Apparently Healthy Cats. J Vet Intern Med 30:733–740. https://doi.org/10.1111/jvim.13931

Häggström J, Andersson O, Falk T, et al (2016) Effect of Body Weight on Echocardiographic Measurements in 19,866 Pure-Bred Cats with or without Heart Disease. J Vet Intern Med 30:1601–1611. https://doi.org/10.1111/jvim.14569

Hill RC, Scott KC (2004) Energy requirements and body surface area of cats and dogs. J Am Vet Med Assoc 225:689–694. https://doi.org/10.2460/javma.2004.225.689

Hoit BD (2017) Evaluation of Left Atrial Function: Current Status. Struct Hear 1:109–120. https://doi.org/10.1080/24748706.2017.1353718

Horwitz DF, Rodan I (2018) Behavioral awareness in the feline consultation: Understanding physical and emotional health. J Feline Med Surg 20:423–436. https://doi.org/10.1177/1098612X18771204

Hu K, Liu D, Herrmann S, et al (2013) Clinical implication of mitral annular plane systolic excursion for patients with cardiovascular disease. Eur Heart J Cardiovasc Imaging 14:205–212. https://doi.org/10.1093/ehjci/jes240

Johnson C, Kuyt K, Oxborough D, Stout M (2019) Practical tips and tricks in measuring strain, strain rate and twist for the left and right ventricles. Echo Res Pract 6:R87–R98. https://doi.org/10.1530/ERP-19-0020

Johnson K, Page A, Williams H, et al (2002) The use of melatonin as an alternative to sedation in uncooperative children undergoing an MRI examination. Clin 115

Radiol 57:502–506. https://doi.org/10.1053/crad.2001.0923

Karbić VO, Škoda M, Antončić D, et al (2014) Gabapentin-induced changes of plasma cortisol level and immune status in hysterectomized women. Int Immunopharmacol 23:530–536. https://doi.org/10.1016/j.intimp.2014.09.029

Kessler M., Turner DC (1997) Stress and adaptation of cats (Felis silvestris catus) housed singly, in pairs and in groups in boarding catteries. Anim Welf 6:243–254

Kiland JA, Voss AM, McLellan GJ (2016) Effect of timolol maleate gel-forming solution on intraocular pressure, pupil diameter, and heart rate in normal and glaucomatous cats. Vet Ophthalmol 19:91–96. https://doi.org/10.1111/vop.12376

Kirberger RM, Bland-vanden Berg P, Grimbeek RJ (1992) DOPPLER ECHOCARDIOGRAPHY IN THE NORMAL DOG: PART II: Factors Influencing Blood Flow Velocities And a Comparison between Left and Right Heart Blood Flow. Vet Radiol Ultrasound 33:380–386. https://doi.org/10.1111/j.1740-8261.1992.tb00163.x

Klaeboe LG, Edvardsen T (2019) Echocardiographic assessment of left ventricular systolic function. J Echocardiogr 17:10–16. https://doi.org/10.1007/s12574-018-0405-5

Klerman GL, Dimascio A, Havens LL SJ (1960) Sedation and Tranquilization: a Comparison of the Effects of a Number of Psychopharmacologic Agents upon Normal Human Subjects. Arch Gen Psychiatry 3:4–13. https://doi.org/10.1001/archpsyc.1960.01710010016002

Kocica MJ, Corno AF, Carreras-Costa F, et al (2006) The helical ventricular myocardial band: global, three-dimensional, functional architecture of the ventricular myocardium. Eur J Cardio-thoracic Surg 29:. https://doi.org/10.1016/j.ejcts.2006.03.011 116

Koffas H, Dukes-McEwan J, Corcoran BM, et al (2006) Pulsed tissue Doppler imaging in normal cats and cats with hypertrophic cardiomyopathy. J Vet Intern Med 20:65–77. https://doi.org/10.1892/0891-6640(2006)20[65:PTDIIN]2.0.CO;2

Koo TK, Li MY (2016) A Guideline of Selecting and Reporting Intraclass Correlation Coefficients for Reliability Research. J Chiropr Med 15:155–163. https://doi.org/10.1016/j.jcm.2016.02.012

Kruszka M, Graff E, Medam T, Masson S (2021) Clinical evaluation of the effects of a single oral dose of gabapentin on fear-based aggressive behaviors in cats during veterinary examinations. J Am Vet Med Assoc 259:1–7. https://doi.org/10.2460/javma.20.06.0307

Kusunose K, Penn MS, Zhang Y, et al (2012) How similar are the mice to men? Between-species comparison of left ventricular mechanics using strain imaging. PLoS One 7:. https://doi.org/10.1371/journal.pone.0040061

Kusunose K, Zhang Y, Mazgalev TN, et al (2013) Left ventricular strain distribution in healthy dogs and in dogs with tachycardia-induced dilated cardiomyopathy. Cardiovasc Ultrasound 11:43. https://doi.org/10.1186/1476-7120-11-43

Lakkatta EG (2004) Beyond Bowditch: The convergence of cardiac chronotropy and inotropy. Cell Calcium 35:629–642. https://doi.org/10.1016/j.ceca.2004.01.017

Levine ED (2008) Feline Fear and Anxiety. Vet Clin North Am - Small Anim Pract 38:1065–1079. https://doi.org/10.1016/j.cvsm.2008.04.010

Lim CY, In J (2019) Randomization in clinical studies. Korean J Anesthesiol 72:221–232. https://doi.org/10.4097/kja.19049

Liu L, Tuo S, Zhang J, et al (2014) Reduction of left ventricular longitudinal global and segmental systolic functions in patients with hypertrophic cardiomyopathy: Study of two-dimensional tissue motion annular displacement. Exp Ther Med 117

7:1457–1464. https://doi.org/10.3892/etm.2014.1617

Lotfy M, Ayaad M (2021) Preoperative oral melatonin can reduce preoperative anxiety and postoperative analgesia in a dose-dependent manner. Ain-Shams J Anesthesiol 13:13–32. https://doi.org/10.1186/s42077-021-00146-6

Luis Fuentes V, Abbott J, Chetboul V, et al (2020) ACVIM consensus statement guidelines for the classification, diagnosis, and management of cardiomyopathies in cats. J Vet Intern Med 1–16. https://doi.org/10.1111/jvim.15745

Luis SA, Chan J, Pellikka PA (2019) Echocardiographic Assessment of Left Ventricular Systolic Function: An Overview of Contemporary Techniques, Including Speckle-Tracking Echocardiography. Mayo Clin Proc 94:125–138. https://doi.org/10.1016/j.mayocp.2018.07.017

Lunkenheimer PP, Redmann K, Cryer CW, et al (2007) Beta-blockade at low doses restoring the physiological balance in myocytic antagonism. Eur J Cardio-thoracic Surg 32:225–230. https://doi.org/10.1016/j.ejcts.2007.03.048

Lunkenheimer PP, Redmann K, Florek J, et al (2004) The forces generated within the musculature of the left ventricular wall. Heart 90:200–207. https://doi.org/10.1136/hrt.2003.011650

Madsen BK, Zetner D, Møller AM, Rosenberg J (2020) Melatonin for preoperative and postoperative anxiety in adults. Cochrane Database Syst Rev 2020:. https://doi.org/10.1002/14651858.CD009861.pub3

Malik M (2009) Drug-induced changes in the T-wave morphology. Drug Saf 32:613–617. https://doi.org/10.2165/00002018-200932070-00007

Mauermann E, Bouchez S, Bove T, et al (2020) Rapid, Single-View Speckle-Tracking–Based Method for Examining Left Ventricular Systolic and Diastolic 118

Function in Point of Care Ultrasound. J Ultrasound Med 39:2151–2164. https://doi.org/10.1002/jum.15324

McCobb EC, Patronek GJ, Marder A, et al (2005) Assessment of stress levels among cats in four animal shelters. J Am Vet Med Assoc 226:548–555. https://doi.org/10.2460/javma.2005.226.548

Mccune S (1992) Temperament and the welfare of caged cats. University of Cambridge

McLellan GJ, Miller PE (2011) Feline glaucoma-a comprehensive review. Vet Ophthalmol 14:15–29. https://doi.org/10.1111/j.1463-5224.2011.00912.x

McLellan GJ, Teixeira LBC (2015) Feline Glaucoma. Vet Clin North Am - Small Anim Pract 45:1307–1333. https://doi.org/10.1016/j.cvsm.2015.06.010

Mizuguchi Y, Oishi Y, Miyoshi H, et al (2008) The Functional Role of Longitudinal, Circumferential, and Radial Myocardial Deformation for Regulating the Early Impairment of Left Ventricular Contraction and Relaxation in Patients With Cardiovascular Risk Factors: A Study With Two-Dimensional Strain Im. J Am Soc Echocardiogr 21:1138–1144. https://doi.org/10.1016/j.echo.2008.07.016

Mondillo S, Galderisi M, Ballo P, Marino PN (2006) Left Ventricular Systolic Longitudinal Function: Comparison Among Simple M-Mode, Pulsed, and M-Mode Color Tissue Doppler of Mitral Annulus in Healthy Individuals. J Am Soc Echocardiogr 19:1085–1091. https://doi.org/10.1016/j.echo.2006.04.005

Müller ME, Van Der Velde N, Krulder JWM, Van Der Cammen TJM (2006) Syncope and falls due to timolol eye drops. Br Med J 332:960–961. https://doi.org/10.1136/bmj.332.7547.960

Nagueh SF, Bachinski LL, Meyer D, et al (2001) Tissue Doppler imaging consistently detects myocardial abnormalities in patients with hypertrophic cardiomyopathy 119 nd provides a novel means for an early diagnosis before and independently of hypertrophy. Circulation 104:128–30. https://doi.org/10.1161/01.cir.104.2.128

Negishi K, Lucas S, Negishi T, et al (2013) What is the Primary Source of Discordance in Strain Measurement Between Vendors: Imaging or Analysis? Ultrasound Med Biol 39:714–720. https://doi.org/10.1016/j.ultrasmedbio.2012.11.021

Ng KY, Leong MK, Liang H, Paxinos G (2017) Melatonin receptors: distribution in mammalian brain and their respective putative functions. Brain Struct Funct 222:2921–2939. https://doi.org/10.1007/s00429-017-1439-6

Niggemann JR, Tichy A, Eberspächer-Schweda MC, Eberspächer-Schweda E (2019) Preoperative calming effect of melatonin and its influence on propofol dose for anesthesia induction in healthy dogs. Vet Anaesth Analg 46:560–567. https://doi.org/10.1016/j.vaa.2019.02.009

Nishihara K, Mikami T, Takatsuji H, et al (2000) Usefulness of early diastolic flow propagation velocity measured by color M-mode Doppler technique for the assessment of left ventricular diastolic function in patients with hypertrophic cardiomyopathy. J Am Soc Echocardiogr 13:801–808. https://doi.org/10.1067/mje.2000.106205

O'Sullivan ML, O'Grady MR, Minors SL (2014) Assessment of diastolic function by Doppler echocardiography in normal Doberman Pinschers and Doberman Pinschers with dilated cardiomyopathy. J Vet Intern Med 21:81–91. https://doi.org/10.1892/0891-6640(2007)21[81:aodfbd]2.0.co;2

Pankratz KE, Ferris KK, Griffith EH, Sherman BL (2018) Use of single-dose oral gabapentin to attenuate fear responses in cage-trap confined community cats: a double-blind, placebo-controlled field trial. J Feline Med Surg 20:535–543. 120

https://doi.org/10.1177/1098612X17719399

Payne JR, Borgeat K, Connolly DJ, et al (2013) Prognostic indicators in cats with hypertrophic cardiomyopathy. J Vet Intern Med 27:1427–1436. https://doi.org/10.1111/jvim.12215

Penk JS, Zaidi SJH, Lefaiver CA, et al (2018) Tissue Motion Annular Displacement Predicts Mortality/Transplant After the Bidirectional Glenn. World J Pediatr Congenit Heart Surg 9:171–176. https://doi.org/10.1177/2150135117742650

Peterson BL (2009) Prevalence of gabapentin in impaired driving cases in Washington State in 2003-2007. J Anal Toxicol 33:545–549. https://doi.org/10.1093/jat/33.8.545

Piotrowski G, Goch A, Wlazłowski R, et al (2014) Non-invasive methods of atrial function evaluation in heart diseases. Med Sci Monit 6:827–39

Pongkan W, Piamsiri C, Dechvongya S, et al (2022) Short-term melatonin supplementation decreases oxidative stress but does not affect left ventricular structure and function in myxomatous mitral valve degenerative dogs. BMC Vet Res 18:1–11. https://doi.org/10.1186/s12917-021-03125-z

Popovic ZB, Thomas JD (2017) Assessing observer variability: A user's guide. Cardiovasc Diagn Ther 7:317–324. https://doi.org/10.21037/cdt.2017.03.12

Quimby J, Gowland S, Carney HC, et al (2021) 2021 AAHA/AAFP Feline Life Stage Guidelines. J Feline Med Surg 57:51–72. https://doi.org/10.5326/JAAHA-MS-7189

Ramlogan S, Aly D, France R, et al (2020) Reproducibility and Intervendor Agreement of Left Ventricular Global Systolic Strain in Children Using a Layer-Specific Analysis. J Am Soc Echocardiogr 33:110–119. https://doi.org/10.1016/j.echo.2019.08.004 121

Riesen SC, Schober KE, Cervenec RM, Bonagura JD (2011) Comparison of the Effects of Ivabradine and Atenolol on Heart Rate and Echocardiographic Variables of Left Heart Function in Healthy Cats. J Vet Intern Med 25:469–476. https://doi.org/10.1111/j.1939-1676.2011.0705.x

Rios ERV, Venâncio ET, Rocha NFM, et al (2010) Melatonin: Pharmacological Aspects and Clinical Trends. Int J Neurosci 120:583–590. https://doi.org/10.3109/00207454.2010.492921

Rishniw M, Erb HN (2000) Evaluation of four 2-dimensional echocardiographic methods of assessing left atrial size in dogs. J Vet Intern Med 14:429–435. https://doi.org/10.1111/j.1939-1676.2000.tb02252.x

Rivara S, Pala D, Bedini A, Spadoni G (2015) Therapeutic uses of melatonin and melatonin derivatives: A patent review (2012 - 2014). Expert Opin Ther Pat 25:425–441. https://doi.org/10.1517/13543776.2014.1001739

Roberto Santilli, Sidney Moïse, Romain Pariaut MP (2018) Electrocardiography of the dog and cat. Diagnosis of arrhythmias., 2nd Ed. Florida : Edra Pulishing

Rodan I (2010) Understanding Feline Behavior and Application for Appropriate Handling and Management. Top Companion Anim Med 25:178–188. https://doi.org/10.1053/j.tcam.2010.09.001

Sahn DJ, DeMaria A, Kisslo J, Weyman A (1978) Recommendations regarding quantitation in M-mode echocardiography: Results of a survey of echocardiographic measurements. Circulation 58:1072–1083. https://doi.org/10.1161/01.CIR.58.6.1072

Salavati S, Mogheiseh A, Nazifi S, et al (2021) The effects of melatonin treatment on oxidative stress induced by ovariohysterectomy in dogs. BMC Vet Res 17:1–8. https://doi.org/10.1186/s12917-021-02882-1 122

Santarelli G, Baron Toaldo M, Bouvard J, et al (2019) Variability among strain variables derived from two-dimensional speckle tracking echocardiography in dogs by use of various software. Am J Vet Res 80:347–357. https://doi.org/10.2460/ajvr.80.4.347

Schmidt CM, Knief A, Deuster D, et al (2007) Melatonin is a useful alternative to sedation in children undergoing brainstem audiometry with an age dependent success rate - A field report of 250 investigations. Neuropediatrics 38:2–4. https://doi.org/10.1055/s-2007-981467

Schmitt B (2010) Accelerated whole-heart 3D CSPAMM reveals impact of beta-blocker therapy on myocardial architecture. J Cardiovasc Magn Reson 12:3. https://doi.org/10.1186/1532-429x-12-s1-p122

Schober KE, Chetboul V (2015) Echocardiographic evaluation of left ventricular diastolic function in cats: Hemodynamic determinants and pattern recognition. J Vet Cardiol 17:S102–S133. https://doi.org/10.1016/j.jvc.2015.02.002

Schober KE, Fuentes VL (2001) Mitral annulus motion as determined by M-mode echocardiography in normal dogs and dogs with cardiac disease. Vet Radiol Ultrasound 42:52–61. https://doi.org/10.1111/j.1740-8261.2001.tb00904.x

Schober KE, Wetli E, Drost WT (2014) Radiographic and echocardiographic assessment of left atrial size in 100 cats with acute left-sided congestive heart failure. Vet Radiol Ultrasound 55:359–367. https://doi.org/10.1111/vru.12131

Schober P, Schwarte LA (2018) Correlation coefficients: Appropriate use and interpretation. Anesth Analg 126:1763–1768. https://doi.org/10.1213/ANE.0000000000002864

Seo J-S, Kim D-H, Kim W-J, et al (2010) Peak systolic velocity of mitral annular longitudinal movement measured by pulsed tissue Doppler imaging as an index 123

of global left ventricular contractility. Am J Physiol Heart Circ Physiol 298:H1608-15. https://doi.org/10.1152/ajpheart.01231.2009

Sharma JB, Deora S, Choudhary R, Kaushik A (2021) Comparison of mitral annular displacement and global longitudinal strain imaging for predicting significant coronary atherosclerotic disease in patients of chronic stable angina pectoris. Int J Cardiovasc Imaging 37:861–870. https://doi.org/10.1007/s10554-020-02058-2

Shiuey Y, Eisenberg MJ (1996) Cardiovascular effects of commonly used ophthalmic medications. Clin Cardiol 19:5–8. https://doi.org/10.1002/clc.4960190104

Shukla AK, Pinard CL, Flynn BL, Bauman CA (2020) Effects of orally administered gabapentin, tramadol, and meloxicam on ocular variables in healthy dogs. Am J Vet Res 81:973–984. https://doi.org/10.2460/ajvr.81.12.973

Siao KT, Pypendop BH, Ilkiw JE (2010) Pharmacokinetics of gabapentin in cats. Am J Vet Res 71:817–821. https://doi.org/10.2460/ajvr.71.7.817

Silva AC, Muzzi RAL, Oberlender G, et al (2013) Longitudinal strain and strain rate by two-dimensional speckle tracking in non-sedated healthy cats. Res Vet Sci 95:1175–1180. https://doi.org/10.1016/j.rvsc.2013.07.020

Simpson KE, Gunn-Moore DA, Shaw DJ, et al (2009) Pulsed-wave Doppler tissue imaging velocities in normal geriatric cats and geriatric cats with primary or systemic diseases linked to specific cardiomyopathies in humans, and the influence of age and heart rate upon these velocities. J Feline Med Surg 11:293–304. https://doi.org/10.1016/j.jfms.2008.08.003

Slenter IJM, Djajadiningrat-Laanen SC, Elders DJ, et al (2019) The effects of topical dorzolamide 2% and brinzolamide 1%, either alone or combined with timolol 0.5%, on intraocular pressure, pupil diameter, and heart rate in healthy cats. Vet Ophthalmol 1–9. https://doi.org/10.1111/vop.12679 124

Smith DN, Schober KE (2013) Effects of vagal maneuvers on heart rate and Doppler variables of left ventricular filling in healthy cats. J Vet Cardiol 15:33–40. https://doi.org/10.1016/j.jvc.2012.08.003

Spalla I, Boswood A, Connolly DJ, Luis Fuentes V (2019) Speckle tracking echocardiography in cats with preclinical hypertrophic cardiomyopathy. J Vet Intern Med 33:1232–1241. https://doi.org/10.1111/jvim.15495

Spalla I, Payne JR, Borgeat K, et al (2018) Prognostic value of mitral annular systolic plane excursion and tricuspid annular plane systolic excursion in cats with hypertrophic cardiomyopathy. J Vet Cardiol 20:154–164. https://doi.org/10.1016/j.jvc.2018.04.005

Spalla I, Payne JRR, Borgeat K, et al (2017) Mitral Annular Plane Systolic Excursion and Tricuspid Annular Plane Systolic Excursion in Cats with Hypertrophic Cardiomyopathy. J Vet Intern Med 31:691–699. https://doi.org/10.1111/jvim.14697

Steagall PVM, Taylor PM, Rodrigues LCC, et al (2009) Analgesia for cats after ovariohysterectomy with either buprenorphine or carprofen alone or in combination. Vet Rec 164:359–363. https://doi.org/10.1136/vr.164.12.359

Strachinaru M, Annis C, Catez E, et al (2016) The mitral annular displacement by two-dimensional speckle tracking. J Cardiovasc Med 17:344–353. https://doi.org/10.2459/JCM.0000000000000346

Sugimoto K, Aoki T, Fujii Y (2021) Longitudinal evaluation of cardiovascular function in six healthy cats aged 1–8 years. J Feline Med Surg 23:98–104. https://doi.org/10.1177/1098612X20932255

Sugimoto K, FUJII Y, Sunahara H, AOKI T (2015) Assessment of left ventricular longitudinal function in cats with subclinical hypertrophic cardiomyopathy using 125

tissue Doppler imaging and speckle tracking echocardiography. J Vet Med Sci 77:1101–1108. https://doi.org/10.1292/jvms.14-0354

Sugimoto K, Kawase N, Aoki T (2020) Assessment of diastolic function using mitral flow propagation velocity in cats. Can J Vet Res 84:124–130

Suzuki R, Mochizuki Y, Yoshimatsu H, et al (2019a) Layer-specific myocardial function in asymptomatic cats with obstructive hypertrophic cardiomyopathy assessed using 2-dimensional speckle-tracking echocardiography. J Vet Intern Med 33:37–45. https://doi.org/10.1111/jvim.15339

Suzuki R, Mochizuki Y, Yuchi Y, et al (2019b) Assessment of myocardial function in obstructive hypertrophic cardiomyopathy cats with and without response to medical treatment by carvedilol. BMC Vet Res 15:1–8. https://doi.org/10.1186/s12917-019-2141-0

Taylor KS, Murai H, Millar PJ, et al (2016) Arousal from Sleep and Sympathetic Excitation during Wakefulness. Hypertension 68:1467–1474. https://doi.org/10.1161/HYPERTENSIONAHA.116.08212

Teraguchi I, Hozumi T, Emori H, et al (2021) Prognostic value of tissue-tracking mitral annular displacement by speckle-tracking echocardiography in asymptomatic aortic stenosis patients with preserved left ventricular ejection fraction. J Echocardiogr 19:95–102. https://doi.org/10.1007/s12574-020-00490-w

Teraguchi I, Hozumi T, Takemoto K, et al (2019) Assessment of decreased left ventricular longitudinal deformation in asymptomatic patients with organic mitral regurgitation and preserved ejection fraction using tissue-tracking mitral annular displacement by speckle-tracking echocardiography. Echocardiography 36:678–686. https://doi.org/10.1111/echo.14290

Thomas WP, Gaber CE, Jacobs GJ, et al (1994) Recommendations for Standards in 126

Transthoracic Two-Dimensional Echocardiography in the Dog and Cat. Vet Radiol Ultrasound 35:173–178. https://doi.org/10.1111/j.1740-8261.1994.tb01588.x

Tidholm A, Ljungvall I, HÃ¶glund K, et al (2009) Tissue Doppler and Strain Imaging in Dogs with Myxomatous Mitral Valve Disease in Different Stages of Congestive Heart Failure. J Vet Intern Med 23:1197–1207. https://doi.org/10.1111/j.1939-1676.2009.0403.x

Tomochika Y, Tanaka N, Wasaki Y, et al (1993) Assessment of flow profile of left anterior descending coronary artery in hypertrophic cardiomyopathy by transesophageal pulsed Doppler echocardiography. Am J Cardiol 72:1425–1430. https://doi.org/10.1016/0002-9149(93)90191-E

Trivedi SJ, Altman M, Stanton T, Thomas L (2019) Echocardiographic Strain in Clinical Practice. Hear Lung Circ 28:1320–1330. https://doi.org/10.1016/j.hlc.2019.03.012

Tsang W, Ahmad H, Patel AR, et al (2010) Rapid Estimation of Left Ventricular Function Using Echocardiographic Speckle-Tracking of Mitral Annular Displacement. J Am Soc Echocardiogr 23:511–515. https://doi.org/10.1016/j.echo.2010.03.003

Van Dalen BM, Bosch JG, Kauer F, et al (2009) Assessment of Mitral Annular Velocities by Speckle Tracking Echocardiography versus Tissue Doppler Imaging: Validation, Feasibility, and Reproducibility. J Am Soc Echocardiogr 22:1302–1308. https://doi.org/10.1016/j.echo.2009.08.004

Van Haaften KA, Forsythe LRE, Stelow EA, Bain MJ (2017) Effects of a single preappointment dose of gabapentin on signs of stress in cats during transportation and veterinary examination. J Am Vet Med Assoc 251:1175–1181. 127

https://doi.org/10.2460/javma.251.10.1175

Vinereanu D, Khokhar A, Fraser AG (1999) Reproducibility of pulsed wave tissue Doppler echocardiography. J Am Soc Echocardiogr 12:492–499. https://doi.org/10.1016/S0894-7317(99)70086-6

Visser LC, Sloan CQ, Stern JA (2017) Echocardiographic Assessment of Right Ventricular Size and Function in Cats With Hypertrophic Cardiomyopathy. J Vet Intern Med 31:668–677. https://doi.org/10.1111/jvim.14688

Wang Z, Denys I, Chen F, et al (2019) Complete atrioventricular block due to timolol eye drops: a case report and literature review. BMC Pharmacol Toxicol 20:73. https://doi.org/10.1186/s40360-019-0370-2

Ward JL, Schober KE, Fuentes VL, Bonagura JD (2012) Effects of sedation on echocardiographic variables of left atrial and left ventricular function in healthy cats. J Feline Med Surg 14:678–685. https://doi.org/10.1177/1098612X12447729

Welty DF, Schielke GP, Vartanian MG, Taylor CP (1993) Gabapentin anticonvulsant action in rats: disequilibrium with peak drug concentrations in plasma and brain microdialysate. Epilepsy Res 16:175–181. https://doi.org/10.1016/0920-1211(93)90078-L

Wilkie DA, Latimer CA (1991) Effects of topical administration of timolol maleate on intraocular pressure and pupil size in cats. Am J Vet Res 52:436–40

Willis AM (2004) Ocular hypotensive drugs. Vet Clin North Am - Small Anim Pract 34:755–776. https://doi.org/10.1016/j.cvsm.2004.02.001

Wolf M, Lucina SB, Silva VBC, et al (2021) Assessment of longitudinal systolic function using tissue motion annular displacement in dogs with degenerative mitral valve disease. J Vet Cardiol 38:44–58. 128

https://doi.org/10.1016/j.jvc.2021.10.004

Wolf M, Lucina SBSB, Brüler BCBC, et al (2018) Assessment of longitudinal systolic function using tissue motion annular displacement in healthy dogs. J Vet Cardiol 20:. https://doi.org/10.1016/j.jvc.2018.04.004

Yang H, Marwick TH, Fukuda N, et al (2015) Improvement in Strain Concordance between Two Major Vendors after the Strain Standardization Initiative. J Am Soc Echocardiogr 28:642–648.e7. https://doi.org/10.1016/j.echo.2014.12.009

Yingchoncharoen T, Agarwal S, Popović ZB, Marwick TH (2013) Normal Ranges of Left Ventricular Strain: A Meta-Analysis. J Am Soc Echocardiogr 26:185–191. https://doi.org/10.1016/j.echo.2012.10.008

Zacà V, Ballo P, Galderisi M, Mondillo S (2010) Echocardiography in the assessment of left ventricular longitudinal systolic function: current methodology and clinical applications. Heart Fail Rev 15:23–37. https://doi.org/10.1007/s10741-009-9147-9

Zois NE, Tidholm A, Nägga KM, et al (2012) Radial and Longitudinal Strain and Strain Rate Assessed by Speckle-Tracking Echocardiography in Dogs with Myxomatous Mitral Valve Disease. J Vet Intern Med 26:1309–1319. https://doi.org/10.1111/j.1939-1676.2012.01017.x

R Core Team. R: a language and environment for statistical computing. Vienna: R Foundation for Statistical Computing, 2021 129

ANEXOS

UNIVERSIDADE FEDERAL DO PARANÁ
SETOR DE CIÊNCIAS AGRÁRIAS
COMISSÃO DE ÉTICA NO USO DE ANIMAIS

CERTIFICADO

Certificamos que o protocolo número 014/2019, referente ao projeto **"Estudo da função cardíaca em gatos saudáveis e cardiopatas",** sob a responsabilidade **Marlos Gonçalves Sousa** – que envolve a produção, manutenção e/ou utilização de animais pertencentes ao filo Chordata, subfilo Vertebrata (exceto o homem), para fins de pesquisa científica ou ensino – encontra-se de acordo com os preceitos da Lei nº 11.794, de 8 de Outubro, de 2008, do Decreto nº 6.899, de 15 de julho de 2009,e com as normas editadas pelo Conselho Nacional de Controle da Experimentação Animal (CONCEA), e foi aprovado pela COMISSÃO DE ÉTICA NO USO DE ANIMAIS (CEUA) DO SETOR DE CIÊNCIAS AGRÁRIAS DA UNIVERSIDADE FEDERAL DO PARANÁ - BRASIL, com grau 2 de invasividade, em reunião de 17/04/2019.

Vigência do projeto	Junho/2019 até Junho/2020
Espécie/Linhagem	*Felis catus* (gato)
Número de animais	350
Peso/Idade	Variável
Sexo	Macho e fêmea
Origem	Particulares e Hospital Veterinário da Universidade Federal do Paraná, Curitiba, Brasil.

CERTIFICATE

We certify that the protocol number 014/2019, regarding the project **"Assessment of cardiac function in healthy cats and cats with cardiac diseases"** under **Marlos Gonçalves Sousa** supervision – which includes the production, maintenance and/or utilization of animals from Chordata phylum, Vertebrata subphylum (except Humans), for scientific or teaching purposes – is in accordance with the precepts of Law nº 11.794, of 8 October, 2008, of Decree nº 6.899, of 15 July, 2009, and with the edited rules from Conselho Nacional de Controle da Experimentação Animal (CONCEA), and it was approved by the ANIMAL USE ETHICS COMMITTEE OF THE AGRICULTURAL SCIENCES CAMPUS OF THE UNIVERSIDADE FEDERAL DO PARANÁ (Federal University of the State of Paraná, Brazil), with degree 2 of invasiveness, in session of 17/04/2019.

Duration of the project	June/2019 until June/2020
Specie/Line	*Felis catus* (cat)
Number of animals	350
Wheight/Age	Variable
Sex	Male and female
Origin	Private and Veterinary Hospital of the Federal University of Paraná, Curitiba, Brazil.

Curitiba, 17 de abril de 2019

Chayane da Rocha

Chayane da Rocha

Coordenadora CEUA-SCA

Veterinary Research Communications
https://doi.org/10.1007/s11259-022-09907-6

ORIGINAL ARTICLE

Tissue motion annular displacement to assess the left ventricular systolic function in healthy cats

Giovana Lais Ruviaro Tuleski[1] · Marcela Wolf[1] · Maria Jose Garcia Ribeiro Pscheidt[2] · Júlio Pereira dos Santos[1] · Marlos Gonçalves Sousa[1]

Received: 17 November 2021 / Accepted: 16 February 2022

Abstract

The tissue motion annular displacement (TMAD) measures the longitudinal displacement of the mitral annulus during systole, using speckle-tracking echocardiography (STE). The main objective was to determine the TMAD means in healthy cats, exploring the correlations with systolic surrogates. The influence of age, body surface area (BSA), heart rate, and systemic blood pressure on the indices was also analyzed. One hundred ninety-three healthy, client-owned cats participated in this prospective, cross-sectional observational study undergoing conventional and STE. Apical four-chamber (AP4) and two-chamber (AP2) images were recorded for offline calculations. Mean TMAD values were similar to mitral annulus plane systolic excursion (MAPSE), varying between 4 to 4.8 mm depending on the annulus and image used. No significant differences between age and BSA categories were detected, except for AP4 MP%, reduced in the heavier group. TMAD variables showed moderate correlation with longitudinal strain (LSt) and MAPSE, but not with fraction shortening (FS) and ejection fraction (EF). The median time required for the offline calculation was 12.2 s for AP4 and 11.8 s for AP2. The technique showed moderate inter and intraobserver variation, proving a reliable tool for assessing left ventricular longitudinal systolic function in cats.

Keywords Speckle tracking · Strain · Longitudinal function · Reference range

Abbreviations

AP2	Apical 2-chamber image
AP4	Apical 4-chamber image
BSA	Body surface area
ECG	Electrocardiography
FS	Fractional shortening
FW	Free wall
EF	Ejection fraction
GLS	Global longitudinal strain
HCM	Hypertrophic cardiomyopathy
HR	Heart rate
IVS	Interventricular septum
LA	Left atrium
LSt	Longitudinal strain
LV	Left ventrilce
MAPSE	Mitral Annular Plane Systolic Excursion
ROI	Regions of interest
SBP	Systolic blood pressure
STE	Speckle-tracking echocardiography
TDI	Tissue Doppler imaging
TMAD	Tissue Motion Annular Displacement
TMAD MP	The displacement (in mm) of a virtual midpoint between the two mitral annular regions towards the left ventricular apex
TMAD MP%	The proportional displacement of that midpoint concerning the total length of the left ventricle
TMAD MV1	Displacement of the septal (AP4) or anterior (AP2) annulus towards the apex
TMAD MV2	Displacement of the lateral (AP4) or inferior (AP2) annulus towards the apex

✉ Giovana Lais Ruviaro Tuleski
gtuleski@yahoo.com.br

[1] Laboratory of Comparative Cardiology, Department of Veterinary Medicine, Federal University of Paraná (UFPR), Rua dos Funcionários, 1540, Curitiba, Paraná CEP 80035-050, Brazil

[2] Autonomous veterinarian, Curitiba, Paraná, Brazil

Published online: 08 March 2022

Introduction

Assessment of systolic function is a cornerstone of echocardiographic examination. In conventional echocardiography, fractional shortening (FS) and ejection fraction (EF) are widely used as surrogates for systolic function, despite their limitations. Measurement of both parameters requires good image quality, has sub-optimal test-retest reproducibility, fails to evaluate the longitudinal myocardial contraction, and neither detects regional dysfunction on the left ventricle (Mizuguchi et al. 2008; Zacà et al. 2010; Klaeboe and Edvardsen 2019; Luis et al. 2019).

While FS measures only the heart's circumferential contraction, EF represents longitudinal and circumferential contraction (Hu et al. 2013). However, the longitudinal systolic function is routinely less evaluated on echocardiographic examinations. The contraction of the longitudinal fibers during systole causes a shortening of the left ventricular chamber along its longitudinal axis, promoting the displacement of the atrioventricular plane towards the cardiac apex (Zacà et al. 2010). In humans, their contraction is the primary contributor to left ventricular pumping, representing up to 60% of the total cardiac stroke (Carlsson et al. 2007). Previous studies have demonstrated that longitudinal systolic dysfunction may be apparent before impaired transverse function becomes overt (Luis et al. 2019; Spalla et al. 2019). For this reason, practical and easy-to-apply techniques are sought to assess longitudinal systolic function in cats.

The Mitral Annular Plane Systolic Excursion (MAPSE) is more sensitive than EF to detect early longitudinal fibers abnormalities (Hu et al. 2013). When low, MAPSE and its right counterpart, Tricuspid Annular Plane Systolic Excursion (TAPSE), reveal longitudinal systolic dysfunction in cats with asymptomatic hypertrophic cardiomyopathy (HCM), being even smaller in congestive heart failure (Spalla et al. 2017). The systolic wave S′ from tissue Doppler imaging (TDI) is a more sensitive index of global contractility of the left ventricle (LV) than EF, reflecting both longitudinal shortening and torsional deformation (Chetboul et al. 2004; Simpson et al. 2009; Seo et al. 2010). Regrettably, both MAPSE and TDI are angle-dependent (Vinereanu et al. 1999; Chetboul et al. 2004; van Dalen et al. 2009; Zacà et al. 2010; Hu et al. 2013; Aloia et al. 2016; Spalla et al. 2017).

In contrast, speckle-tracking echocardiography (STE) is angle-independent and determines tissue velocities accurately (van Dalen et al. 2009). The longitudinal strain (LSt) has been used to assess the longitudinal systolic function in people (Collier et al. 2017; Trivedi et al. 2019), dogs (Tidholm et al. 2009; Chetboul and Tissier 2012; Zois et al. 2012), and cats (Silva et al. 2013; Spalla et al. 2019; Suzuki et al. 2019a; Caivano et al. 2020). Cats with preclinical HCM have a decrease in LSt (Spalla et al. 2019), highlighting the use of this technique in the early detection of this disease.

Another STE method to estimate the longitudinal function is the Tissue Motion Annular Displacement (TMAD), which measures the systolic displacement of two regions of interest (ROI) located in the mitral annulus, tracking them towards a third ROI at the cardiac apex (Buss et al. 2012). Previous studies observed that TMAD is faster than LSt and requires lower image quality (Buss et al. 2012; Black et al. 2014; Asada et al. 2018). Another advantage of the TMAD concerning the LSt is that the last one presents a variation in its values according to the software and equipment used, this problem being observed in humans (Bansal et al. 2008; Negishi et al. 2013; Yingchoncharoen et al. 2013; Yang et al. 2015; Ramlogan et al. 2020) and dogs (Santarelli et al. 2019). Finally, TMAD was considered a viable method for rapid assessment of longitudinal systolic function in humans with HCM (Liu et al. 2014). Therefore, TMAD may be useful in the early diagnosis of HCM in cats, although further studies are needed to confirm this supposition.

Our research group was the first to describe the relevance of TMAD to evaluate longitudinal systolic function in dogs, both in healthy animals and those with heart disease (Wolf et al. 2018, 2021). However, no articles reported a study of TMAD in cats on a recent search (January 2022) on two platforms: PubMed and ProQuest. In this study, we aimed to explore the potential applicability of TMAD for the assessment of longitudinal systolic function in healthy cats. Our goal was to clarify whether TMAD is a reliable method compared with LSt and other echocardiographic surrogates in cats. Another objective was to determine whether a correlation exists between TMAD and LSt, and other echocardiographic parameters such as FS, EF, TDI, and MAPSE. Lastly, we investigated whether TMAD alters with age, body surface area (BSA), heart rate (HR), and systemic blood pressure (SBP).

Animals, materials and methods

Animals

Client-owned healthy cats were recruited for this prospective, cross-sectional observational study at the cardiology section of a veterinary teaching facility between May and July 2019. The experimental unit was the individual animal. All procedures were previously approved by the Institutional Animal Care and Use Committee (protocol 014/2019) and complied with the National Institutes of Health Guide for the Care and Use of Laboratory Animals. Written consent

from owners allowing their cats to participate in the study was mandatory.

All cats underwent a complete physical examination before enrollment, as well as SBP measurement, electrocardiography (ECG), conventional and speckle-tracking echocardiography. The Doppler technique (Binns et al. 1995) was used to obtain SBP indirectly by a trained observer (GLRT), acquiring at least five reliable values to measure the average. Subsequently, a 2-min recording of a computer-based ECG was performed.

The inclusions criteria were: cats more than one year, considered adults (Quimby et al. 2021), absence of murmur on cardiac auscultation, no previously diagnosed disease, and standard examinations (ECG, SBP, and echocardiography). The SBP before the echocardiogram was considered normal up to 160 mmHg (Acierno et al. 2018). Animals whose SBP exceeded this value were only included if they were patients without a record of arterial hypertension, with at least three normal SBP measurements in the last five years. Free plasma T4 excluded hyperthyroidism in cats over 11 years old or whenever this disease was suspected.

Exclusion criteria were established in an attempt to select only healthy cats, rejecting cats receiving topical or systemic medication and those previously diagnosed with any illness, including chronic systemic hypertension, arrhythmias, acquired or congenital heart disease.

Echocardiography

All cats underwent echocardiographic examinations[1] with electrocardiography monitoring using only gentle restraint and no sedation. Positioning followed the recommendations of the Echocardiography Committee of the Specialty of Cardiology of the American College of Veterinary Internal Medicine (Thomas et al. 1994). The same operator (GLRT) performed all examinations and measurements.

The FS of the left atrium (LA) was estimated based on the minimum and maximum LA diameter from the right parasternal short-axis view image at the aortic valve level, using anatomic M-mode (Abbott and MacLean 2013). The ratio between LA and aorta was measured at the maximum LA diameter, right after the T wave from the ECG, as described before (Rishniw and Erb 2000). A normal relation of LA and aorta (LA/Ao <1.6, at the final of the T wave) was considered evidence of normal diastolic pressure, combined with a normal diastolic pattern defined by the transmitral outflow (E/A > 1) and TDI waves (E´/A´ > 1) (Schober and Chetboul 2015).

The HCM was ruled out after examining the LV in the right and left parasternal long-axis LV outflow view and in the right parasternal short axis view of the left ventricle at the level of the papillary muscles. The M-Mode measurements of the LV at the papillary level were measured before the QRS to characterize the end of diastole as described (Sahn et al. 1978), being 5.5 mm the cut-off point for HCM (Häggström et al. 2016).

The left parasternal window allowed the acquisition of apical 4-chamber (AP4) and 2-chamber (AP2) images (Thomas et al. 1994). AP4 was used to measure the TDI velocities (Koffas et al. 2006) and MAPSE from the interventricular septum mitral annulus (MAPSE IVS) and from and free wall (MAPSE FW) as described elsewhere (Mondillo et al. 2006; Spalla et al. 2017). Recording of at least five cardiac cycles of AP4 and AP2 images enabled the offline calculation of all TMAD and LSt values.

Both TMAD and LSt required the measure of the aortic valve closure time from the apical 5-chamber image. It corresponds to the time, in milliseconds, from the beginning of the QRS complex to the end of the aortic valve spectra obtained with the pulsed Doppler gate positioned distal to the aortic valve.

Longitudinal strain

The LSt was measured offline using speckle-tracking software[2] and AP4 and AP2 images containing at least five cardiac cycles obtained from standard echocardiography. To calculate AP4 LSt, three ROIs were defined from the selected frame: the septal and lateral portions of the mitral valve leaflets and the epicardial region of the left ventricular apex (Spalla et al. 2019). The equipment's software automatically tracked the myocardium and calculated longitudinal deformation (Fig. 1a). Manual corrections were made whenever auto-tracking was obviously incorrect. The mean value from three cardiac cycles in the same frame was used for analysis. A similar procedure was used for AP2 images, and the ROIs were defined at the anterior and inferior aspects of the mitral annulus (Fig. 1c).

The average of the LSt values obtained with AP2 and AP4 was assumed as a modified global deformation index (Wolf et al. 2018), as it did not include the apical three-chamber (AP3) view, as follows:

$$GLS = (AP2\ LSt + AP4\ LSt)/2.$$

[1] Philips Affiniti 50 ultrasound system equipped with 12 MHz phased-array transducer

[2] QLAB Software with automatic cardiac motion quantification (aCMQ)

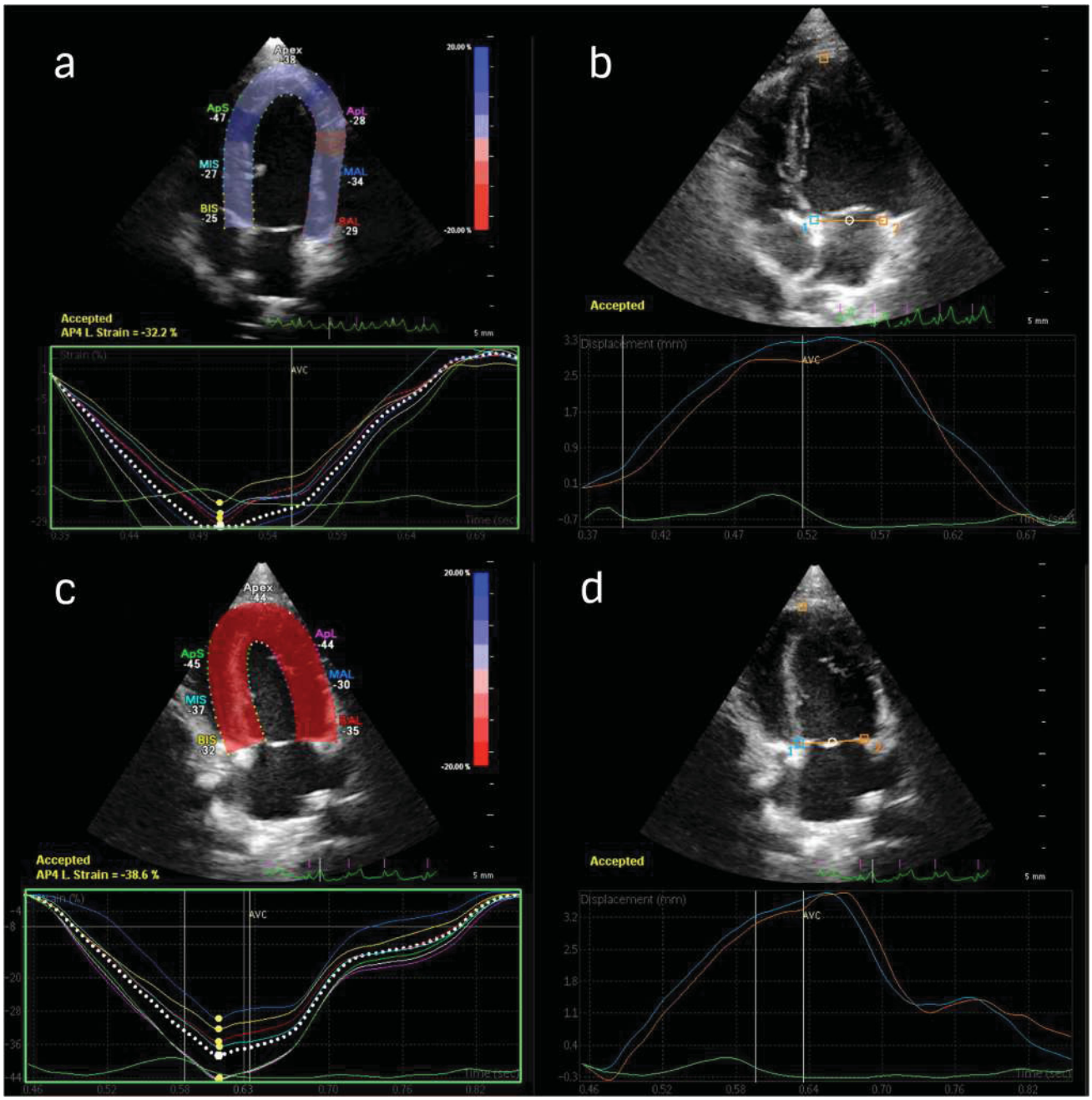

Fig. 1 Above: two apical 4-chamber images demonstrate the longitudinal strain on the left (**a**) and the tissue motion annular displacement on the right (**b**). Below: two apical 2-chamber images display the longitudinal strain on the left (**c**) and the tissue motion annular displacement on the right (**d**). The line in blue describes the displacement of the septal mitral annulus towards the left ventricular apex. Similarly, the orange displays the displacement of the free wall mitral annulus towards the left ventricular Apex

Tissue motion annular displacement

Mitral annular motion was measured offline as described for LSt, using the same ROIs. The displacement of both annuli towards the apex (in mm) was automatically calculated. The abbreviation MV1 refers to the displacement of the septal (AP4) or anterior (AP2) annulus, while MV2 corresponds to the lateral (AP4) or inferior (AP2) annulus. The software also defined a virtual midpoint (MP) between the two annular ROIs and calculated its displacement (in mm) towards the left ventricular apex, as well as the proportional displacement of that midpoint concerning the total length of the left ventricle (MP%) (Fig. 1b, d). The

mean values from three cardiac cycles in the same recording were used to calculate the TMAD.

The average of the indices obtained by AP2 and AP4 was called global TMAD values (Wolf et al. 2021), calculated as follows:

$$\text{Global TMAD MP} = (\text{AP2 MP} + \text{AP4 MP})/2\text{Global TMAD MP\%} = (\text{AP2 MP\%} + \text{AP4 MP\%})/2$$

Intra-observer and inter-observer variability and time requirements

The same observer (GLRT) randomly reassessed AP4 images from 18 patients at least 30 days after the first evaluation to estimate intra-observer variability. A co-investigator blinded to the previous results (MW) assessed the same examinations, whose results were used to calculate inter-observer variation.

Different 23 echocardiographic records were selected to calculate the time spent for the offline calculation of the TMAD and LSt, both for AP2 and AP4 views.

Age and body surface area categories

Cats were divided into groups according to age and BSA, allowing the investigation of their action on TMAD. The age distribution followed the most recent age classification of cats by the American Animal Hospital Association (AAHA) and the American Association of Feline Practitioners (AAFP) (Quimby et al. 2021): 1–6 years (young adult); 7 to 10 years (mature adult); and 11 years or older (senior). The BSA categories were: less than 0.252 m^2 (<4 kg), 0.253 to 0.292 m^2 (4.01 to 5 kg), 0.293 to 0.330 m^2 (5.1 to 6 kg), and more than 0.330 m^2 (>6.01 kg). The BSA was calculated as described before (Hill and Scott 2004), following the formula:

$$\text{BSA}\left(m^2\right) = 0.1 \times (\text{bodyweight in kg})^{2}/_{3}$$

Statistical analysis

The *Statistica Single User* software version 13.2 performed most of the analyses, with a significant level of 0.05 (P value <0.05). Descriptive data analysis included mean and standard deviation calculations, minimum and maximum of all quantitative variables, and pure frequencies of qualitative variables. The Shapiro-Wilk test was used to investigate the normality of the data. Group comparison was performed with ANOVA followed by Tukey's or Dunn's posthoc test. The parameters with not normally distributed data were adequate for the Kruskal-Wallis test (LSt and TMAD MP%).

The correlations were investigated using Pearson's correlation coefficient, scaled and ranged from −1 to +1, where 0 indicates no linear association. The relationship gets stronger as the coefficient approaches an absolute value of 1. They were considered weak between 0 and 1 to 0.39, moderate from 0.40 to 0.69, strong from 0.7 to 0.89, and very strong above 0.9 (Schober and Schwarte 2018).

The intra- and inter-observer agreement analysis was performed using the interclass correlation coefficient (ICC) with its respective 95%CI and standard error of measurement (SEM) (Fleiss 1986; Popovic and Thomas 2017). From the ten different ICC formulas, it was used the two-way mixed-effects model (Koo and Li 2016) defined for the formula:

$$\text{ICC} = \text{MSR} - \text{MSE}/\text{MSR};\text{where MSR} = \text{mean square for rows};\text{MSE} = \text{mean square for error}$$

The minimum sample size for using the ICC was calculated with a power of 80%, with a drop of 10%, minimum acceptable reliability of 0.6, and expected reliability of 0.85. Its interpretation was based on a Fleiss study: low for values below 0.40; moderate between 0.40 and 0.75; substantial between 0.75 and 0.90; and excellent greater than 0.90 (Fleiss 1986). The Bland-Altman test was used to better represent non-normal data as it does not necessarily require a normal distribution (Bland and Altman 2010).

Wilcoxon test was used to compare the median time spent to calculate the TMAD and LSt variables on AP4 and AP2.

Results

A total of 193 client-owned cats (1–19 y/2.5–11.8 kg) were recruited for this study (105 females; 56%). The population included crossbred cats ($n = 172$; 89.1%), Persian ($n = 10$; 5.2%), Siamese ($n = 6$; 3.1%), Angora ($n = 2$; 1%), Maine Coon ($n = 2$; 1%), American Shorthair ($n = 1$; 0.5%), and Bengal ($n = 1$; 0.5%). Most of the cats weighed less than 5 kg, i.e., the BSA category below 0.292 m^2 ($n = 127$; 65.8%). The BSA distribution was as follow: 32.64% (63) less then 0.252 m^2 (< 4 kg), 33.16% (64) between 0.253 to 0.292 m^2 (4.01 to 5 kg), 20.72% (40) between 0.293 to 0.330 m^2 (5.1 to 6 kg), and 13.47% (26) with more than 0.331 m^2 (> 6.01 kg). The age distribution was: 108 (55.96%) young adults; 48 (24.87%) mature adults; 36 (18.65%) seniors, and 1 (0.52%) unknown.

Table 1 displays the TMAD and LSt results for the studied population. Table 2 presents TMAD and LSt results according to BSA categories. From all TMAD variables analyzed, only AP4 MP% differed by BSA. In contrast, all LSt values were lower in heavier cats. The age categories of

Table 1 Conventional and speckle-tracking echocardiographic parameters obtained in healthy non-sedated cats

Variables	n	Mean	Min	Max	SD
Age (years)	192	6.6	1	19	4
Weight (kg)	193	4.8	2.5	11.6	1.3
SBP (mmHg)	191	141.1	100	220	19.5
HR (bpm)	193	193.5	145	260	25.9
FS (%)	193	53.2	25.1	68.5	8.1
EF (%)	193	86	68.6	95.7	6.3
MAPSE IVS (mm)	136	4.4	2.3	7.7	0.9
MAPSE FW (mm)	174	4.7	2.2	7.9	0.9
Sep S′ (cm/s)	189	7.6	4.1	14.3	1.8
Lat S′ (cm/s)	165	7.3	3.9	11.4	1.5
TMAD Parameters					
AP2 MV1 (mm)	104	4.4	2	6.8	0.9
AP2 MV2 (mm)	104	4.8	2.2	8.2	1.1
AP2 MP (mm)	104	4.7	2.5	7.8	1
AP2 MP% (%)	104	18.5	11.3	26.4	3.4
AP4 MV1 (mm)	193	4.0	1.6	6.9	1
AP4 MV2 (mm)	193	4.2	1.8	7.4	1.1
AP4 MP (mm)	193	4.3	1.9	7.5	1
AP4 MP%	193	17.6	8.4	30.6	4
Global MP (mm)	104	4.6	3	7.6	0.8
Global MP%	104	18	12.7	26	2.7
Longitudinal Strain					
AP2 LSt (%)	104	28.9	19.9	45	4.6
AP4 LSt (%)	192	28.3	14.7	45.9	5.1
GLS (%)	104	29.4	20.4	42.3	4.6

SBP: systemic blood pression; HR: hear rate; FS: Fractional Shortening; EF: ejection fraction; MAPSE FW: mitral annular plane systolic excursion from the lateral annulus; MAPSE IVS: mitral annular plane systolic excursion from the septal annulus; Sep S′: systolic myocardium wave from tissular Doppler from the septal annulus; Lat S′: systolic myocardium wave from tissular Doppler from the lateral annulus; TMAD: tissue motion annular displacement; AP2: apical 2-chamber; MV1: point of septal mitral annulus; MV2: point of lateral mitral annulus; MP: displacement of a virtual midpoint between the two mitral annulus towards the left ventricle apex; MP%: percentage value of the midpoint in relation to the total length of the left ventricle; AP4: apical 4-chamber; LSt: longitudinal strain of the left ventricle; GLS: global longitudinal strain

n: total number of individuals; Min: minimum; Max: maximum; SD: standard deviation

the animals did not influence LSt and TMAD values, as can be seen in Table 3.

Significant correlations between TMAD and echocardiographic variables are shown in Table 4. The scatter plots of the moderate correlations between TMAD and echocardiographic variables are in Fig. 2. When comparing all variables, all significant correlations were considered low, such as those with BSA (MAPSE IVS, r = 0.221; TAPSE, r = 0.206; AP4 LSt, r = − 0.251; AP2 LSt, r = − 0.341; GLS, r = − 0.286; Lat s', r = 0.161; Sep s', r = 0.341), HR (SBP, r = 0.138; FS, r = 0.243, EF, r = 0.255; Sep s', r = 0.341; Lat s', r = 0.242; TRIV, r = − 0.219), Sep s' (IVRT, r = AP,4) LSt (MAPSE IVS, r = − 0.173; TAPSE, r = − 0.182), AP2 LSt (TAPSE, r = − 0.201), and GLS (TAPSE, r = − 0.256; EF, r = −0.256).

The inter and intra-observer variations are demonstrated in Table 5 for all the TMAD indexes, including the one without normality, TMAD MP%. Figure 3 displays the Bland-Altman graphics for this variable. Most TMAD variables had a moderate agreement, except the interobserver TMAD MP and MP%, which showed a substation correlation.

Concerning the time spent, although there was a numerical difference between the median time of AP4 LSt and AP4 TMAD (16.9 and 12.2 s, respectively), it was not significant ($p = 0.107$, Wilcoxon test). The same happened for AP2 LSt and AP2 TMAD (17.46 and 11.8 s, respectively; $p = 0.301$).

Discussion

This investigation sought to investigate whether TMAD would be a reliable surrogate for systolic function in apparently healthy cats. To date, TMAD has been extensively evaluated in people and proved to be a valuable and reproducible technique (Buss et al. 2012; Black et al. 2014; Asada et al. 2018; Teraguchi et al. 2019; Sharma et al. 2021; Teraguchi et al. 2021). In dogs, we recently evaluated TMAD and demonstrated its correlation with LSt of the left ventricle (Wolf et al. 2018). It was speculated that the results were at least as promising as those observed in the species mentioned above.

Interestingly, most of the mean TMAD values obtained in cats in this investigation were lower than those found in dogs within a comparable weight, between 1.7 and 8.5 kg (Wolf et al. 2018). A reasonable justification was that the mean bodyweight in cats was lower than in dogs, even within a similar weight range. Heavier animals with larger hearts present a more significant absolute mitral displacement towards the apex (Schober and Fuentes 2001).

On the contrary, the mean AP4 LSt in this study was higher than those observed in cats by other authors (Silva et al. 2013; Spalla et al. 2019; Suzuki et al. 2019b; Caivano et al. 2020). An explanation may be using different equipment and software to acquire the LSt, which has been discussed in human medicine lately (Bansal et al. 2008; Negishi et al. 2013; Yingchoncharoen et al. 2013; Yang et al. 2015; Ramlogan et al. 2020). A study with children found that the mean LSt differed between QLAB 10.5 and all other software packages, including contemporary versions of QLAB (Ferraro et al. 2020). Coincidentally, the LSt obtained in dogs using QLAB 10.5 was also higher than the average found by other researchers with different equipment (Kusunose et al. 2013; Wolf et al. 2018), pointing to a tendency

Table 2 Tissue motion annular displacement and longitudinal strain obtained in healthy non-sedated cats according to body surface area categories

BAS (m^2)	< 0.252 m		0.253 to 0.292 m2		0.293 to 0.330		> 0.331		P value*
Bodyweight (kg)	< 4		4.01 to 5		5.01 to 6		> 6.01		
	Mean (n)	SD	Mean (n)	SD	Mean (n)	SD	Mean (n)	SD	
TMAD values									
AP2 MV1 (mm)	4.22 (32)	0.97	4.31 (32)	0.88	4.47 (26)	0.88	4.81 (14)	0.78	0.2099
AP2 MV2 (mm)	4.60 (32)	1.27	4.75 (32)	1.09	4.86 (26)	0.96	5.04 (14)	1.08	0.6261
AP2 MP (mm)	4.59 (32)	1.1	4.64 (32)	0.98	4.82 (26)	0.83	4.99 (14)	0.87	0.5409
AP2 MP%	18.65 (32)	3.73	18.96 (32)	3.72	17.4 (26)	2.26	18.94 (14)	3.46	0.3132
AP4 MV1 (mm)	3.89 (63)	1.00	4.02 (64)	0.94	4.16 (40)	0.89	3.87 (26)	0.94	0.9985
AP4 MV2 (mm)	4.2 (63)	1.22	4.23 (64)	1.08	4.21 (40)	1.00	4.18 (26)	1.04	0.496
AP4 MP (mm)	4.28 (63)	1.05	4.29 (64)	0.98	4.31 (40)	0.91	4.13 (26)	0.87	0.8836
AP4 MP%	18.66[a] (63)	4.61	17.57 (64)	3.99	16.7 (40)	3.1	16.18[b] (26)	3.12	**0.0205**
Global MP (mm)	4.48 (32)	1.01	4.56 (32)	0.75	4.68(26)	0.69	4.62 (14)	0.58	0.8169
Global MP%	18.35 (32)	3.08	18.57 (32)	2.69	17.11 (26)	2.03	17.78 (14)	2.29	0.1706
LSt values (%)									
AP2 LSt	30.25[a] (32)	4.54	30.19 (32)	4.82	26.35[b] (26)	3.08	27.42 (14)	4.41	**0.0013**
AP4 LSt	29.54[a] (63)	5.21	28.80 (63)	4.66	26.42[b] (40)	4.61	27.02 (26)	5.9	**0.0095**
GLS	30.94[a] (32)	4.57	30.27[a] (33)	4.61	26.80[b] (26)	3.81	28.46 (14)	4.18	**0.0025**

*p value<0.05 means a significant difference

a, b: Lowercase letters indicate significant differences between the categories ($p < 0.05$)

BAS: body surface area

AP2: apical 2-chamber; MV1: point of septal mitral annulus; MV2: point of lateral mitral annulus; MP: displacement of a virtual midpoint between the two mitral annulus towards the left ventricle apex; MP%: percentage value of the midpoint in relation to the total length of the left ventricle; AP4: apical 4-chamber; LSt: longitudinal strain of the left ventricle; GLS: global longitudinal strain

n: total number of individuals; SD: standard deviation

Table 3 Comparison of tissue motion annular displacement (TMAD) values between the age categories

Variables	Age category	n	Mean	SD	*p-valor**
AP4 MP	Young	108	4.32	0.94	0.4700
	Mature	48	4.28	1.03	
	Senior	36	4.09	1.00	
AP4 MP%	Young	108	17.51	3.73	0.9930
	Mature	48	17.53	4.18	
	Senior	36	17.61	4.68	
AP4 MV1	Young	108	4.09	0.92	0.1382
	Mature	48	3.93	1.05	
	Senior	36	3.73	0.89	
AP4 MV2	Young	108	4.30	1.05	0.2647
	Mature	48	4.19	1.16	
	Senior	36	3.96	1.18	

*p value<0.05 means a significant difference

AP4: apical 4-chamber; MP: displacement of a virtual midpoint between the two mitral annulus towards the left ventricle apex; MP%: percentage value of the midpoint in relation to the total length of the left ventricle; MV1: point of septal mitral annulus; MV2: point of lateral mitral annulus

n: total number of individuals; SD: standard deviation

of this software to acquire higher LSt indexes. Furthermore, the LSt means obtained in the present study were similar to small dogs (up to 8.5 kg) using the same software version (Wolf et al. 2018). A study with dogs observed significant variability of strain variables obtained using different software, being the GLS the most reproducible measurement (Santarelli et al. 2019). Still, there is a need to standardize the abbreviation GLS in veterinary medicine, which can represent a weighted mean of the regional strains, using a single view (AP4) (Santarelli et al. 2019), or performing the average of the values from two apical images, AP2 and AP4 (Wolf et al. 2018, 2021). A reasonable option would be to follow human medicine, which refers to the GLS as the average of the values obtained from three apical views: AP2, AP3, and AP4 (Johnson et al. 2019).

As observed in children (Asada et al. 2018), the age categories did not influence TMAD values (Table 3). In dogs, although a significant correlation between TMAD and age happened, it disappeared when TMAD was normalized by body surface area (Wolf et al. 2018). Consequently, there is a need for a longitudinal study measuring TMAD values to clarify the effect of age, similarly to what was done previously with strain values, having been detected a reduction in

Table 4 Correlations detected between echocardiographic variables and TMAD indices

Variable	TMAD indices	r	CI	p-valor
Age	AP4 MV1	-0,155	-0,290 to -0,0140	0,0314
	AP2 MP	-0,208	-0,397 to -0,0321	0,0226
	Global MP	-0,208	-0,3838 to -0,0183	0,0321
HR	AP2 MV2	-0,207	-0,3809 to -0,0130	0,0353
	AP2 MP	-0,195	-0,3680 to 0,0020	0,0468
	Global MP	-0,194	-0,3676 to 0,0006	0,0469
BSA	AP4 MP%	-0,200	-0,3313 to -0,0605	0,0052
	Global MP%	-0,209	-0,3828 to -0,0171	0,0322
SBP	AP4 MV1	0,185	-0,1354 to 0,1464	0,0102
	AP4 MV2	0,171	-0,1183 to 0,1633	0,0178
	AP4 MP	0,194	-0,1685 to 0,1131	0,0072
	AP2 MP	0,208	0,0148 to 0,3858	0,0352
MAPSE FW	AP4 MV1	0,192	0,0396 to 0,3261	0,0113
	AP4 MV2	0,278	0,1345 to 0,4089	0,0002
	AP4 MP	0,244	0,0964 to 0,3762	0,0012
	AP2 MV1	0,337	0,1376 to 0,4842	0,0005
	AP2 MV2	0,411	0,0274 to 0,3948	0,0001
	AP2 MP	0,401	0,2139 to 0,5422	0,0001
	AP2 MP%	0,227	0,0274 to 0,3948	0,0213
	Global MP	0,390	0,2058 to 0,5349	0,0001
	Global MP%	0,179	-0,0178 to 0,3543	0,0001
MAPSE IVS	AP4 MV1	0,216	0,0522 to 0,3721	0,0114
	AP2 MV1	0,320	0,1365 to 0,4834	0,0001
	AP2 MV2	0,268	0,0814 to 0,4395	0,0061
	AP2 MP	0,297	0,0769 to 0,4343	0,0024
	AP2 MP%	0,265	0,0769 to 0,4343	0,0064
	Global MP%	0,253	-0,0962 to 0,2837	0,0071
Lat S'	AP4 MV1	0,185	0,03361 to 0,3289	0,0017
	AP4 MV2	0,207	0,0556 to 0,3484	0,0078
	AP4 MP	0,190	0,0385 to 0,3333	0,0144
AP4 LSt	AP4 MP	0,147	0,0048 to 0,2813	0,0422
	AP4 MP%	0,337	0,2054 to 0,4564	0,0001
	AP2 MP%	0,255	0,0628 to 0,4227	0,0091
	Global MP%	0,280	0,0920 to 0,4450	0,0038
AP2 LSt	AP4 MP%	0,242	0,0599 to 0,4203	0,013
	AP2 MP%	0,458	0,2706 to 0,5821	0,00001
	Global MP%	0,444	0,2557 to 0,5715	0,00001
GLS	AP4 MP%	0,209	0,0168 to 0,3825	0,0327
	AP2 MP%	0,285	0,0854 to 0,4412	0,0033
	Global MP%	0,307	0,1140 to 0,4627	0,0014

the rate of maximum longitudinal strain during diastole after six years of follow-up (Sugimoto et al. 2021).

Regarding the BSA, a positive correlation existed between BSA and AP4 MP% and Global MP% (Table 4). However, most TMAD parameters did not differ among cats of different BSA categories, the only exception being AP4 MP%, which decreased with the increase in BSA (Table 2). On the contrary, all TMAD variables evaluated in dogs changed following bodyweight, reducing when in percentage (MP%) and increasing when measured in millimeters (Wolf et al. 2018). One possible explanation might be the slight difference between BSA categories in cats compared to dogs. This hypothesis is supported by the fact that dogs showed a much more pronounced decrease in LSt as weight increased, justified by the considerable variation in heart size within this species.

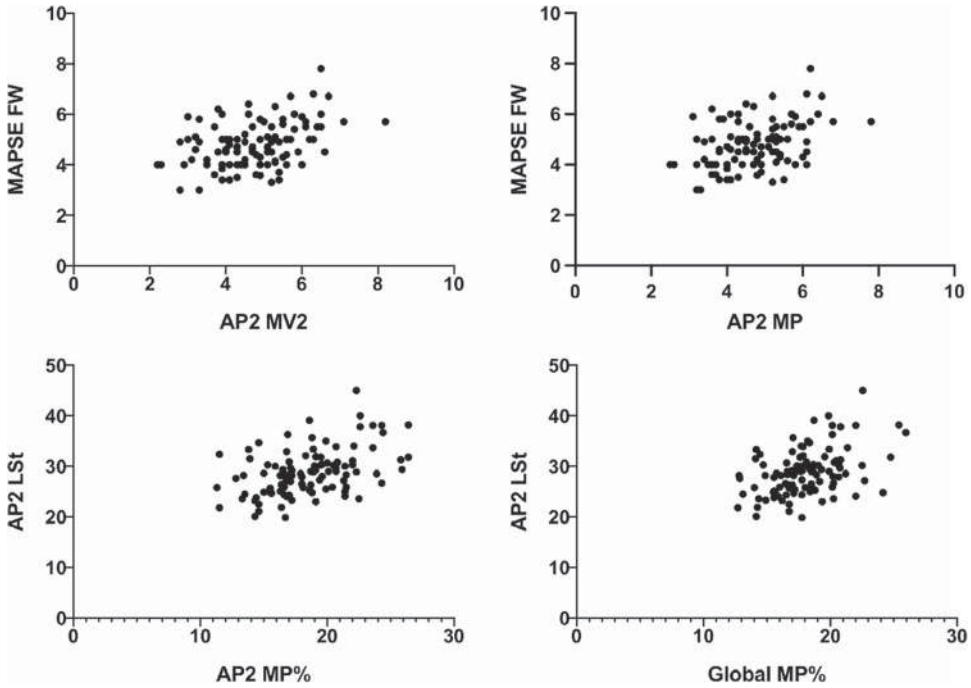

Fig. 2 Scatter plots of the moderate correlations between TMAD and echocardiographic variables

A low correlation appeared between SBP in almost all AP4 TMAD indices, except MP%. Sympathetic activity may explain it, affecting both SBP and contraction force. However, there was no correlation between HR and TMAD indices measured in AP4. This lack of correlation was also previously reported in children (Asada et al. 2018) and dogs (Wolf et al. 2018). Nevertheless, a negative correlation occurred between HR and AP2 MV2, AP2 MP, and Global MP (Table 4). The contrary would be expected: an increase in HR would raise contraction, called the Bowditch staircase effect (Lakkatta 2004), confirmed by the positive correlation between HR and FS. The arrangement of the myofibrils may explain these contrasting results. It was recently observed that the ventricular mass is organized in a mesh shape with myocytes aggregated in tangential alignment and some obliquely in the wall, with antagonistic function (Lunkenheimer et al. 2004). If this also occurs in the cat's heart, these antagonistic fibers may predominate in the inferior portion of the mitral annulus, corresponding to MV2 from AP2 image, explaining the negative correlations found. However, it is still a conjecture.

Concerning the most commonly used systolic indices, FS and EF, TMAD did not correlate with them, coinciding with the results from dogs (Wolf et al. 2018) and children (Black et al. 2014). A likely explanation for this finding is that both FS and EF acquired from M-mode echocardiography reflect the transversal and circumferential fibers (Kocica et al. 2006; Buss et al. 2012; Trivedi et al. 2019), not the target of TMAD. On the contrary, TMAD strongly correlated with the EF based on magnetic resonance imaging (MRI) in normal children (Black et al. 2014). The same happened in adult humans comparing a TMAD algorithm with EF MRI (Tsang et al. 2010). Future studies can confirm whether TMAD values in cats correlate with EF MRI.

The best correlation between LSt and TMAD occurred in AP2 (Table 4 and Fig. 2), obtaining two moderate correlations: LSt with MP%; and LSt with Global MP%. These findings were not surprising since both methods use STE.

Table 5 Intra and inter-observer variations for tissue motion annular displacement (TMAD) variables obtained for the apical four-chamber image

Variable	ICC (0–1)	SEM	M	SD	95%CI
		mm or %			
Intraobserver variation					
TMAD MV1 (mm)	0.72	0.44	3.9	0.8	3.05–4.71
TMAD MV2 (mm)	0.55	0.43	3.7	0.6	2.87–4.58
TMAD MP (mm)	0.68	0.34	3.9	0.6	3.34–4.66
TMAD MP%*	0.71	1.42	16.5	2.6	14.98–20.53
Interobserver variation					
TMAD MV1 (mm)	0.64	0.65	3.9	1.1	Not calculated
TMAD MV2 (mm)	0.52	0.83	3.8	1.2	Not calculated
TMAD MP (mm)	0.75	0.52	4.0	1.0	Not calculated
TMAD MP%*	0.85	1.78	17.7	4.6	Not calculated

*Variable without normal distribution

ICC: interclass correlation coefficient; SEM: Standard error of measurement; M: mean; SD: Standard deviation; 95%CI: range of 95% confidence interval calculated from the mean value

MV1: point of septal mitral annulus; MV2: point of lateral mitral annulus; MP: displacement of a virtual midpoint between the two mitral annulus towards the left ventricle apex; MP%: percentage value of the midpoint in relation to the total length of the left ventricle

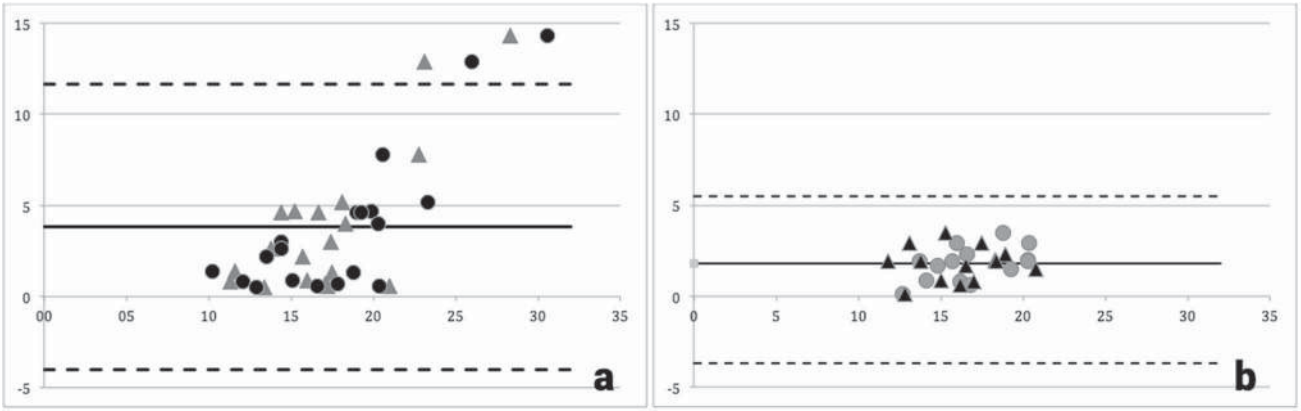

Fig. 3 Bland-Altmann graphic representing inter and intra-observer agreement for the variable TMAD MP% (**a**) interobserver variation; (**b**) intraobserver variation

Nonetheless, a low correlation was observed between Global MP% and GLS, while studies with people (Asada et al. 2018) and dogs (Wolf et al. 2018) found a moderate one.

Apparently, despite using speckle-tracking technology, TMAD and LSt have some very distinct characteristics. For example, TMAD was not influenced by cardiac rhythm in dogs, while GLS presented higher GLS values in sinus arrhythmia than sinus tachycardia or sinus rhythm (Wolf et al. 2018). The predominant rhythm in cats in hospital settings is tachycardia due to the fear reaction (Abbott 2005), requiring an investigation with sleeping or sedated cats to verify whether the GLS would be higher in sinus arrhythmia or if the mean TMAD values would change in sinus arrhythmia.

There were moderate correlations between TMAD and MAPSE, while in in humans it was observed a strong correlation (Hoit 2017; Mauermann et al. 2020). In cats, the strongest correlations were documented when comparing results obtained at the same mitral annulus, i.e., MV1 (septal) correlated better with MAPSE IVS and MV2 (lateral) with MAPSE FW (Table 4). These results were expected since both techniques follow the displacement of the mitral annulus in the longitudinal plane, except that the angle-independency from STE presumably makes the TMAD more accurate. For this reason, TMAD was also called $MAPSE_{STE}$ by some authors (Mauermann et al. 2020), highlighting that both techniques measure the displacement of the mitral annulus by different methods, M-mode and STE, respectively. Unlike the mentioned authors, who concluded that the TMAD underestimates the MAPSE values in M-mode, the TMAD indices in the present study were quite similar to the MAPSE ones.

Comparing IVS and FW annulus for MAPSE acquisition, it seemed that the first had better performance, obtaining more correlations with the TMAD variables (Table 4). Moreover, FW annulus also presented more correlations with TDI, having Lat s' correlated with all AP4 variables, except MP%. In humans, a strong correlation was seen with both s' waves (Buss et al. 2012), although others authors have not found it (Teraguchi et al. 2019).

About the inter-and intra-observer variations, most variables presented ICC classified as moderate (Table 4). Surprisingly, two interobserver comparisons were substantial (Fleiss 1986), MP and MP%, achieving better performance than the intraobserver assessment. Nevertheless, the visual interpretation given by the Bland-Altman plot of the MP% variability revealed satisfactory repeatability and reproducibility (Fig. 2). Earlier studies with TMAD obtained a satisfactory coefficient of variation in dogs (Wolf et al. 2018) and people (Tsang et al. 2010; Buss et al. 2012; Black et al. 2014; Penk et al. 2018; Teraguchi et al. 2019). The moderate agreement observed in this study may be due to more significant variability in the TMAD indices. An increase in the variability of STE indices was verified by an investigation that compared the left ventricular mechanics of mice, rats, rabbits, dogs, and humans, using strain imaging (Kusunose et al. 2012; Popovic and Thomas 2017). Another unproven possibility is that the HR three times greater than the human could make it difficult to correctly track the myocardium since the software was initially developed for humans.

Nevertheless, the SEM results shown in Table 5 provide an expected random variation in the scores of normal cats, which may be helpful in further studies with cats with HCM and compromised systolic function.

Concerning time, TMAD was faster to obtain in cats (MD = 12.2 s) compared to dogs (MD = 19.7 s) (Wolf et al. 2018) and slightly longer than reported in humans (8.22 and 10 s, respectively) (Tsang et al. 2010; Buss et al. 2012). Although it takes less than 15 s to be calculated, the real-time spent with TMAD should also compute the image

acquisition for later offline calculation and the time spent selecting the best record. The need for the three measurements to obtain the mean is advisable for most echocardiographic parameters in cats, so it does not count. However, all these mentioned steps also occur to acquire LSt, inherent to the STE. The authors consider that the TMAD calculation does not interfere negatively with the day-to-day exam. In addition, adequate tracking for calculating the TMAD was possible in all images obtained, like dogs (Wolf et al. 2018) and humans (Teraguchi et al. 2019).

Presumably, this was the first study to mention difficulties in obtaining STE in cats due to very low amplitude QRS complexes, even using the maximum magnification to increase ECG sensitivity. In general, the software can automatically detect QRS complexes and select a frame immediately before the ventricular systole, allowing the observer to determine the ROIs. However, sometimes very low QRS complexes resulted in incorrect P or T waves identification instead of QRS, producing unusual TMAD waves and unreliable LSt values. Provided the echocardiographer identifies this problem, TMAD can still be calculated, but failure to recognize this limitation can result in incorrect measurements being recorded.

Some limitations are recognized in this study. First, despite all efforts to include only healthy individuals, asymptomatic comorbidities may not have been identified based on clinical evaluation and ancillary examinations. In addition, the number and variability of cats included in the study may not represent feline populations from other countries, as Brazilian crossbred cats have an average weight of four to five kilograms, lighter than observed elsewhere. Lastly, the technique may have some disadvantages seen in STE, including the necessity of a simultaneous ECG, which can cause more stress depending on the cat's sensibility and the need for offline analysis.

Conclusion

This investigation led us to conclude that TMAD is viable to assess left ventricular longitudinal systolic function in healthy cats, with acceptable repeatability and reproducibility. Since the mitral motion can be easily tracked, TMAD has the advantage of not requiring an image quality as high as LSt, encouraging its application in routine. In addition, TMAD does not present remarkable discrepancies due to the equipment's software as occurs with strain. Even so, like most echocardiographic parameters, the TMAD may not be recommended as a single surrogate, but it complements the use of other parameters in the assessment of systolic function.

Although diastolic dysfunction predominates in cats' cardiomyopathies, little is comprehended about how the impairment of systolic function can contribute to the progression of the disease. Based on the reference values obtained for the species, further investigations may verify whether this technique can early detect systolic dysfunction in cats with subclinical HCM, and how this information could help in the primary care clinic. Another good purpose would be to define a cutoff value to aid in the prognosis of symptomatic patients.

Acknowledgements The researchers acknowledge the Veterinary Hospital of UPPR for allowing the use of the facilities during the study period and all the staff from the Laboratory of Comparative Cardiology, Department of Veterinary Medicine.

Special gratitude to Vera Hubner, who brought healthy cats and brightened our laboratory with her experience and love for the animals.

Code or data availability The datasets generated during and/or analysed during the current study are available from the corresponding author on reasonable request.

Authors' contribution - Giovana Lais Ruviaro Tuleski, M.Sc: electrocardiographys, echocardiography, blood pressure measurements, analysis of the results, text writing;

- Marcela Wolf, M.Sc: blood pressure measurements, TMAD measurements as co-observer, advice from her practice with TMAD in dogs;

- Maria José Garcia Ribeiro Pscheidt, BSc: animal recruitment, physical examination, blood pressure measurements, literature research;

- Júlio Pereira dos Santos, M.Sc: physical examination, electrocardiographys, blood pressure measurements, research assistance, text revision;

- Marlos Gonçalves Sousa, PhD: research design, guidance, statistical support, analysis of results, final review.

Declarations

Ethics approval The study was ethically approved by an established committee as established in the manuscript, protocol number 014/2019 of the Animal Use and Care Committee, and all procedures followed the National Institutes of Health Guide for the Care and Use of Animals of Laboratory.

Consent to participate Written informed consent was obtained from the owners.

Consent for publication statement of animal ethics The written consent from owners allowing their cats to participate in the study included permission to publish the echocardiographic images obtained.

Conflicts of interest/competing The authors do not have any conflicts of interest to declare.

References

Abbott JA (2005) Heart rate and heart rate variability of healthy cats in home and hospital environments. J Feline Med Surg 7:195–202. https://doi.org/10.1016/j.jfms.2004.12.003

Abbott JA, MacLean HN (2013) Two-dimensional echocardiographic assessment of the feline left atrium. J Vet Intern Med 20:111–119. https://doi.org/10.1892/0891-6640(2006)20[111:teaotf]2.0.co;2

Acierno MJ, Brown S, Coleman AE et al (2018) ACVIM consensus statement: guidelines for the identification, evaluation, and management of systemic hypertension in dogs and cats. J Vet Intern Med 32:1803–1822. https://doi.org/10.1111/jvim.15331

Aloia E, Cameli M, D'Ascenzi F et al (2016) TAPSE: an old but useful tool in different diseases. Int J Cardiol 225:177–183. https://doi.org/10.1016/j.ijcard.2016.10.009

Asada D, Okumura K, Ikeda K, Itoi T (2018) Tissue motion annular displacement of the mitral valve can be a useful index for the evaluation of left ventricular systolic function by echocardiography in Normal children. Pediatr Cardiol 39:976–982. https://doi.org/10.1007/s00246-018-1847-2

Bansal M, Cho GY, Chan J et al (2008) Feasibility and accuracy of different techniques of two-dimensional speckle based strain and validation with harmonic phase magnetic resonance imaging. J Am Soc Echocardiogr 21:1318–1325. https://doi.org/10.1016/j.echo.2008.09.021

Binns SH, Sisson DD, Buoscio DA, Schaeffer DJ (1995) Doppler Ultrasonographic, Oscillometric Sphygmomanometric, and Photoplethysmographic techniques for noninvasive blood pressure measurement in anesthetized cats. J Vet Intern Med 9:405–414. https://doi.org/10.1111/j.1939-1676.1995.tb03301.x

Black DE, Bryant J, Peebles C et al (2014) Tissue motion annular displacement of the mitral valve using two-dimensional speckle tracking echocardiography predicts the left ventricular ejection fraction in normal children. Cardiol Young 24:640–648. https://doi.org/10.1017/S1047951113000863

Bland JM, Altman DG (2010) Statistical methods for assessing agreement between two methods of clinical measurement. Int J Nurs Stud 47:931–936. https://doi.org/10.1016/j.ijnurstu.2009.10.001

Buss SJ, Mereles D, Emami M et al (2012) Rapid assessment of longitudinal systolic left ventricular function using speckle tracking of the mitral annulus. Clin Res Cardiol 101:273–280. https://doi.org/10.1007/s00392-011-0389-x

Caivano D, Rishniw M, Baiona L et al (2020) Assessment of longitudinal left ventricle deformation by 2-dimensional speckle tracking echocardiography obtained from different views in cats. Vet Sci 7:104. https://doi.org/10.3390/vetsci7030104

Carlsson M, Ugander M, Mosén H et al (2007) Atrioventricular plane displacement is the major contributor to left ventricular pumping in healthy adults, athletes, and patients with dilated cardiomyopathy. Am J Physiol Circ Physiol 292:H1452–H1459. https://doi.org/10.1152/ajpheart.01148.2006

Chetboul V, Athanassiadis N, Carlos C et al (2004) Quantification, repeatability, and reproducibility of feline radial and longitudinal left ventricular velocities by tissue Doppler imaging. Am J Vet Res 65:566–572. https://doi.org/10.2460/ajvr.2004.65.566

Chetboul V, Tissier R (2012) Echocardiographic assessment of canine degenerative mitral valve disease. J Vet Cardiol 14:127–148. https://doi.org/10.1016/j.jvc.2011.11.005

Collier P, Phelan D, Klein A (2017) A test in context: myocardial strain measured by speckle-tracking echocardiography. J Am Coll Cardiol 69:1043–1056. https://doi.org/10.1016/j.jacc.2016.12.012

Ferraro AM, Adar A, Ghelani SJ et al (2020) Speckle tracking echocardiographically-based analysis of ventricular strain in children: an intervendor comparison. Cardiovasc Ultrasound 18:15. https://doi.org/10.1186/s12947-020-00199-x

Fleiss JL (1986) Reliability of measurement. John Wiley & Sons, Inc

Häggström J, Andersson O, Falk T et al (2016) Effect of body weight on echocardiographic measurements in 19,866 pure-bred cats with or without heart disease. J Vet Intern Med 30:1601–1611. https://doi.org/10.1111/jvim.14569

Hill RC, Scott KC (2004) Energy requirements and body surface area of cats and dogs. J Am Vet Med Assoc 225:689–694. https://doi.org/10.2460/javma.2004.225.689

Hoit BD (2017) Evaluation of left atrial function: current status. Struct Hear 1:109–120. https://doi.org/10.1080/24748706.2017.1353718

Hu K, Liu D, Herrmann S et al (2013) Clinical implication of mitral annular plane systolic excursion for patients with cardiovascular disease. Eur Heart J Cardiovasc Imaging 14:205–212. https://doi.org/10.1093/ehjci/jes240

Johnson C, Kuyt K, Oxborough D, Stout M (2019) Practical tips and tricks in measuring strain, strain rate and twist for the left and right ventricles. Echo Res Pract 6:R87–R98. https://doi.org/10.1530/ERP-19-0020

Klaeboe LG, Edvardsen T (2019) Echocardiographic assessment of left ventricular systolic function. J Echocardiogr 17:10–16. https://doi.org/10.1007/s12574-018-0405-5

Kocica MJ, Corno AF, Carreras-Costa F et al (2006) The helical ventricular myocardial band: global, three-dimensional, functional architecture of the ventricular myocardium. Eur J Cardio-thoracic Surg 29. https://doi.org/10.1016/j.ejcts.2006.03.011

Koffas H, Dukes-McEwan J, Corcoran BM et al (2006) Pulsed tissue Doppler imaging in normal cats and cats with hypertrophic cardiomyopathy. J Vet Intern Med 20:65–77. https://doi.org/10.1892/0891-6640(2006)20[65:PTDIIN]2.0.CO;2

Koo TK, Li MY (2016) A guideline of selecting and reporting Intraclass correlation coefficients for reliability research. J Chiropr Med 15:155–163. https://doi.org/10.1016/j.jcm.2016.02.012

Kusunose K, Penn MS, Zhang Y et al (2012) How similar are the mice to men? Between-species comparison of left ventricular mechanics using strain imaging. PLoS One 7. https://doi.org/10.1371/journal.pone.0040061

Kusunose K, Zhang Y, Mazgalev TN et al (2013) Left ventricular strain distribution in healthy dogs and in dogs with tachycardia-induced dilated cardiomyopathy. Cardiovasc Ultrasound 11:43. https://doi.org/10.1186/1476-7120-11-43

Lakkatta EG (2004) Beyond Bowditch: the convergence of cardiac chronotropy and inotropy. Cell Calcium 35:629–642. https://doi.org/10.1016/j.ceca.2004.01.017

Liu L, Tuo S, Zhang J et al (2014) Reduction of left ventricular longitudinal global and segmental systolic functions in patients with hypertrophic cardiomyopathy: study of two-dimensional tissue motion annular displacement. Exp Ther Med 7:1457–1464. https://doi.org/10.3892/etm.2014.1617

Luis SA, Chan J, Pellikka PA (2019) Echocardiographic assessment of left ventricular systolic function: an overview of contemporary techniques, including speckle-tracking echocardiography. Mayo Clin Proc 94:125–138. https://doi.org/10.1016/j.mayocp.2018.07.017

Lunkenheimer PP, Redmann K, Florek J et al (2004) The forces generated within the musculature of the left ventricular wall. Heart 90:200–207. https://doi.org/10.1136/hrt.2003.011650

Mauermann E, Bouchez S, Bove T et al (2020) Rapid, single-view speckle-tracking–based method for examining left ventricular systolic and diastolic function in point of care ultrasound. J Ultrasound Med 39:2151–2164. https://doi.org/10.1002/jum.15324

Mizuguchi Y, Oishi Y, Miyoshi H et al (2008) The functional role of longitudinal, circumferential, and radial myocardial deformation for regulating the early impairment of left ventricular contraction and relaxation in patients with cardiovascular risk factors: a study with two-dimensional strain Im. J Am Soc Echocardiogr 21:1138–1144. https://doi.org/10.1016/j.echo.2008.07.016

Mondillo S, Galderisi M, Ballo P, Marino PN (2006) Left ventricular systolic longitudinal function: comparison among simple M-mode, pulsed, and M-mode color tissue Doppler of mitral annulus in healthy individuals. J Am Soc Echocardiogr 19:1085–1091. https://doi.org/10.1016/j.echo.2006.04.005

Negishi K, Lucas S, Negishi T et al (2013) What is the primary source of discordance in strain measurement between vendors: imaging

or analysis? Ultrasound Med Biol 39:714–720. https://doi.org/10.1016/j.ultrasmedbio.2012.11.021

Penk JS, Zaidi SJH, Lefaiver CA et al (2018) Tissue motion annular displacement predicts mortality/transplant after the bidirectional Glenn. World J Pediatr Congenit Heart Surg 9:171–176. https://doi.org/10.1177/2150135117742650

Popovic ZB, Thomas JD (2017) Assessing observer variability: a user's guide. Cardiovasc Diagn Ther 7:317–324. https://doi.org/10.21037/cdt.2017.03.12

Quimby J, Gowland S, Carney HC et al (2021) 2021 AAHA/AAFP Feline Life Stage Guidelines. J Feline Med Surg 57:51–72. https://doi.org/10.5326/JAAHA-MS-7189

Ramlogan S, Aly D, France R et al (2020) Reproducibility and Intervendor agreement of left ventricular global systolic strain in children using a layer-specific analysis. J Am Soc Echocardiogr 33:110–119. https://doi.org/10.1016/j.echo.2019.08.004

Riffel JH, Mereles D, Emami M et al (2015) Prognostic significance of semiautomatic quantification of left ventricular long axis shortening in systemic light-chain amyloidosis. Amyloid 22:45–53. https://doi.org/10.3109/13506129.2014.992515

Rishniw M, Erb HN (2000) Evaluation of four 2-dimensional echocardiographic methods of assessing left atrial size in dogs. J Vet Intern Med 14:429–435. https://doi.org/10.1111/j.1939-1676.2000.tb02252.x

Sahn DJ, DeMaria A, Kisslo J, Weyman A (1978) Recommendations regarding quantitation in M-mode echocardiography: results of a survey of echocardiographic measurements. Circulation 58:1072–1083. https://doi.org/10.1161/01.CIR.58.6.1072

Santarelli G, Baron Toaldo M, Bouvard J et al (2019) Variability among strain variables derived from two-dimensional speckle tracking echocardiography in dogs by use of various software. Am J Vet Res 80:347–357. https://doi.org/10.2460/ajvr.80.4.347

Schober KE, Chetboul V (2015) Echocardiographic evaluation of left ventricular diastolic function in cats: hemodynamic determinants and pattern recognition. J Vet Cardiol 17:S102–S133. https://doi.org/10.1016/j.jvc.2015.02.002

Schober KE, Fuentes VL (2001) Mitral annulus motion as determined by M-mode echocardiography in normal dogs and dogs with cardiac disease. Vet Radiol Ultrasound 42:52–61. https://doi.org/10.1111/j.1740-8261.2001.tb00904.x

Schober P, Schwarte LA (2018) Correlation coefficients: appropriate use and interpretation. Anesth Analg 126:1763–1768. https://doi.org/10.1213/ANE.0000000000002864

Seo J-S, Kim D-H, Kim W-J et al (2010) Peak systolic velocity of mitral annular longitudinal movement measured by pulsed tissue Doppler imaging as an index of global left ventricular contractility. Am J Physiol Heart Circ Physiol 298:H1608–H1615. https://doi.org/10.1152/ajpheart.01231.2009

Sharma JB, Deora S, Choudhary R, Kaushik A (2021) Comparison of mitral annular displacement and global longitudinal strain imaging for predicting significant coronary atherosclerotic disease in patients of chronic stable angina pectoris. Int J Cardiovasc Imaging 37:861–870. https://doi.org/10.1007/s10554-020-02058-2

Silva AC, Muzzi RAL, Oberlender G et al (2013) Longitudinal strain and strain rate by two-dimensional speckle tracking in non-sedated healthy cats. Res Vet Sci 95:1175–1180. https://doi.org/10.1016/j.rvsc.2013.07.020

Simpson KE, Gunn-Moore DA, Shaw DJ et al (2009) Pulsed-wave Doppler tissue imaging velocities in normal geriatric cats and geriatric cats with primary or systemic diseases linked to specific cardiomyopathies in humans, and the influence of age and heart rate upon these velocities. J Feline Med Surg 11:293–304. https://doi.org/10.1016/j.jfms.2008.08.003

Spalla I, Boswood A, Connolly DJ, Luis Fuentes V (2019) Speckle tracking echocardiography in cats with preclinical hypertrophic cardiomyopathy. J Vet Intern Med 33:1232–1241. https://doi.org/10.1111/jvim.15495

Spalla I, Payne JRR, Borgeat K et al (2017) Mitral annular plane systolic excursion and tricuspid annular plane systolic excursion in cats with hypertrophic cardiomyopathy. J Vet Intern Med 31:691–699. https://doi.org/10.1111/jvim.14697

Sugimoto K, Aoki T, Fujii Y (2021) Longitudinal evaluation of cardiovascular function in six healthy cats aged 1–8 years. J Feline Med Surg 23:98–104. https://doi.org/10.1177/1098612X20932255

Suzuki R, Mochizuki Y, Yoshimatsu H et al (2019a) Layer-specific myocardial function in asymptomatic cats with obstructive hypertrophic cardiomyopathy assessed using 2-dimensional speckle-tracking echocardiography. J Vet Intern Med 33:37–45. https://doi.org/10.1111/jvim.15339

Suzuki R, Mochizuki Y, Yuchi Y et al (2019b) Assessment of myocardial function in obstructive hypertrophic cardiomyopathy cats with and without response to medical treatment by carvedilol. BMC Vet Res 15:1–8. https://doi.org/10.1186/s12917-019-2141-0

Teraguchi I, Hozumi T, Emori H et al (2021) Prognostic value of tissue-tracking mitral annular displacement by speckle-tracking echocardiography in asymptomatic aortic stenosis patients with preserved left ventricular ejection fraction. J Echocardiogr 19:95–102. https://doi.org/10.1007/s12574-020-00490-w

Teraguchi I, Hozumi T, Takemoto K et al (2019) Assessment of decreased left ventricular longitudinal deformation in asymptomatic patients with organic mitral regurgitation and preserved ejection fraction using tissue-tracking mitral annular displacement by speckle-tracking echocardiography. Echocardiography 36:678–686. https://doi.org/10.1111/echo.14290

Thomas WP, Gaber CE, Jacobs GJ et al (1994) Recommendations for standards in transthoracic two-dimensional echocardiography in the dog and cat. Vet Radiol Ultrasound 35:173–178. https://doi.org/10.1111/j.1740-8261.1994.tb01588.x

Tidholm A, Ljungvall I, HÃglund K et al (2009) Tissue Doppler and strain imaging in dogs with Myxomatous mitral valve disease in different stages of congestive heart failure. J Vet Intern Med 23:1197–1207. https://doi.org/10.1111/j.1939-1676.2009.0403.x

Trivedi SJ, Altman M, Stanton T, Thomas L (2019) Echocardiographic strain in clinical practice. Hear Lung Circ 28:1320–1330. https://doi.org/10.1016/j.hlc.2019.03.012

Tsang W, Ahmad H, Patel AR et al (2010) Rapid estimation of left ventricular function using echocardiographic speckle-tracking of mitral annular displacement. J Am Soc Echocardiogr 23:511–515. https://doi.org/10.1016/j.echo.2010.03.003

van Dalen BM, Bosch JG, Kauer F et al (2009) Assessment of mitral annular velocities by speckle tracking echocardiography versus tissue Doppler imaging: validation, feasibility, and reproducibility. J Am Soc Echocardiogr 22:1302–1308. https://doi.org/10.1016/j.echo.2009.08.004

Vinereanu D, Khokhar A, Fraser AG (1999) Reproducibility of pulsed wave tissue Doppler echocardiography. J Am Soc Echocardiogr 12:492–499. https://doi.org/10.1016/S0894-7317(99)70086-6

Wolf M, Lucina SB, Silva VBC et al (2021) Assessment of longitudinal systolic function using tissue motion annular displacement in dogs with degenerative mitral valve disease. J Vet Cardiol 38:44–58. https://doi.org/10.1016/j.jvc.2021.10.004

Wolf M, Lucina SBSB, Brüler BCBC et al (2018) Assessment of longitudinal systolic function using tissue motion annular displacement in healthy dogs. J Vet Cardiol 20. https://doi.org/10.1016/j.jvc.2018.04.004

Yang H, Marwick TH, Fukuda N et al (2015) Improvement in strain concordance between two major vendors after the strain standardization initiative. J Am Soc Echocardiogr 28:642–648.e7. https://doi.org/10.1016/j.echo.2014.12.009

Yingchoncharoen T, Agarwal S, Popović ZB, Marwick TH (2013) Normal ranges of left ventricular strain: a Meta-analysis. J Am Soc Echocardiogr 26:185–191. https://doi.org/10.1016/j.echo.2012.10.008

Zacà V, Ballo P, Galderisi M, Mondillo S (2010) Echocardiography in the assessment of left ventricular longitudinal systolic function: current methodology and clinical applications. Heart Fail Rev 15:23–37. https://doi.org/10.1007/s10741-009-9147-9

Zois NE, Tidholm A, Nägga KM et al (2012) Radial and longitudinal strain and strain rate assessed by speckle-tracking echocardiography in dogs with Myxomatous mitral valve disease. J Vet Intern Med 26:1309–1319. https://doi.org/10.1111/j.1939-1676.2012.01017.x

Original Article

jfms Journal of Feline Medicine and Surgery

Journal of Feline Medicine and Surgery
1–13

DOI: 10.1177/1098612X221083372
journals.sagepub.com/home/jfm

This paper was handled and processed by the American Editorial Office (AAFP) for publication in *JFMS*

SAGE

Timolol 0.5% ophthalmic solution influences cardiac function in healthy cats

Giovana LR Tuleski[1], Maria Jose Garcia Ribeiro Pscheidt[2], Júlio Pereira dos Santos[1] and Marlos Gonçalves Sousa[1]

Abstract

Objectives The aim of this study was to ascertain the effect of a drop of timolol 0.5% ophthalmic solution on the systolic function of the left ventricle (LV) and left atrium (LA), and to confirm if timolol helped appraisal of diastolic function by reducing heart rate (HR) and separating the transmitral outflow waves from tissue Doppler imaging (TDI).

Methods A total of 41 client-owned healthy cats underwent two echocardiograms 20 mins apart. The timolol group (33 cats) received a drop of timolol solution after the first examination. Standard and speckle-tracking echocardiography evaluated the LV and LA function of both groups at the two time points evaluated.

Results Timolol reduced HR (19%), and fractional shortening from LV (20.3%) and LA (16.6%). Septal S' decreased by 51% (from 7.7 to 5.2 cm/s) and lateral S' dropped by 43.1% (7.3 to 5.1 cm/s). Most longitudinal techniques did not change after timolol, including the mitral annular plane systolic excursion from the interventricular annulus, tricuspid annular plane systolic excursion, LV longitudinal strain and LV tissue motion annular displacement. The isovolumic relaxation time increased by 15.2% (from 54 to 64.6 ms), with most cats presenting this variable above the reference (>60 ms). Timolol did not support diastolic assessment, enabling evaluation in only 2/11 cats when using lateral TDI and 1/9 cats using septal TDI. Regarding side effects, miosis occurred in 18 cats (54.5%).

Conclusions and relevance Timolol reduced systolic function, decreasing standard echocardiographic variables. Regarding diastolic evaluation, although timolol decreased HR, it did not separate the mitral diastolic waves, as expected.

Keywords: Beta blocker; tissue motion annular displacement; speckle tracking; atrial function

Accepted: 7 February 2022

Introduction

An echocardiogram in cats usually activates the fear response, causing an increase in heart rate (HR),[1,2] systemic blood pressure (SBP)[3] and respiratory rate. Tachycardia is an undesirable consequence of stress, as it can impede or complicate diastolic evaluation.[4] At a lower HR, there are two transmitral outflow waves: the E wave, which corresponds to the filling of the left ventricle (LV) in early diastole, followed by the A wave, with the peak resulting from atrial systole.[5,6] In most cats with normal diastolic function, E is greater than A (E/A>1). An HR above 170–180 beats per min (bpm) during echocardiography in cats leads to fusion of the mitral outflow waves (EAfus). The same occurs with tissue Doppler imaging (TDI): the summation of waves with tachycardia (E'A'fus). This technique reflects the myocardial velocity rather than blood movement by placing the Doppler gate at the mitral annulus (interventricular septum [IVS] or free wall [FW]). The E' wave, called early diastolic mitral annular velocity, is produced during early LV diastole, while A' reflects annulus movement during contraction of the left atrium (LA).[5] Normally, E' is expected to be

[1]Laboratory of Comparative Cardiology, Department of Veterinary Medicine, Federal University of Paraná (UFPR), Curitiba, Paraná, Brazil
[2]Curitiba, Paraná, Brazil

Corresponding author:
Giovana LR Tuleski MSc, Laboratory of Comparative Cardiology, Department of Veterinary Medicine, Federal University of Paraná (UFPR), Rua dos Funcionários, 1540, Curitiba, Paraná CEP 80035-050, Brazil
Email: gtuleski@yahoo.com.br

greater than A', although a slightly inverted ratio (E'/A' between 0.8 and 1.0) can be considered normal in cats with a high HR.[4]

Fused waves do not allow diastolic assessment, which is essential for diagnosis, as the most prevalent heart diseases in cats (ie, cardiomyopathies with hypertrophic or restrictive phenotypes) start with impairment of diastolic function.[4,7,8] It is highly recommended that diastolic function is evaluated and its pattern classified using a combination of spectral Doppler and TDI. Precocious detection of dysfunction can help diagnose early-stage disease. In cats that have already developed signs of congestive heart failure or arterial thromboembolism (ie, those classified as stage C), diastolic information helps establish a prognosis.[9]

An alternative to avoiding summation and enabling diastolic assessment is to apply a vagal maneuver at the time of mitral outflow Doppler or TDI acquisition.[10] It requires the presence of an assistant to perform the parasympathetic stimulation correctly at the appropriate moment. Another option is to administer timolol ophthalmic solution to block the sympathetic tone and decrease the HR, separating the transmitral and TDI waves.[11] The topical application of timolol has a systemic absorption,[12,13] reducing the HR when administered alone in cats[11] or associated with topically applied carbonic anhydrase inhibitors, such as dorzolamide or brinzolamide.[14]

Timolol maleate is the most frequently used drug in managing open-angle glaucoma,[15] although long-term treatment may have adverse effects in humans, such as low systolic or diastolic blood pressure.[16] A non-selective beta-adrenergic antagonist such as timolol may reduce the contraction force of the heart,[17,18] compromising the commonly used systolic variables. In consequence, it may also modify the LA activity, directly affected by the LV.[19]

This study assumed that timolol would alter cardiac function in cats undergoing an echocardiogram. In this case, the objective was to determine how much a single drop of timolol interferes with the systolic variables obtained by standard and speckle-tracking echocardiography. Furthermore, it was expected that the echocardiographic indices of the control group would not change after 20 mins of waiting and second handling, even though it could be stressful for cats.

Materials and methods

Animals

This prospective longitudinal observational study recruited client-owned healthy cats between May and July 2019. Before enrollment, all cats underwent a thorough physical examination, SBP measurement with Doppler, electrocardiography (ECG) and standard transthoracic echocardiography.

The Institutional Animal Care and Use Committee (protocol 014/2019) previously approved all the procedures and they complied with the National Institutes of Health Guide for the Care and Use of Laboratory Animals. Owners were required to formally agree to participate in this research by signing an informed consent form.

An age limitation was adopted to avoid possible changes in drug metabolism in younger or older animals; cats <1 year or >14 years of age were excluded. Cats with an elevated SBP prior to the first echocardiogram (>160 mmHg) did not participate, nor did any cat with a history or signs of heart disease or other chronic illness, or that had received any treatment in the past 6 months.

Echocardiography

All cats underwent two echocardiographic examinations with only gentle restraint and no sedation. Positioning followed the recommendations of the Echocardiography Committee of the Specialty of Cardiology of the American College of Veterinary Internal Medicine.[20] The same operator (GLRT) performed all examinations and measurements.

A drop of timolol 0.5% ophthalmic solution containing approximately 0.17 mg timolol (1 mm = 30 drops) was instilled at the left eye immediately after the first echocardiogram (control timolol). A second echocardiogram (timolol) was performed 20 mins later, following the same protocols mentioned. The control group consisted of eight cats not receiving the timolol eyedrop, submitted to two echocardiograms 20 mins apart (control 1 and control 2, respectively).

LV systolic function

LV M-mode measurements at the papillary level were determined, as described previously,[21] allowing the calculation of the most common systolic variables, such as fractional shortening (FS) and ejection fraction (EF). The end-diastolic and end-systolic LV diameters were measured using a leading-edge-to-leading-edge technique, with a simultaneous ECG allowing us to distinguish the two cardiac phases. The cut-off point for hypertrophic cardiomyopathy (HCM) was considered to be 5.5 mm for any LV image,[22] including IVS thickness in the LV outflow tract view from the right parasternal window.

Evaluation of the longitudinal systolic function of the LV required acquisition of apical four-chamber (AP4) and two-chamber (AP2) images from the left parasternal window. At least five cardiac cycles were recorded to allow off-line calculation of tissue motion annular displacement (TMAD) measures and the longitudinal strain (LSt) values, considering the mean of AP4 and AP2 values as global indices. In addition, AP4 was applied to measure the mitral annular plane systolic excursion (MAPSE) from the IVS annulus and FW annulus, the tricuspid annular plane systolic excursion (TAPSE), and the mitral annular velocities with the gate of investigation on the IVS and FW annulus, as described elsewhere.[5,23]

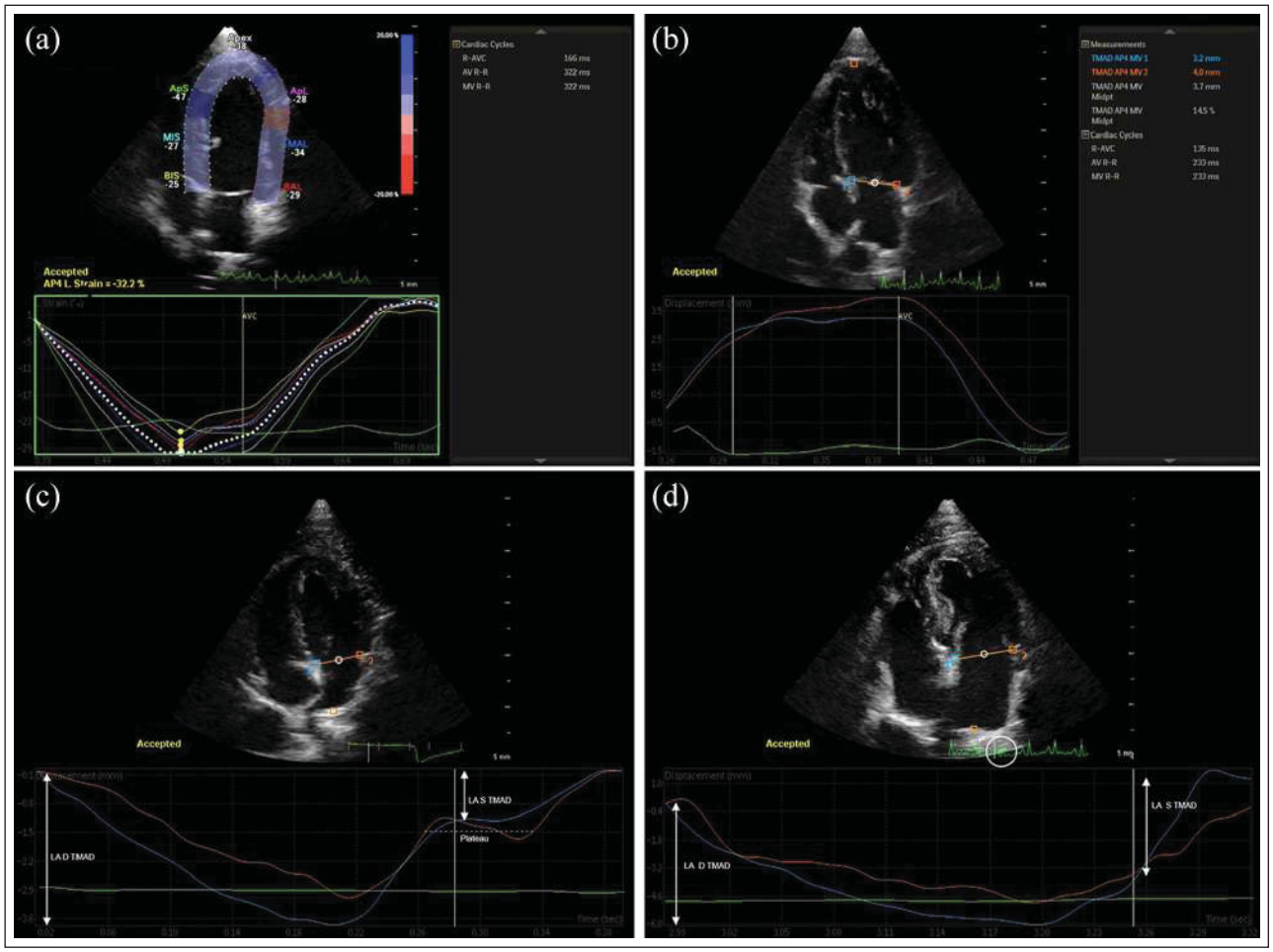

Figure 1 Apical four-chamber (AP4) images demonstrating: (a) longitudinal strain of the left ventricle (LV); (b) tissue motion annular displacement (TMAD) of the LV; (c) TMAD of the left atrium (LA) in a patient with a low heart rate (150 beats per minute [bpm]) and a visible plateau (dashed line); and (d) TMAD of the LA in a cat with a faster heart rate (186 bpm), with diastasis determined by pausing the electrocardiogram (ECG) cursor just before the P wave on the ECG (white circle). TMAD AP4 MV1 (in blue) describes the displacement of mitral septal annulus towards the LV apex; TMAD AP4 MV2 (in orange) is the displacement of mitral lateral annulus towards the LV apex; TMAD AP4 MV midpoint (in white) signifies the displacement of a virtual point determined in between the septal and lateral hinge points of mitral annulus towards the LV apex. In (c) and (d), the larger arrows designate the total displacement of the mitral annulus towards the farthest point of the LA (LA D TMAD); the shorter ones represent systolic displacement to the same point (LA S TMAD)

Both LV TMAD and LV LSt required the aortic valve closure time, measured from the apical five-chamber image. It corresponds to the time (ms) from the beginning of the QRS complex to the end of the aortic valve spectra obtained with the pulsed Doppler gate positioned distally to the valve.[24]

The hinge points of mitral valve leaflets (septal and lateral) and the LV apex epicardial region were the three regions of interest (ROIs) used to calculate the LV LSt[25] (Figure 1a), which was measured automatically by the equipment software (QLAB ACMQ; Auto Cardiac Motion Quantification). Manual corrections were made whenever the automatic myocardial tracking was obviously incorrect. For LV TMAD, the same three ROIs were defined (Figure 1b). The displacement of both annuli towards the apex (in mm) was automatically calculated. Also, the software defined a virtual midpoint between the two annular ROIs (LV MP TMAD) and calculated its displacement towards the LV apex (mm), as well as the proportional displacement of that midpoint concerning the total length of the LV (LV MP% TMAD).

LA function

LA FS was estimated based on the minimum and maximum LA diameter from the right parasternal short-axis view image at the aortic valve level, using anatomic M-mode.[26] The ratio between the LA and aorta was measured at the maximum LA diameter (LAD), right after the T wave from the ECG, as described previoulsy.[27] The LAD measure was acquired from the right parasternal long-axis four-chamber view, being performed as explained before, with a maximum reference value of 1.6 cm.[28] The

AP4 image was used to measure LA dimensions at three different moments based on the LA cycle (before P wave, before QRS complex and after T wave), enabling later calculation of the passive (pEF), active (aEF) and complete (cEF) LA EF, as detailed elsewhere.[29]

To calculate LA LSt and LA TMAD, the first two ROIs had the same position as the LV at the mitral leaflet hinge points, while the third ROI was defined at the cranial inner edge of the LA. The total displacement (LA D TMAD) between the maximal negative and positive positions was the average of the displacements documented individually for each of the two annular points. The systolic displacement (LA S TMAD) was the average movement of the two ROIs between diastasis and the maximal positive position. In humans, diastasis is easily recognized by a plateau wave (Figure 1c).[30] However, as the mean HR in cats is approximately three times higher, a plateau phase might not happen. In these cases, it is possible to determine the diastasis based exclusively on the simultaneous ECG, pausing the marker immediately before the P wave (Figure 1d).

Statistical analysis

The study aimed to determine whether ophthalmic timolol would cause differences in the echocardiographic variables of cats after its application. The same group of animals was compared before and after application (paired quantitative variable). The sample size was calculated using GPower 3.1.9.4,[31] with an expected effect of 80%, a sampling power of 95% and an error of 5% for quantitative measurements and using two dependent samples, reaching a total number of 23 cats for the timolol group.

Analysis was conducted in R 4.0.5 (R Core Team 2021).[32] Initially, a descriptive analysis of the data was accomplished with an estimate of the mean, median, SD, range and interquartile range of the quantitative variables, and simple and relative frequencies of the qualitative variables.

The Shapiro–Wilk normality test was performed to determine the parametric and non-parametric approaches to evaluate the quantitative variables. For variables with a normal distribution, the difference between two independent groups was verified with a Student's *t*-test or paired *t*-test for dependent groups (crossover). For variables without a normal distribution, this difference was verified using the Mann–Whitney or Wilcoxon U-test. *P* values <0.05 were considered to be significantly different. Finally, Spearman's correlation was adopted to analyze the relationship between HR and body weight (BW) for both timolol and control groups.

Results

Forty-one client-owned healthy cats were enrolled in the study. The timolol group was composed of 33 cats, including 18 females (mean age 6.1 years [range 1–13]; mean weight 5.1 kg [range 2.1–11]). This group included Persian (n = 2), Maine Coon (n = 1), Siamese (n = 1) and mixed breed (n = 29) cats. Eight mixed-breed (including six females) were included as a control group (mean age 8.8 years [range 3–13]; mean weight 4.5 kg [range 2.1–7.6]).

Most data were normally distributed, except BW, HR, LA and aorta measurements on the right transversal image, isovolumic relaxation time (IVRT), TDI velocities, MAPSE IVS, MAPSE FW and TAPSE.

The mean SBP (140 mmHg) of the control groups (control timolol and control 1) did not differ significantly. All animals had normal sinus rhythm on ECG recording.

The echocardiographic indices of the control group presented no significant differences between the two examinations performed after a 20 min interval (control 1 and control 2). On the contrary, the echocardiogram of cats after timolol administration showed differences in many indices, as shown in Table 1 and Figure 2. Figure 3 displays the variations in some of the variables affected by timolol (control timolol and timolol).

Table 2 presents the assessment results of the LV filling pattern before and after timolol administration. The lower HR resulted in an increase in IVRT by 15.2% (from 54.8 to 64.6 ms), with most cats having this variable above the reference (>60 ms)[4] after drug administration. Of 33 cats, only 11 (33.3%) presented fused transmitral waves before timolol administration. Similarly, few diastolic TDI waves were fused on the control echocardiogram (control timolol): only five when measured at the IVS annulus (15.1%) and eight at the FW annulus (24.2%). The 'impossibility of diastolic assessment' described in Table 2 refers to the fusion of mitral waves or TDI waves preventing diastolic interpretation, as the presence of unfused waves is required in both techniques.

Spearman's test revealed a moderate negative correlation between HR and BW ($r = -0.290$ and -0.393, respectively) for both the control and timolol groups, with evidence of statistical significance for the timolol group ($P = 0.025$).

Concerning the LA TMAD results, most cats did not show a plateau phase (Figure 1d). A horizontal line during LA diastasis similar to that seen in a human graph (Figure 1c)[30] occurred in a few cats: three in the first echocardiogram of the control group (control 1) and two in the second (control 2). In the timolol group, four cats showed a plateau phase on the first echocardiogram (control timolol), increasing to eight on the second (timolol), without statistical significance.

Regarding side effects, miosis occurred in 18 cats (54%) and lasted an average of 18 h, reaching up to 80 h in one cat. A contralateral effect on pupil diameter was not seen in the non-treated eye, ending in anisocoria (Figure 4). Short-lived ptyalism (<3 mins) was observed immediately after timolol application in 4/33 cats (12%).

Discussion

This investigation sought to assess whether timolol administered in eye drops interfered with cardiac variables assessed by echocardiography. In general, cats are more sensitive to stressful conditions, although they may

Table 1 Standard and speckle-tracking echocardiographic variables in the timolol group, before the drug administration (control timolol) and after (timolol), and in the control group, before (control 1) and after (control 2) the 20 min interval

	Control timolol		Timolol		*P* value* control timolol × timolol	Control 1		Control 2		*P* value* control 1 × control 2
	Mean	SD	Mean	SD		Mean	SD	Mean	SD	
Parameters										
HR	190.8	26.1	160.3	18	<0.001	212.5	20.7	210.6	25.7	0.832
LAD	12.9	1.5	13.3	1.5	0.251	13.1	<1	13.4	1	0.637
LA FS	35.2	7	30.2	5.3	0.02	34.1	6.7	38	4.3	0.225
IVSd	3.3	0.7	3.5	0.6	0.34	3.7	0.8	3.4	0.6	0.445
LVIDd	15.5	2.1	16.4	2	0.093	15.5	1.5	14.3	1.9	0.139
LVPWd	3.7	0.8	3.8	0.7	0.9	3.6	0.7	3.6	0.5	0.939
IVSs	6.2	1.4	5.8	1.3	0.374	7.1	1.4	6.4	1	0.4
LVIDs	7.6	1.6	9.4	1.4	<0.001	6.6	1.1	6.1	1.3	0.101
LVPWs	6.1	1.1	5.9	1.2	0.567	6.4	0.9	6.3	0.6	1
FS	51	7.8	42.4	5.6	<0.001	60.4	9.3	58.3	6.4	0.944
EF	83.3	6.5	76.4	5.8	<0.001	89.7	3.3	90.1	3.4	0.288
A flow	89.9	17.1	74.1	13.6	<0.001	92.2	20.8	97.3	12.9	0.637
P flow	83.8	16.6	65.9	15.2	<0.001	82	18.1	78	8.1	0.843
Sep S'	7.7	2	5.1	0.9	<0.001	8.3	1.4	7.9	1.4	0.554
Lat S'	7.3	1.7	5.1	0.6	<0.001	7.1	0.7	6.9	1.2	0.64
IVRT	54.8	8.5	64.6	9.5	0.001	54	8.7	54.5	5.8	0.932
MAPSE FW	4.5	0.7	4.1	0.7	0.01	4.9	1.4	4.6	1	0.621
MAPSE IVS	4.4	1	3.9	0.9	0.064	4.7	0.8	4.5	0.8	0.546
TAPSE	8	1.8	7.5	2.1	0.362	8.8	0.7	8.6	1.5	0.742
Parameters from AP4										
LV LSt	29.6	5.2	28.3	5.9	0.325	24.4	4.3	25.4	4.1	0.723
LV MP TMAD	4	0.9	4	0.8	0.855	4.3	0.6	4	0.8	0.335
LV MP% TMAD	17.2	3.4	16.1	3.1	0.236	17.3	3	16.2	2.4	0.363
LA LSt	36.2	6.6	33.1	6.9	0.052	33.7	7.2	37.2	7.5	0.261
LA D TMAD	2.5	1.2	2.2	1.1	0.618	2.7	1.3	2.3	1.1	0.880
LA S TMAD	2.5	1.7	2	1.3	0.415	2.5	1.3	3.2	2.3	0.47
LA cEF	57.8	6.3	52.8	6.4	0.011	65.1	4.8	62.2	4.8	0.283
LA aEF	43	7.6	39.4	7.6	0.094	43.5	31.1	50.4	9.1	0.812
LA pEF	25.8	8.4	21.8	8.4	0.194	21.9	5.9	22.7	10.2	0.893

(Continued)

Table 1 (Continued)

	Control timolol		Timolol		*P* value* control timolol × timolol	Control 1		Control 2		*P* value* control 1 × control 2
	Mean	SD	Mean	SD		Mean	SD	Mean	SD	
Parameters from AP2										
LV LSt	31.5	5.5	30.7	7.5	0.616	27.1	3	24.6	4.1	0.096
LV MP TMAD	4.2	1	4.2	1	0.858	4.6	0.8	4	0.5	0.169
LV MP% TMAD	17.6	4.3	17	4.1	0.492	18.2	2.5	15.7	3	0.155
LA LSt	37.2	7.6	32.9	7.7	0.049	38.3	7.6	35.7	7	0.536
LA D TMAD	3.8	1.1	4	1.2	0.397	4	1.1	4.8	1.7	0.303
LA S TMAD	2.3	1.3	2.5	1.1	0.188	3.2	1.7	2.6	0.6	0.234
LA cEF	56.8	5	51.7	6.4	0.001	63	4.5	60.8	4.9	0.074
LA aEF	44	8.4	40.7	8.9	0.006	52.7	7.5	48.7	8.1	0.594
LA pEF	22.3	8	21.1	10.6	1	25.8	5.1	21.6	10.8	0.296
Global parameters										
LV LSt	33.9	3.9	31.8	5.4	0.092	25.7	2.7	25	3.3	0.686
LV MP TMAD	4.1	0.8	4.1	0.7	0.918	4.4	0.4	4	0.4	0.076
LV MP% TMAD	17.5	3	16.6	2.9	0.287	17.8	2.3	15.9	2.1	0.167
LA LSt	36.9	4.4	32.9	6.1	0.004	36.4	6.5	36.5	4.2	0.971
LA D TMAD	2.4	0.6	2.4	0.7	0.885	4.2	0.9	4.4	1.1	0.876
LA S TMAD	4	0.8	4.1	0.8	0.747	2.7	1.6	1.9	0.4	0.239
LA cEF	57.4	4.6	52.7	4.2	0.001	64	3.5	61.5	4.5	0.132
LA aEF	43.5	5.9	39	5.5	0.006	46.7	14.9	49.9	7.5	0.594
LA pEF	24.2	7.4	22.3	6.5	0.434	23.8	3	22.1	9.8	0.716

*P value <0.05

HR = heart rate; LAD = left atrium diameter; LA FS = left atrium fractional shortening; IVSd = interventricular septum thickness end diastole; LVIDd = left ventricular internal dimension at end-diastole; LVPWd = left ventricular posterior wall thickness at end-diastole; IVSs = interventricular septum thickness at end-systole; LVIDs = left ventricular internal dimension at end-systole; LVPWs = left ventricular posterior wall thickness at end-systole; FS = fractional shortening; EF = ejection fraction; IVRT = isovolumic relaxation time; MAPSE = mitral annular plane systolic excursion; FW = free wall; IVS = intraventricular septum; TAPSE = tricuspid annular plane systolic excursion; AP4 = apical four-chamber; LV = left ventricle; LSt = longitudinal strain; MP = midpoint (virtual midpoint determined between the septal and lateral points of the mitral annulus); TMAD = tissue motion annular displacement; LA D TMAD = total displacement of the mitral annulus towards the farthest point of the left atrium; LA S TMAD = systolic displacement of the mitral annulus towards the farthest point of the left atrium; LA = left atrium; cEF = complete ejection fraction; aEF = active ejection fraction; pEF = passive ejection fraction; AP2 = apical two-chamber

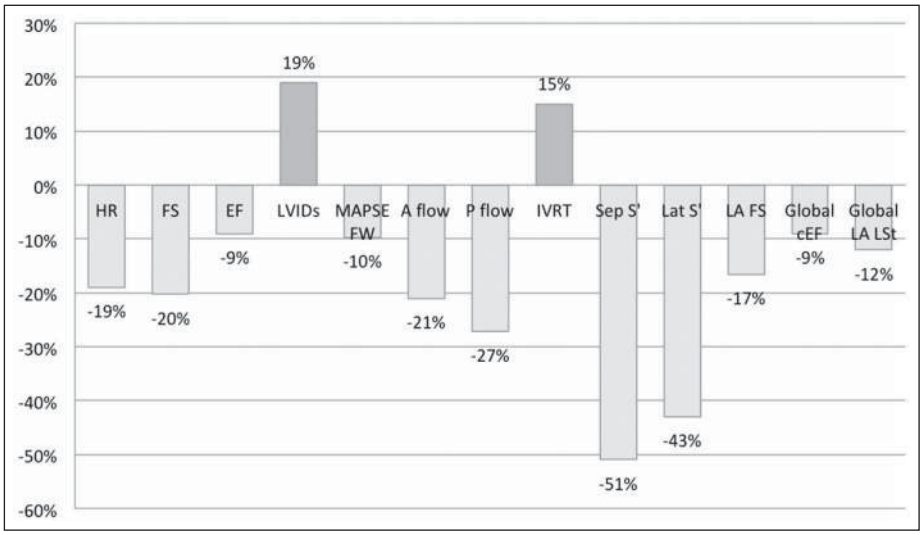

Figure 2 Percentage of change in echocardiographic indices significantly affected by timolol administration. HR = heart rate; FS = fractional shortening of the left ventricle; EF = ejection fraction of the left ventricle; LVIDs = left ventricular internal dimension at end-systole; MAPSE FW = mitral annular plane systolic excursion measured at the free wall annulus; A flow = peak velocity of aortic valve flow; P flow = peak velocity of pulmonary valve flow; Sep S' = peak velocity of systolic mitral annular motion as determined by pulsed wave Doppler at the septal annulus; Lat S' = peak velocity of systolic mitral annular motion as determined by pulsed wave Doppler at the lateral annulus; LA FS = fractional shortening of the left atrium; global cEF = complete ejection fraction of the left atrium; global LA LSt = global longitudinal strain of the left atrium

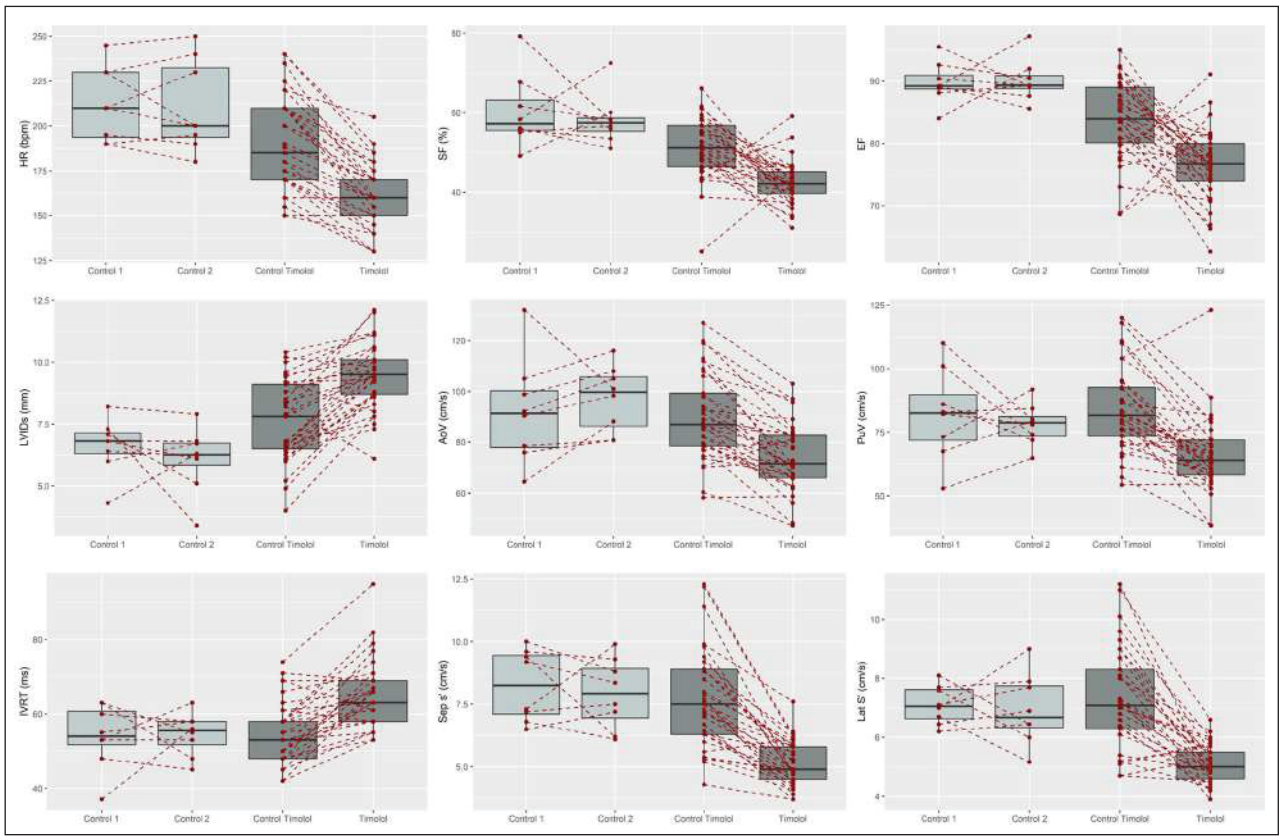

Figure 3 Boxplots representing echocardiographic indices altered significantly after timolol administration. Comparison between the first and second echocardiograms in the timolol group (control timolol and timolol) and the control group (control 1 and control 2). HR = heart rate; bpm = beats per min; SF = shortening fraction of the left ventricle; EF = ejection fraction; LVIDs = left ventricular internal dimension at end-systole; AoV = peak velocity of aortic valve flow; PuV = peak velocity of pulmonary valve flow; IVRT = isovolumic relaxation time

Table 2 Echocardiographic diastolic alterations before and after timolol administration

Diastolic alteration	Control (n = 33)	Timolol (n = 33)	*P* value
Enlarged IVRT (>60 ms)	8 (24.2)	20 (60.6)	0.003
EAfus	8 (24.2)	8 (24.2)	0.613
E'A'fus FW	8 (24.2)	2 (6.1)	0.041
Impossibility of diastolic assessment (FW)	11 (33.3)	8 (24.2)	0.552
E'A'fus IVS	5 (15.1)	5 (15.1)	0.500
Impossibility of diastolic assessment (IVS)	9 (27.3)	8 (24.2)	0.625

Data are n (%)
IVRT = isovolumetric relaxation time; EAfus = peak velocity of summated E and A waves; E'A'fus = peak velocity of summated E' and A' waves; FW = free wall; IVS = interventricular septum

Figure 4 Left eye of the cat with miosis owing to timolol resulting in anisocoria

hide signs of stress owing to their survival strategy.[33] Continued restraint during echocardiography exacerbates sympathetic activation, resulting in tachycardia and changes in several variables to assess cardiac function. The administration of a beta blocker could lead to a condition closer to the normal physiologic pattern, reflecting the condition the cat was in before sympathetic activation, or it could go beyond this point and lead to parasympathetic activation. It is likely that the latter occurred, given the high number of significantly altered variables (17/46) in the second echocardiogram of the timolol group (Table 1). In contrast, in the control group no significant differences were observed between the variables in the two echocardiographs performed. Hence, handling twice for echocardiography and the waiting period in a hospital environment did not stress the cats sufficiently to raise the HR and affect the indices.

Although timolol has its maximum effect in cats between 6 and 12 h after administration,[12] we chose to repeat the echocardiogram 20 mins later to follow the same protocol for the diastolic assessment detailed previously,[11] which coincides with the onset of its action after topical administration. As previously mentioned, timolol applied topically to the eyes has systemic effects, with a reduction in HR being the easiest to observe. Timolol effectively decreased HR by 19%, from ~190 to ~160 bpm. The mean decrease of 30 bpm was close to that previously reported (25 bpm).[11] Interestingly, another research group reported that a drop of timolol gel-forming solution did not affect HR 4 and 8 h later,[34] suggesting the bradycardic effect may not last long.

As there was a difference in BW between the animals, the dose of assimilated timolol was not the same, which may have influenced the variations observed. One drop of timolol contains approximately 0.17 mg, with most cats receiving around 0.033 mg/kg, considering an average BW of 5.1 kg. The dose that the lightest animal (2 kg) received was 5.6 times that of the heaviest cat (11 kg): 0.085 and 0.015 mg/kg, respectively. The difference in dose may explain the non-alteration of HR between the two echocardiograms of the heaviest animal; the HR remained at 150 bpm, which is a low HR for the species. However, excluding this outlier cat, the others weighed a maximum of 7.5 kg, and all showed a significant drop in HR after timolol administration. Moreover, Spearman's test showed a significant negative correlation between HR and BW after timolol, amplifying a tendency seen by the control group, although without statistical significance. The correlation with the control group would also presumably be significant in a larger sample, as previously observed in healthy cats,[22] with HR decreasing as BW increases.

Comparing the results of timolol administration and the vagal maneuver previously investigated is challenging. Their advantages and limitations are pretty balanced, and it is difficult to determine which is more suitable. Timolol required a 20 min waiting interval and the HR reduction lasted throughout the echocardiographic examination. The vagal maneuver produced a more pronounced reduction in HR (42 bpm) within a few seconds,[10] lasting a maximum of 15 s, allowing systolic assessment with usual HR. However, about one-quarter of animals submitted to vagal stimulation had an inadequate response (HR reduction <20 bpm). Although the cited investigation did not observe it, a paradoxical tachycardia might result from the oculocardiac reflex.[35] Besides, to separate both the spectral and TDI waves, it might be necessary to repeat the stimuli, with the risk of reducing the intensity of the decrease in HR caused by fatigue, as reported in children.[36] Finally, the administration of

timolol seems to be less invasive and more suitable for stressed cats. They may be disturbed by the mechanical procedure for parasympathetic stimulation in addition to the restraint required for the echocardiography. In dogs, fear and pain may be associated with the procedure, and potential reasons for a paradoxical elevation in HR or the absence of response after the maneuver.[10]

Most systolic surrogates decreased with the use of timolol, such as FS and EF (Table 1). The FS, a classical echocardiographic variable used to evaluate radial systolic function, reduced by 20.3% (from 51% to 42.4%), coinciding with what has been previously reported.[11] However, post-timolol FS was still within the reference interval for cats (ie, between 39% and 51%).[22] Timolol is not likely, at least in normal cats, to impair the interpretation of the echocardiogram. Nonetheless, in cats with HCM, the reduction in FS has already been demonstrated to be a prognostic surrogate.[9,37] A mean FS of 42.4% is much closer to what has been seen in cats with heart failure owing to HCM than in healthy cats.[38]

Interestingly, the variables known to assess longitudinal ventricular systolic function, including LV LSt, MAPSE IVS and TMAD, were less impaired by timolol. A possible explanation would be a more potent action of timolol on the transversal myocardial fibers. In humans, transverse cardiomyocytes have been shown to be significantly more sensitive to beta blockers, with studies suggesting a physiological balance of antagonism between myocytes.[39,40] Another explanation lies with HR variation itself, which affects the radial fibers more than the longitudinal ones, as previously described.[41]

A surprising result was the significant reduction (9.8%) in MAPSE FW after timolol administration, while there was no corresponding reduction in MAPSE IVS. This finding reinforces the perception that MAPSE does not behave similarly when measured on the FW or the IVS annulus, with the IVS annulus somehow affected by the right ventricle, as previously reported.[42] A previous study with HCM cats concluded that the MAPSE IVS was the only factor predicting pleural effusion on a multivariable regression model,[43] pointing to the influence of the right ventricle on this index. The researchers assumed that the IVS mitral annulus acts differently from the FW, and changes in its longitudinal function could lead to pleural effusion rather than pulmonary edema. In any case, the decrease in MAPSE FW indicated that timolol may also have influenced longitudinal fibers, although not sufficiently to change other longitudinal indices, as previously discussed.

Many LA variables changed significantly after timolol administration. Considerable LA area measures obtained from AP2 and AP4 images increased on the second echocardiogram in the timolol group, affecting LA cEF on both AP4 and AP2. The reductions in LA FS (17%), global LA LSt (12%) and global LA cEF (9%) suggest a compromise in atrial function once timolol was administered. On the contrary, LA TMAD values did not change between examinations, requiring more understanding of this LA assessment technique to justify its non-alteration. Despite presenting potential advantages, such as not demanding high-quality images, the use of TMAD to evaluate the LA function has not been validated in cats, and has previously only been applied to one research group in humans.[30] Interestingly, the reduction in HR promoted by timolol was insufficient to significantly increase the number of graphics, with a plateau phase signaling the diastasis of the LA, as occurs in human LA TMAD, suggesting a need for an even lower HR.

Of the 17 variables that changed after timolol administration (Table 1), peak systolic mitral annular velocity presented the most remarkable change, as determined by tissue Doppler (S'). The S' obtained from the interventricular annulus reduced by 51% (from 7.7 to 5.2 cm/s) and 43.1% from the FW (from 7.3 to 5.1 cm/s). Consequently, timolol lowered the S' velocity to $<$5.2 cm/s, below the reference interval.[5] Similar results on S' velocity have been reported previously.[5,8] There is a positive relationship between the S' wave and HR; however, it is impossible to delimit how much the reduction in HR may have played a role in such a marked decline. It seems that a combination of factors contributed, such as a systolic impairment evidenced by the lower FS. Of note, cats with HCM are known to have lower S' wave velocity.[5,23] In such patients, timolol might complicate the interpretation of the echocardiogram as the cardiologist will not be able to confirm if a reduced myocardial velocity is a result of the illness or the drug.

The pulmonary and aortic outflow velocities also decreased (by 27.2% and 21.3%, respectively) with timolol administration. This reduction appeared to be a consequence of the reduction in HR. A previous study with dogs concluded that an increase in HR leads to a faster aortic and pulmonary flow velocity,[44] insinuating a directly proportional relationship between them.

Regrettably, a low frequency of fused mitral outflow waves was documented in the first echocardiogram (Table 2). We speculate that having cats undergo a series of procedures (auscultation, hair clip, ECG and SBP measurement) before the echocardiogram might have contributed to their adaptation to the environment. Also, timolol administration did not separate most EAfus and E'A'fus, which impaired the LV filling pressure assessment. In those cats in which fused mitral or TDI waves were observed (11/33, using TDI IVS [33.3%]), timolol produced the desired separation in 3/11 (10.1%). In a previous study with timolol, 13/20 cats had a transmitral fusion, and successful separation was achieved in eight (62%).[11] Investigation with vagal maneuvers had better results, effectively separating 71% of the fused transmitral flows and 72% of the TDI velocity.[10]

The fusion of transmitral waves may be caused by increased HR or indicate diastolic impairment. A previous

study found that cats with HCM tend to have more EAfus at a lower HR than healthy cats, suggesting that summation may indicate diastolic impairment.[5] However, as the present study aimed to evaluate healthy cats, a more likely explanation for the low success of timolol might be due to a combination of factors: an insufficient reduction in HR; few animals with fused waves on the control echocardiogram (control timolol); and the separation of only one variable (mitral outflow or TDI), not both simultaneously.

A noteworthy result was the increase in IVRT post-timolol (Table 2). IVRT is a diastolic variable influenced by HR, lasting longer as HR decreases.[4] Combined with other variables, an enlarged IVRT reveals a diastolic dysfunction.[45] Eight cats in the timolol group had increased TRIV (>60 ms) before instillation (24%), which were maintained in the experiment because they did not manifest alterations in any other variable and had an HR low enough to justify an increase in this index. However, enlarged IVRT more than doubled after using the drug, rising to 20 (60.6%). Consequently, timolol administration might lead to a misinterpretation of the cat's echocardiogram as enlarged IVRT in these cases reflects the action of the beta blocker and is not associated with a diastolic impairment.

The administration of timolol ophthalmic solution was initially proposed to assist in the early diagnosis of HCM[11] as diastolic dysfunction secondary to hypertrophy is characteristic of this disease.[46] However, timolol might not be indicated in cats with HCM as it increases IVRT and interferes negatively with the systolic function of LV and LA. The administration would likely make the diagnosis of subclinical HCM more challenging. In patients already diagnosed with HCM, a low LA FS – a classical indicator of poor prognostic[9,37] – could be due to timolol action and not to the disease itself. There are no data on the effect of timolol in cats with advanced cardiomyopathy.

The ideal situation would be to adopt a technique to assess diastolic function independent of preload and HR. One method that meets this requirement is assessment of the flow velocity profiles of the left anterior descending coronary artery via transesophageal echocardiography.[47] Another, more promising relaxation index, is the velocity of propagation of the mitral flow (Vp),[48] obtained during transthoracic echocardiography. It measures the rapid filling phase determined by M-mode color Doppler echocardiography, with its application reported in humans with HCM[49] and dogs with dilated cardiomyopathy.[50] A recent study in HCM cats concluded that the decline in Vp is correlated with the degree of increase in LA, which is significantly associated with the progression of diastolic dysfunction in HCM.[45]

Interestingly, two cats appeared much calmer on the second echocardiogram. Their HR decreased slightly more than the mean, from 240 to 185 bpm (22.9%) and from 180 to 140 bpm (22.3%). Hence, it is plausible that the observed relaxation resulted from a beta blocker anxiolytic effect[51] and not from the reduction in HR itself. Behavioural assessment was not part of the experimental design, and the tranquillizing effect may have been present in other cats and gone unnoticed. Although this relaxation was not perceived in the control group, it is not possible to exclude the cat's acclimatization in reducing anxiety.

In this investigation, a drop of timolol did not cause any clinically relevant adverse effects. All the cats likely had miosis on the eye that received the drug (Figure 4), but it was only observed in 18/33 cats (54.5%), resulting in anisocoria as the contralateral non-treated eye was not affected.[11,33] A previous study of the administration of timolol in normotensive eyes in healthy cats reported a reduction in pupil diameter of 38.7% at 30 mins after treatment in all cats.[12] Despite going unnoticed by a significant number of owners, anisocoria was a disturbing feature for some of them, who reported non-specific behavioral changes, such as hiding or inactivity, both common alterations in cats exposed to a hospital environment.

Considering that only healthy cats were included, some possible side effects were not observed, such as bronchoconstriction,[52] which is an important reason for contraindication of timolol for cats with feline asthma.[15] This eye solution might also be avoided in elderly cats, as its continued use has been linked to syncope,[53] post-prandial head-drops[54] and atrioventricular block[55] in older people. Some studies do not recommend timolol for long-term treatment of glaucoma in cats with cardiac diseases,[15,56] but nothing is known about the effect of a single administration in cats with advanced heart failure. However, some researchers hypothesize that the negative inotropic effect of timolol may help to elucidate the patient's response to beta blockade, particularly in cats with obstructive cardiomyopathy.[11] In the cited study, all six cats with evidence of dynamic obstruction or hypertrophic obstructive cardiomyopathy on baseline echocardiogram had relief of that obstruction after the administration of timolol.

Moreover, some episodes of ptyalism were reported, which is in line with preliminary data.[11] This excess salivation was not an action of timolol, but simply a normal cat response to the bad taste of the eye solution that passed through the tear duct to the back of the throat. However, as this reaction was short-lived, it may have gone unnoticed in most cats, as they waited in their crate for the second echocardiogram.

There were some limitations to this study. First, despite all efforts to select only healthy individuals, occult cardiomyopathies might not have been identified. Another limitation was the variation in the dose administered, which could be resolved by choosing only cats with similar BWs or manipulating the ophthalmic solution

to administer a similar dose for all. The small number of cats with EAfus and E'A'fus biased the evaluation of timolol as a facilitator in assessing LV filling pressure. In this case, the owner's awareness that their cat would undergo two echocardiograms may have discouraged them from bringing stressed cats to hospital environments, with only calmer cats participating in the experiment. A less pronounced fear response would result in a control echocardiogram with a lower HR and separate transmitral flow. An intraocular pressure measurement after the second echocardiogram could have added relevant information connecting the heart effect and reduction in eye pressure.

Conclusions

A drop of timolol 0.5% ophthalmic solution reduced HR and interfered negatively with the LV and LA systolic function in healthy cats. It affected many variables commonly used in standard echocardiography, such as FS and EF. All the cited changes are not desirable in evaluating cats with suspected cardiomyopathy, with a risk of misinterpretation. The influence of timolol was milder on the echocardiographic indexes known to assess the longitudinal systolic function of the LV, such as TAPSE, MAPSE IVS, LSt and TMAD. The MAPSE FW and de S' wave were two exceptions, with both decreasing significantly after the administration of timolol.

Finally, despite not being the objective of the present study, it was found that diastolic evaluation was not benefited by timolol as the decrease in HR was not enough to separate the transmitral waves. On the contrary, the drug significantly enlarged the IVRT, which was used to classify diastolic function.

Conflict of interest The authors declared no potential conflicts of interest with respect to the research, authorship, and/or publication of this article.

Funding The authors received no financial support for the research, authorship, and/or publication of this article.

Ethical approval The work described in this manuscript involved the use of non-experimental (owned or unowned) animals and procedures that differed from established internationally recognised high standards ('best practice') of veterinary clinical care for the *individual* patient. The study therefore had prior ethical approval from an established (or ad hoc) committee as stated in the manuscript.

Informed consent Informed consent (verbal or written) was obtained from the owner or legal custodian of all animal(s) described in this work (experimental or non-experimental animals, including cadavers) for all procedure(s) undertaken (prospective or retrospective studies). No animals or people are identifiable within this publication, and therefore additional informed consent for publication was not required.

ORCID iD Giovana LR Tuleski https://orcid.org/0000-0002-0817-3470

References

1 Rodan I. **Understanding feline behavior and application for appropriate handling and management.** *Top Companion Anim Med* 2010; 25: 178–188.
2 Abbott JA. **Heart rate and heart rate variability of healthy cats in home and hospital environments.** *J Feline Med Surg* 2005; 7: 195–202.
3 Belew AM, Barlett T and Brown SA. **Evaluation of the white-coat effect in cats.** *J Vet Intern Med* 1999; 13: 134. DOI: 10.1892/0891-6640(1999)013<0134:eotwce>2.3.co;2.
4 Schober KE and Chetboul V. **Echocardiographic evaluation of left ventricular diastolic function in cats: hemodynamic determinants and pattern recognition.** *J Vet Cardiol* 2015; 17: S102–S133.
5 Koffas H, Dukes-McEwan J, Corcoran BM, et al. **Pulsed tissue Doppler imaging in normal cats and cats with hypertrophic cardiomyopathy.** *J Vet Intern Med* 2006; 20: 65–77.
6 Galiuto L, Ignone G and DeMaria AN. **Contraction and relaxation velocities of the normal left ventricle using pulsed-wave tissue Doppler echocardiography.** *Am J Cardiol* 1998; 81: 609–614.
7 Nagueh SF, Bachinski LL, Meyer D, et al. **Tissue Doppler imaging consistently detects myocardial abnormalities in patients with hypertrophic cardiomyopathy and provides a novel means for an early diagnosis before and independently of hypertrophy.** *Circulation* 2001; 104: 128–130.
8 Sugimoto K, Fujii Y, Sunahara H, et al. **Assessment of left ventricular longitudinal function in cats with subclinical hypertrophic cardiomyopathy using tissue Doppler imaging and speckle tracking echocardiography.** *J Vet Med Sci* 2015; 77: 1101–1108.
9 Luis Fuentes V, Abbott J, Chetboul V, et al. **ACVIM consensus statement guidelines for the classification, diagnosis, and management of cardiomyopathies in cats.** *J Vet Intern Med* 2020; 34: 1062–1077.
10 Smith DN and Schober KE. **Effects of vagal maneuvers on heart rate and Doppler variables of left ventricular filling in healthy cats.** *J Vet Cardiol* 2013; 15: 33–40.
11 Gunther-Harrington CT, Ontiveros ES, Hodge TE, et al. **Effects of 0.5% timolol maleate ophthalmic solution on heart rate and selected echocardiographic indices in apparently healthy cats.** *J Vet Intern Med* 2016; 30: 733–740.
12 Wilkie DA and Latimer CA. **Effects of topical administration of timolol maleate on intraocular pressure and pupil size in cats.** *Am J Vet Res* 1991; 52: 436–440.
13 Willis AM. **Ocular hypotensive drugs.** *Vet Clin North Am Small Anim Pract* 2004; 34: 755–776.
14 Slenter IJM, Djajadiningrat-Laanen SC, Elders DJ, et al. **The effects of topical dorzolamide 2% and brinzolamide 1%, either alone or combined with timolol 0.5%, on intraocular pressure, pupil diameter, and heart rate in healthy cats.** *Vet Ophthalmol* 2020; 23: 16–24.
15 McLellan GJ and Teixeira LBC. **Feline glaucoma.** *Vet Clin North Am Small Anim Pract* 2015; 45: 1307–1333.
16 Chen L, Zeng X and Huang X. **Efficacy and safety of intraocular pressure-lowering agents bimatoprost and timolol maleate in glaucoma.** *Int J Pharmacol* 2018; 14: 179–186.

17 Riesen SC, Schober KE, Cervenec RM, et al. **Comparison of the effects of ivabradine and atenolol on heart rate and echocardiographic variables of left heart function in healthy cats.** *J Vet Intern Med* 2011; 25: 469–476.
18 Gorre F and Vandekerckhove H. **Beta-blockers: focus on mechanism of action. Which beta-blocker, when and why?** *Acta Cardiol* 2010; 65: 565–570.
19 Barbier P, Solomon SB, Schiller NB, et al. **Left atrial relaxation and left ventricular systolic function determine left atrial reservoir function.** *Circulation* 1999; 100: 427–436.
20 Thomas WP, Gaber CE, Jacobs GJ, et al. **Recommendations for standards in transthoracic two-dimensional echocardiography in the dog and cat.** *Vet Radiol Ultrasound* 1994; 35: 173–178.
21 Sahn DJ, DeMaria A, Kisslo J, et al. **Recommendations regarding quantitation in M-mode echocardiography: results of a survey of echocardiographic measurements.** *Circulation* 1978; 58: 1072–1083.
22 Häggström J, Andersson O, Falk T, et al. **Effect of body weight on echocardiographic measurements in 19,866 pure-bred cats with or without heart disease.** *J Vet Intern Med* 2016; 30: 1601–1611.
23 Spalla I, Payne JRR, Borgeat K, et al. **Mitral annular plane systolic excursion and tricuspid annular plane systolic excursion in cats with hypertrophic cardiomyopathy.** *J Vet Intern Med* 2017; 31: 691–699.
24 Wolf M, Lucina SBSB, Brüler BCBC, et al. **Assessment of longitudinal systolic function using tissue motion annular displacement in healthy dogs.** *J Vet Cardiol* 2018; 20: 175–185.
25 Spalla I, Boswood A, Connolly DJ, et al. **Speckle tracking echocardiography in cats with preclinical hypertrophic cardiomyopathy.** *J Vet Intern Med* 2019; 33: 1232–1241.
26 Abbott JA and MacLean HN. **Two-dimensional echocardiographic assessment of the feline left atrium.** *J Vet Intern Med* 2013; 20: 111–119.
27 Rishniw M and Erb HN. **Evaluation of four 2-dimensional echocardiographic methods of assessing left atrial size in dogs.** *J Vet Intern Med* 2000; 14: 429–435.
28 Schober KE, Wetli E and Drost WT. **Radiographic and echocardiographic assessment of left atrial size in 100 cats with acute left-sided congestive heart failure.** *Vet Radiol Ultrasound* 2014; 55: 359–367.
29 Piotrowski G, Goch A, Wlazłowski R, et al. **Non-invasive methods of atrial function evaluation in heart diseases.** *Med Sci Monit* 2014; 6: 827–839.
30 Strachinaru M, Annis C, Catez E, et al. **The mitral annular displacement by two-dimensional speckle tracking.** *J Cardiovasc Med* 2016; 17: 344–353.
31 Faul F, Erdfelder E, Lang A-G, et al. **G*Power 3: a flexible statistical power analysis program for the social, behavioral, and biomedical sciences.** *Behav Res Methods* 2007; 39: 175–191.
32 R Core Team. R: a language and environment for statistical computing. Vienna: R Foundation for Statistical Computing, 2021.
33 Horwitz DF and Rodan I. **Behavioral awareness in the feline consultation: understanding physical and emotional health.** *J Feline Med Surg* 2018; 20: 423–436.
34 Kiland JA, Voss AM and McLellan GJ. **Effect of timolol maleate gel-forming solution on intraocular pressure, pupil diameter, and heart rate in normal and glaucomatous cats.** *Vet Ophthalmol* 2016; 19: 91–96.
35 Arnold RW. **The oculocardiac reflex: a review.** *Clin Ophthalmol* 2021; 15: 2693–2725.
36 Blanc VF, Hardy JF, Milot J, et al. **The oculocardiac reflex: a graphic and statistical analysis in infants and children.** *Can Anaesth Soc J* 1983; 30: 360–369.
37 Payne JR, Borgeat K, Connolly DJ, et al. **Prognostic indicators in cats with hypertrophic cardiomyopathy.** *J Vet Intern Med* 2013; 27: 1427–1436.
38 Visser LC, Sloan CQ and Stern JA. **Echocardiographic assessment of right ventricular size and function in cats with hypertrophic cardiomyopathy.** *J Vet Intern Med* 2017; 31: 668–677.
39 Lunkenheimer PP, Redmann K, Cryer CW, et al. **Beta-blockade at low doses restoring the physiological balance in myocytic antagonism.** *Eur J Cardiothoracic Surg* 2007; 32: 225–230.
40 Schmitt B. **Accelerated whole-heart 3D CSPAMM reveals impact of beta-blocker therapy on myocardial architecture.** *J Cardiovasc Magn Reson* 2010; 12: 3. DOI: 10.1186/1532-429X-12-S1-P122.
41 Simpson KE, Gunn-Moore DA, Shaw DJ, et al. **Pulsed-wave Doppler tissue imaging velocities in normal geriatric cats and geriatric cats with primary or systemic diseases linked to specific cardiomyopathies in humans, and the influence of age and heart rate upon these velocities.** *J Feline Med Surg* 2009; 11: 293–304.
42 Hu K, Liu D, Herrmann S, et al. **Clinical implication of mitral annular plane systolic excursion for patients with cardiovascular disease.** *Eur Heart J Cardiovasc Imaging* 2013; 14: 205–212.
43 Spalla I, Payne JR, Borgeat K, et al. **Prognostic value of mitral annular systolic plane excursion and tricuspid annular plane systolic excursion in cats with hypertrophic cardiomyopathy.** *J Vet Cardiol* 2018; 20: 154–164.
44 Kirberger RM, Bland-vanden Berg P and Grimbeek RJ. **Doppler echocardiography in the normal dog: part II: factors influencing blood flow velocities and a comparison between left and right heart blood flow.** *Vet Radiol Ultrasound* 1992; 33: 380–386.
45 Sugimoto K, Kawase N and Aoki T. **Assessment of diastolic function using mitral flow propagation velocity in cats.** *Can J Vet Res* 2020; 84: 124–130.
46 Abbott JA. **Feline hypertrophic cardiomyopathy: an update.** *Vet Clin North Am Small Anim Pract* 2010; 40: 685–700.
47 Tomochika Y, Tanaka N, Wasaki Y, et al. **Assessment of flow profile of left anterior descending coronary artery in hypertrophic cardiomyopathy by transesophageal pulsed Doppler echocardiography.** *Am J Cardiol* 1993; 72: 1425–1430.
48 Garcia MJ, Thomas JD and Klein AL. **New Doppler echocardiographic applications for the study of diastolic function.** *J Am Coll Cardiol* 1998; 32: 865–875.
49 Nishihara K, Mikami T, Takatsuji H, et al. **Usefulness of early diastolic flow propagation velocity measured by color M-mode Doppler technique for the assessment of left ventricular diastolic function in patients with**

hypertrophic cardiomyopathy. *J Am Soc Echocardiogr* 2000; 13: 801–808.
50 O'Sullivan ML, O'Grady MR and Minors SL. **Assessment of diastolic function by Doppler echocardiography in normal Doberman Pinschers and Doberman Pinschers with dilated cardiomyopathy.** *J Vet Intern Med* 2014; 21: 81–91.
51 Carabine UA, Milligan KR and Moore JA. **Adrenergic modulation of preoperative anxiety: a comparison of temazepam, clonidine, and timolol.** *Anesth Analg* 1991; 73: 633–637.
52 Shiuey Y and Eisenberg MJ. **Cardiovascular effects of commonly used ophthalmic medications.** *Clin Cardiol* 1996; 19: 5–8.
53 Müller ME, Van Der Velde N, Krulder JWM, et al. **Syncope and falls due to timolol eye drops.** *BMJ* 2006; 332: 960–961.
54 Bin Waqar SH, Rehan A and Zammam M. **Postprandial head-drops: insight into systemic effects of ocular timolol preparation in elderly.** *Cureus* 2019; 11: e4780. DOI: 10.7759/cureus.4780.
55 Wang Z, Denys I, Chen F, et al. **Complete atrioventricular block due to timolol eye drops: a case report and literature review.** *BMC Pharmacol Toxicol* 2019; 20: 73. DOI: 10.1186/s40360-019-0370-2.
56 McLellan GJ and Miller PE. **Feline glaucoma-a comprehensive review.** *Vet Ophthalmol* 2011; 14: 15–29.

VITA

Médica Veterinária permanente da Universidade Federal do Paraná (UFPR) desde 2004, formada na mesma instituição (1994-1999). Fez aprimoramento nos Estados Unidos (The Ohio International Agricultural & Horticultural Intern Program) e mestrado em Ciências Veterinárias na UFPR (2005-2007), defendendo uma tese sobre otite em cães. 2007.. No mesmo ano ganhou o 9º Prêmio Pesquisa Clínica Schering-Plough ao esdrever um artigo com dados provenientes de sua pesquisa. Especializou-se em Cardiologia Veterinária na Universidade de Buenos Aires (2008-2009).Desde 2007 vem atuando em cardiologia de cães e gatos no Laboratório de Cardiologia Comparada do Hospital Veterinário da UFPR. Durante o doutorado realizado mais de 400 exames cardiológicos completos em gatos para sua pesquisa (aferição de pressão, eletrocardiografia e ecocardiografia).